THE UNIVERSITY
of EDINBURGH

Redox regulation of salicylic acid synthesis in plant immunity

Yuan Li

Doctor of Philosophy
The University of Edinburgh
2015

Declaration

I composed this thesis, the work is my own. No part of this thesis has been submitted for any other degree or qualification.

Name **Date**

Acknowledgement

Foremost, I would like to express my sincere gratitude to my advisor Prof. Gary Loake for the continuous support of my PhD study and research, for his patience, motivation, enthusiasm, and immense knowledge. His guidance helped me in all the time of research and writing of this thesis.

I would like to thank all my colleagues in the University of Edinburgh for their support and help during my study, research and daily life.

Last, I would like to thank my parents for giving birth to me at the first place and loving me unconditionally throughout my life.

Abstract

Salicylic acid (SA) is essential to the establishment of both local and systemic acquired resistance (SAR) against a wide range of phytopathogens. Isochorismate synthase 1 (ICS1) is the key enzyme involved in the synthesis of SA and it is transcriptionally activated by the regulatory proteins SAR deficient 1 (SARD1) and Calmodulin binding protein 60g (CBP60g). It has been demonstrated previously that the loss-of-function mutant, *S*-nitrosogluthione reductase 1-3 (gsnor1-3), increased cellular levels of *S*-nitrosylation. Significantly, accumulation of both free SA and its storage form SA-glucoside (SAG), were substantially reduced, disabling multiple SA-dependent immune responses. However, the molecular mechanism underlying this observation remains to be established. Our data suggests that the transcription of ICS1 and it regulators, SARD and CBP60g, are reduced in the gsnor1-3 mutant, implying that increased cellular *S*-nitrosylation blunts the expression of ICS1 by reducing the transcription of its activators. We demonstrated that SARD1 is *S*-nitrosylated *in vitro* resulting in inhibition of its DNA binding activity. Further, Cys438 of SARD1 was found to be the site of *S*-nitrosylation, demonstrated by the observation that the SARD1 C438S mutant was insensitive to NO regulation in regard to DNA binding activity.

Content

Abbreviations **1**

Chapter 1 Introduction **2**

1. **Nitric Oxide** 4
2. **Salicylic acid** 17
3. **Project aims** 25

Chapter 2 Material and Methods **26**

1. **Plant material and *E. coli* strains** 26
2. **Preparing pathogen and plant leaf samples** 26
3. **Plant RNA extraction and cDNA synthesis** 26
4. **Primer design** 27
5. **Quantitative RT-PCR analysis** 29
6. **Vector construction** 29
7. **Recombinant protein expression, extraction and purification** 31
8. ***S*-nitrosylation assays** 32
9. **Western blot** 33
10. **Plant transformation** 34
11. **Electrophoretic mobility shift assay (EMSA)** 35
12. **GUS stain using X-Gluc** 35

Chapter 3 SA synthesis related gene expression **36**

Chapter 4 SARD1 and CBP60g protein expression **40**

Chapter 5 SARD1 DNA binding assay **49**

Chapter 6 *S*-nitrosylation of SARD1 ..... **55**

Chapter 7 SARD1 C438S analysis **64**

Chapter 8 Constructing *ICS1 promoter::GUS* reporter *Arabidopsis* plants **71**

Chapter 9 Discussion and conclusion **76**

References **82**

Abbreviations

CBP60g	Calmodulin-binding protein 60-like g
DTT	Dithiothreitol
EMSA	Electrophoretic mobility shift assay
ETI	Effector triggered immunity
HR	Hypersensitive response
GR	Glutathione reductase
GSH	Glutathione
GSNO	*S*-nitrosyglutathione
GSNOR	GSNO reductase
GSSG	Glutathione disulfide
ICS	Isochorismate synthase
IPTG	Isopropyl β-D-1-thiogalactopyranoside
PAMP	Pathogen-associated-molecular-pattern
PR	Pathogenesis-related
PRR	Pattern recognition receptor
PTI	PAMP-triggered Immunity
MBP	Maltose-binding protein
NO	Nitric Oxide
NOS	NO synthase
NPR1	Nonexpressor of Pathogenesis-Related Gene 1
NR	Nitrate reducatase
RNS	Reactive nitrogen species
ROS	Reactive oxygen species
SA	Salicylic acid
SAR	Systemic acquired resistance
SARD1	SAR-deficient 1
SDS	Sodium dodecyl sulphate
SNO	*S*-nitrosythiol
SNP	Sodium nitroprusside
TF	Transcription Factors

Chapter 1 Introduction

Plants face numerous biotic stresses in the natural environment and have therefore developed sophisticated defence mechanisms in order to adapt and counter such challenges. In the plant immune system, salicylic acid (SA) plays a vital role in establishing plant defence against biotrophic pathogens and triggering systemic acquired resistance (SAR) (Fu & Dong, 2013; Loake & Grant, 2007; Vlot et al, 2009). On another hand, nitric oxide (NO), a gaseous, redox-active small molecule, has been recognized to play an equally important role in regulating plant defence (Feechan et al, 2005; Yu et al, 2014; Yu et al, 2012). Despite the increased numbers of discoveries on SA signalling (Yan & Dong, 2014) and how NO might be involved in local SA dependent immune responses and SAR (Malik et al, 2011; Yu et al, 2012), surprisingly, there has been less focus on how NO might impact SA synthesis.

Currently, the widely accepted plant-pathogen interaction model is called a 'zig-zag', in which plant and pathogen interactions include multiple stages of defence and counter-defence mechanisms, respectively (Jones & Dangl, 2006) (Fig 1.1). After pathogens penetrate leaf/root surface and cell wall, they will encounter a range of extracellular receptors deployed to recognize pathogen-associated-molecular-patterns (PAMPs) like chitin. Upon recognition PAMP- triggered immunity is initiated (PTI) (Nicaise et al, 2009; Zipfel, 2014), preventing pathogens from further colonization. However, pathogens have developed a series of proteins called effectors to supress PTI. In response, plants have evolved resistance (R) proteins to directly or indirectly recognize effectors, which when recognised are termed as avirulence (avr) factors, to induce effector triggered immunity (ETI) (Okmen & Doehlemann, 2014; Yan & Dong, 2014). An inability of the challenged plant to recognise any one of the pathogens effector repertoire allows pathogens to supress basal plant defence and establish an infection. Following initiation of PTI or ETI, a variety of events occur at the site of infection, including production of ROS, accumulation of SA and expression of *Pathogenesis-related (PR)* genes (Vlot et al, 2009). Additionally, ETI is often associated with hypersensitive response (HR) cell death, which results in necrotic lesions at the

site of infection. Further global accumulation of SA and expression of *PR* genes, leads to a systemic, long lasting, broad ranged resistance against following pathogen infection, which is termed systemic acquired resistance (SAR) (Durner et al, 1997; Durrant & Dong, 2004; Vlot et al, 2009).

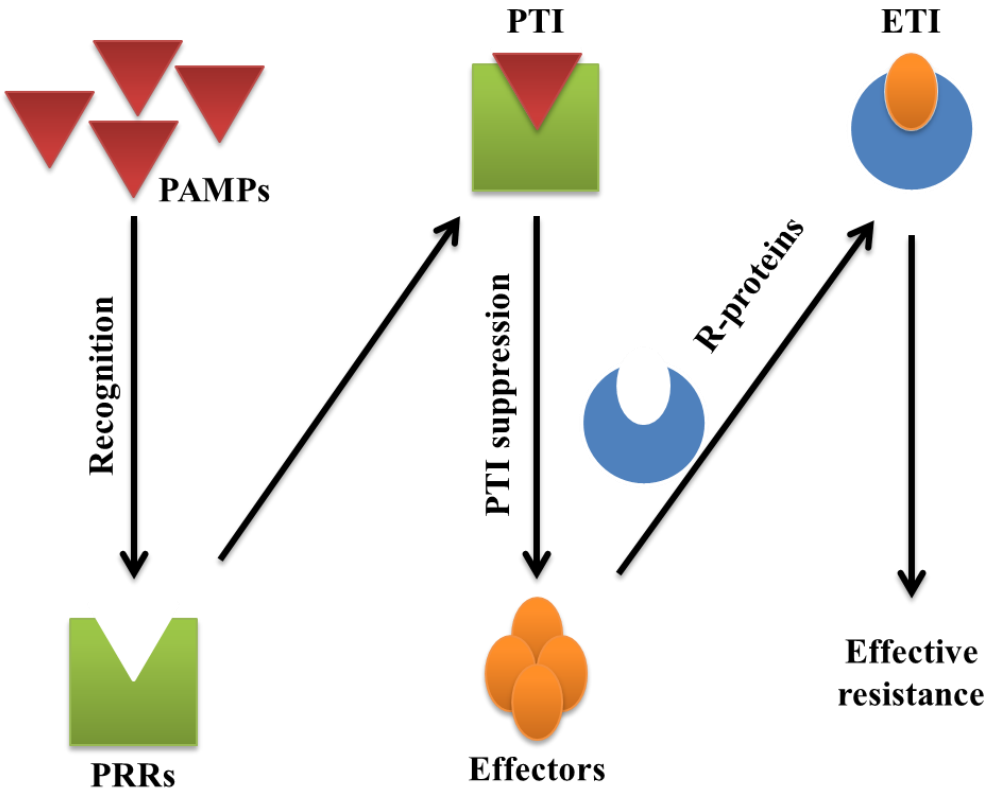

Figure 1.1. Schematic representation of the plant immune response during pathogen infection. Recognition of PAMPs by plant pattern recognition receptors (PRRs) leads to activation of PTI. Successful pathogens have developed effectors to supress PTI. Some effectors can be directly or indirectly recognized or sensed by plant derived R-proteins result in triggering ETI, and further establish an effective resistance in plant. (Jones & Dangl, 2006).

In this chapter, the current knowledge of NO and SA will be introduced with more focus on NO related regulation of plant immunity and SA synthesis. Also, the main purpose of the project will be discussed.

1. Nitric Oxide

1.1 NO synthesis in plants

In mammalian cells, it is known that NO is synthesized via an oxidative mechanism using NO synthase (NOS), which is homologous to P450 cytochrome c reductase. NOS have three isoforms: endothelial (eNOS), neuronal (nNOS) and inducible (iNOS) NOS (Alderton et al, 2001). The major route of NO synthesis in animal involves deamination of arginine by NOS to form citrulline and NO. Besides NOS, it has been reported that in mammal mitochondria, NO can be formed by reducing NO_2^- at complex III or cytochrome c oxidase (Shiva, 2010) or other enzymes with nitrate reductase activity (Jansson et al, 2008). However, unravelling NO synthesis mechanisms in higher plants is far from completion. Following numerous completed genome sequencing projects, genes that encode a structurally related NOS enzyme have not been identified.

At least seven sources have been identified as possible routes for NO production so far (Gupta et al, 2011; Mur et al, 2013; Yu et al, 2014), those sources have been divided into two groups based on chemical natures (Fig 1.2). A reductive route uses nitrite as primary substrate, and includes nitrate reductase (NR), a plasma membrane-bound nitrite-NO reductase (NiNOR) or mitochondrial nitrite reduction. On another hand, an oxidative route includes production of NO from L-arginine (L-Arg), polyamines or hydroxylamines.

1.1.1 Oxidative route of NO production

Although people were not able to find a structurally related NOS enzyme in higher plants, evidence suggested that producing NO from L-arginine via NOS activity may be presented. It has been reported that L-arginine analogs, like NG-Nitro-L-arginine methyl ester (L-NAME) and S,S'-1,3-Phynylene-bis(1,2-ethanediyl)-bis-isothiourea (PBITU), which were used as NOS inhibitors in animal research, are capable to decrease NO accumulation in soybean seedlings and *Arabidopsis* (Corpas et al, 2006; Delledonne et al, 1998). Further, a loss of function mutant, *no overproducer 1* (*nox1*), has been reported to have an excessive amount of L-Arg and thus accumulates a high level of NO and citrulline (He et al, 2004). Also, it has been reported that NOS activity is associated to plant immune response in both tobacco (*Nicotiana tabacum*) and

Arabidopsis (Delledonne et al, 1998; Durner et al, 1998). Further, a NOS enzyme has been identified in a green algae species, *Ostreococcus tauri* (Foresi et al, 2010). Upon characterization, it has been shown the amino acid sequence of *O. tauri*'s NOS shares 45% similarity of human NOS in amino acid sequence, and purified recombinant *O. tauri* NOS has a K_m of 12 μM for L-Arg, which possesses similar property to animal NOS *in vitro*.

Spermine and spermidine are polyamines produced in plant cells which use arginine and other amines as precursors. Previous research has shown addition of spermine induces release of NO from *Arabidopsis* seedlings. Furthermore, the authors demonstrated that polyamine induced NO synthesis is root specific in *Arabidopsis* (Tun et al, 2006). Nevertheless, the molecular detail of how spermine and spermidine are used to produce NO is not clear. Hydroxylamines have also been proposed as substrates that can be oxidized into NO, previous research has shown that hydroxylamines added externally can be oxidized to NO by an NR deficient plant cell (Rumer et al, 2009). Since this research used cell culture, the organ(s) that oxidises hydroxylamine to NO is still unknown.

1.1.2 Reductive route of NO production

The NR pathway is the best characterized NO production pathway in plants (Fig 1.2). NR is a cytosol localized enzyme which is primarily used to convert nitrate (NO_3^-) to nitrite (NO_2^-). Two NR genes have been identified in *Arabidopsis*, *NIA1 and NIA2.* Among two proteins, NIA2 is responsible for the majority of NR enzyme activity (Wilkinson & Crawford, 1993). Later, Yamasaki and Sakihama demonstrated that corn NR is able to convert nitrite to NO with the presence of NADH at neutral pH under aerobic condition (Yamasaki & Sakihama, 2000). Further, this property has been shown *in vivo* (Rockel et al, 2002). Although NR has been shown to have the ability to produce NO from nitrite, it only produces NO at about 1% of its nitrate reducing capacity at optimal condition *in vitro*, and its activation requires accumulation of nitrate, low concentration of nitrite (Rockel et al, 2002) and decreased cellular pH (Gupta et al, 2011; Kaiser & Brendle-Behnisch, 1995). Despite all the limitations, several independent groups have shown NR mediated NO production can be induced by fungal and oomycete infection (Srivastava et al, 2009; Yamamoto-Katou et al, 2006), osmotic and water stress (Kolbert et al, 2010; Sang et al,

2008), flower and root development (Kolbert et al, 2008; Seligman et al, 2008) and in low oxygen environment (Benamar et al, 2008; Blokhina & Fagerstedt, 2010), suggesting the biological importance of this NO synthesis mechanism.

More than a decade ago, a membrane bound nitrite reducing enzyme was isolated from tobacco (*Nicotiana tabacum L. cv. Samsun*) root, exclusively (Stohr et al, 2001), this enzyme has been termed as nitrite-NO reductase (NiNOR). It was assumed a chain of enzymatic reactions are presented to convert nitrate into NO with the aid of NiNR. Unlike NR, NAD(P)H is not the electron donor in such a reaction, instead, cytochrome c has been shown to induce NO production. However, the molecular details of this enzyme still remain elusive. Nevertheless, NiNOR has been suggested to have a role in sensing nitrate availability (Meyer & Stöhr, 2004) and mediating NO production in mycorrhizal fungal infection (Moche et al, 2010).

The peroxisomal enzyme xanthine oxidoreductase (XOR) has been proposed to be an enzyme that catalyses the reduction of nitrite to NO (Fig 1.2). Godber et al were able to show that animal XOR can reduce nitrite to NO using NADH or xanthine as substrate under anaerobic conditions (Godber et al, 2000). Previous research has shown that XOR is also be able to produce the superoxide radical O_2^- (Harrison, 2002). Since the enzyme is peroxisome localized, which is known to produce reactive oxygen species (ROS), it is proposed the NO producing property of XOR may allow its involvement in interaction of ROS and reactive nitrogen species (RNS) (del Rio et al, 2004). Furthermore, it has been reported that XOR was involved in NO production induced by phosphorus deficiency in white lupin (*Lupinus albus*), providing a biological significance for this NO synthesis mechanism (Wang et al, 2010).

Plant mitochondria have been reported to produce NO under anoxia conditions (Planchet et al, 2005) (Fig 1.2). Mitochondria from tobacco root has been reported to reduce nitrite to NO at the expense of NADH (Gupta et al, 2005). Additionally, this NO producing process in mitochondria has been demonstrated to generate a small amount of ATP (Stoimenova et al, 2007).

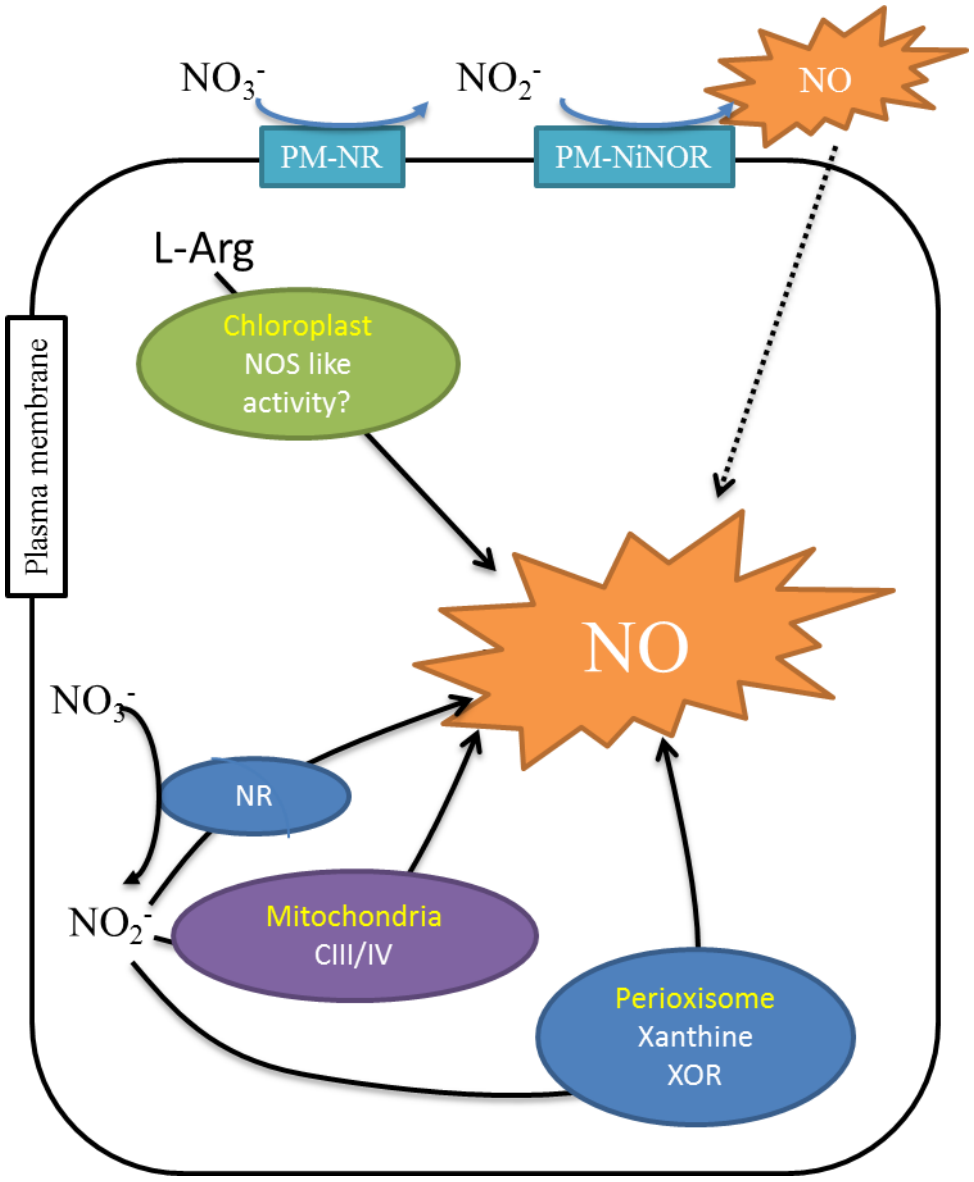

Figure 1.2. Overview of NO production routes. Various NO production pathways have been suggested. Production of NO and citrulline from L-arginine catalysed by NOS activity has been described in plant leaf tissue and its activity is inhibited by animal NOS inhibitors (Corpas et al, 2009). NR, found in cytosol, has been reported to convert nitrite to NO with low efficiency (Rockel et al, 2002; Yamasaki & Sakihama, 2000). Also, a plasma bound nitrite-NO reductase has been identified in tobacco root to convert nitrite into NO in a possible enzymatic chain reaction (Stohr et al, 2001). Also, mitochondria and perioxisome have been reported to produce NO from nitrite (Godber et al, 2000; Planchet et al, 2005). (Gupta et al, 2011).

1.2 NO signalling

It is important to understand how elevated NO levels lead to NO signalling and further regulation. Unlike macromolecules, NO is a gaseous small molecule that chemically reacts with a specific amino acid of its target protein, which results in a covalent modification (Nathan, 2003). Nitrosylation is a chemical process that covalently incorporates the NO moiety into another molecule. In biology, NO has been reported to oxidize a reactive cysteine thiol, forming an *S*-nitrosothiol (SNO) (Stamler et al, 1992). In contrast to many cysteine residues (Cys) which are embedded by their protein tertiary structures, a rare sets of cysteines with low pKa sulfhydryl group are termed as reactive cysteines (Spadaro et al, 2010). These reactive cysteines are targets of a variety of redox modifications (Fig 1.3). Besides *S*-nitrosylation, oxidation of a Cys can form a sulphenic acid via *S*-sulphenation (SOH). However, a protein sulphenic acid is relatively unstable and a disulphide bond (S-S) can be formed between two sulphenic acid residues by further oxidation. Additionally, intra and intermolecular disulphide bonds formation is important in controlling protein folding and multimerization (D'Autreaux & Toledano, 2007). *S*-glutathionylation (SSG) is the disulphide bond formation between glutathione (GSH) and a protein Cys residue. *S*-sulphination (SO_2H) and irreversible *S*-sulphonation (SO_3H) are more extreme oxidation of Cys residues (Spadaro et al, 2010). These modifications can be reversed in response to changes in cellular redox environment or enzymatically (Benhar et al, 2009; Tada et al, 2008), further providing strategies for plants to adapt environmental changes and stresses. Among all these redox modifications, *S*-nitrosylation has a central role in translating NO bioactivity. *S*-nitrosylation has been found to be involved in many biological processes in animals (Hess et al, 2005). Further, emerging evidence suggests this modification also regulates enzyme activity (Lindermayr et al, 2005; Romero-Puertas et al, 2007; Wang et al, 2015a; Wang et al, 2009b; Yun et al, 2011), protein localization (Tada et al, 2008) and protein-protein interactions (Hara et al, 2006) in plants.

Apart from cysteine, specific protein tyrosine residues were suggested to be oxidized by NO_2 to form 3-nitrotyrosine and result in protein conformational change (Astier & Lindermayr, 2012). NO can interact with iron, zinc or copper centres of metalloproteins resulting metal-nitrosyl

complexes. In mammal, binding between NO and the heme centre of soluble guanylate cyclase activate the enzyme via conformational change and further lead to the production of cyclic GMP (Russwurm & Koesling, 2004).

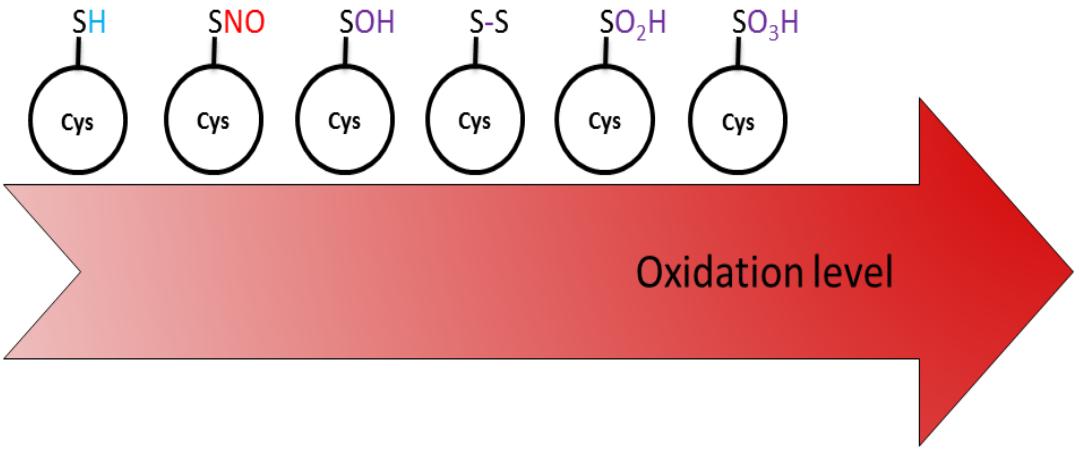

Figure 1.3. Schematic sketch of cysteine modifications according to an increasing of oxidation. S-nitrosothiol (SNO), sulfenic acid (SOH), disulfide bond (SS), sulfinic acid (SO_2H) and sulfonic acid (SO_3H), which is irreversible.

Glutahinone (GSH) is a highly abundant tripeptide which has been recognized as an antioxidant barrier to protect cells from excessive oxidant damage (Noctor et al, 2012). Two reduced GSH are oxidized to disulphide to form glutathione disulfide (GSSG) by enzyme activity or in response to reactive oxygen species (ROS). Later, GSSG can be reduced to GSH by glutathione reductase (GR) (May et al, 1998). The antioxidant and widely distributed properties of GSH enable its role in effectively scavenging radicals. *S*-nitrosyglutathione (GSNO) is formed by addition of an NO moiety to GSH by an O_2 dependent reaction. As the half-life of NO in biological system is only a few seconds, GSNO has been suggested as a stable reservoir of NO (Liu et al, 2001; Sakamoto et al, 2002). The mechanism of GSNO formation in biological systems remains elusive. By using submitochondrial particles and cell lysate, Basu et al were able to show cytochrome C may catalyse the formation of GSNO from GSH and NO (Basu et al, 2010).

In plants, maintaining the optimal GSH level is crucial for plant immunity. A mutation study

performed by Parisy et al (Parisy et al, 2007) has revealed that *phytoalexin deficient 2-1* (*pad 2-1*) plant, which is a knock-out of γ-glutamylcysteine synthetase thus has reduced GSH level, is susceptible to pathogens. In contrast to NO, GSNO is more stable and also mobile in biological systems, this makes GSNO a good intermediate in transporting redox signals over long distance. It has been reported that NO can be release by homolytic cleavage of S-N bond in GSNO (Singh et al, 1996). In addition, research on *Saccharomyces cerevisiae* suggested the presence of an SNO-lyase activity, which could catalyse release of NO from GSNO (Foster et al, 2009). Apart from releasing of NO, GSNO has been reported to transfer an NO group on to a Cys residue, which has been termed as trans-nitrosylation (Pawloski et al, 2001). Taken together, GSNO serves not only as a reservoir of NO, but also function as a messenger in transmission of NO bioactivity.

1.3 GSNO reductase (GSNOR)

In vivo, the GSNO level controls the degree of peptide and protein nitrosylation, thus affecting functions and activities of varies enzymes and transcription factors, thus having an impact on plant stresses adaptation and development (Yu et al, 2014). Cellular levels of GSNO are controlled by GSNO reductase (GSNOR) (Liu et al, 2001). GSNOR is glutathione-dependent formaldehyde dehydrogenase and catalyses the oxidation of *S*-(hydroxymethyl)glutathione to *S*-formylglutathinone using NAD^+ as a coenzyme (Jensen et al, 1998). But the main role of GSNOR is to catalyse the reduction GSNO into N-hydroxysulphenamide intermediate. The unstable intermediate spontaneously rearrange to form glutathione sulphonamide which hydrolysed into glutathione sulphinic acid and ammonia in acidic condition; or in excessive GSH environment, the intermediate can form GSSG with GSH and releasing hydroxylamine (Hedberg et al, 2003; Kubienova et al, 2013; Liu et al, 2001; Singh et al, 1996). The function of GSNOR is conserved in animals, plants and bacteria (Feechan et al, 2005; Liu et al, 2001). GSNOR structures from human and tomato (*Solanum lycoperscum*) have been resolved previously (Kubienova et al, 2013; Sanghani et al, 2002). SlGSNOR is a homodimer of 81,085 Da, the entrances of both active sites are present on one side of dimer, and both co-enzyme binding sites are on the opposite sides of the dimer, similar to hGSNOR (Kubienova et al, 2013).

Arabidopsis thaliana S-nitrosoglutathione Reductase (*AtGSNOR1*) was cloned from cDNA library

and further functional complementary study revealed its GSNO reduction activity in yeast (Sakamoto et al, 2002). Later, study on a *GSNOR1* T-DNA insertion plant *gsnor1-3* demonstrated *Arabidopsis* with no GSNOR activity exhibit reduced GSNO turn-over activity and increased total SNO. In contrast, enhanced GSNO activity promoted the turnover of GSNO (Feechan et al, 2005). Furthermore, the loss of function *gsnor* mutant showed compromised plant immunity (Feechan et al, 2005) as well as defects in plant growth and development (Kwon et al, 2012).

Apart from biotic stresses, GSNOR has been found to be critical in thermotolerance. By selecting a plant line that failed to develop after exposed in high temperature, a mutant, *hot5*, has been uncovered (Lee et al, 2008). As well as *gsnor1-3*, *hot5* also exhibit an increased nitrate and SNO concentration phenotype. Later genetic study has revealed that *hot5* is in fact a mutation in *GSNOR*. Further analysis has shown that exogenous administration of NO scavenger, CPTIO, partially rescued the heat sensitive phenotype in *hot5* mutant; in contrast, applying NO donor to wild type plant increased the heat sensitivity of wild type plant seedlings and leaves (Lee et al, 2008). There is no evidence suggest that GSNOR may regulate thermotolerance directly, which is similar to the regulatory role of GSNOR in immunity. The ubiquitous presences in plants of GSNOR regulate the redox statues of the most abundant antioxidant GSH, and unbalancing its redox situation may directly and/or indirectly regulate many signalling pathways within plant.

Paraquat (1,1'-dimethyl-4,4'-bipyridinium dichloride) is a non-selective, effective herbicide. It causes photooxidative stresses by accepting electrons from photosystem I and transferring them to molecular oxygens, and results in production of ROS, and paraquat is oxidized and recycled during this process (Babbs et al, 1989). Interestingly, GSNOR mutant, par2-1, has been found to be resistant to paraquat (Chen et al, 2009b). It has been suggested that GSNOR may act downstream of superoxide to regulate cell death signalling pathways. A later report has suggested that paraquat induced cell death is reduced by *rbohd* mutant (Straus et al, 2010). It has been demonstrated that RbohD activity is blunted by *S*-nitrosylation (Yun et al, 2011). In animal cell, knocking down NADPH oxidase activity has been reported to reduce paraquat induced cell death (Cristovao et al, 2009). Taken together, reduced RbohD activity in *gsnor1-3* may contribute largely in paraquat resistance phenotype of this mutant. Despite be reported in different

independent research, *hot5*, *par2-1* and *gsnor1-3* are the same loss of GSNOR function mutant due to mutation in *AtGSNOR1*.

1.4 NO function in plant immunity

Plant transcriptional co-activator Non-Expresser of Pathogenesis Related Gene 1 (NPR1) is a key regulator of the SA-dependent immune response (Loake & Grant, 2007). Loss of NPR1 function in *Arabidopsis* results in compromised SA signalling upon pathogen challenge or SA treatment, and further prevents induction of *Pathogenesis-Related* (*PR*) gene expression and SAR (Cao et al, 1994). Without pathogen challenge, NPR1 monomers form intermolecular disulphide bonds between conserved cysteine residues, promoting the formation of NPR1 oligomers in the cytosol (Mou et al, 2003). Furthermore, cytosolic localization of oligomer NPR1 suppresses its movement into the nucleus, thereby inhibiting its ability to promote binding between transcription factors *PR* genes and subsequent establishment of SAR.

After pathogen or elicitor induction, SA-induced redox changes promote reduction of intermolecular disulphide bonds and result in NPR1 monomer formation, this facilitates translocation of NPR1 from the cytoplasm into the nucleus, enabling target gene activation and NPR1-dependent immune responses (Fu & Dong, 2013). Further studies have revealed how NPR1 translocation is regulated by redox changes and NO (Mou et al, 2003; Tada et al, 2008). Two conserved Cys residues, Cys82 and Cys216, are responsible for intermolecular disulphide bond formation. Experiments have shown mutating both Cys residues results in constitutive nuclear localization of NPR1 monomers and *PR-1* expression (Mou et al, 2003). Later study revealed that reduction of Cys82 and Cys216 is catalysed by thioredoxins (TRXs), TRX-h3 and TRX-h5, which are induced by SA (Tada et al, 2008).

A later study suggested that another conserved Cys, Cys156, is also important in facilitating NPR1 oligomerization (Tada et al, 2008). Cys156 has been reported to be *S*-nitrosylated by GSNO, such modification facilitates its oligomerization by promoting disulphide bond formation (Fig 1.4). Interestingly, mutation of Cys156 leads to constitutively nuclear localization of NPR1 monomer and enhanced resistance against *Pseudomonas syringae pv. maculicola* ES4326 (*Psm* ES4326).

However, after SA treatment, unlike wild type plants, Cys156 mutant plants fail to show enhanced immunity as Cys156 NPR1 is depleted 48 hours after SA treatment (Tada et al, 2008). As NPR1 oligomerization is mediated by *S*-nitrosylation of Cys156, these findings suggest that *S*-nitrosylation of Cys156 is important in maintaining NPR1 homeostasis, and further, promoting a sustained immune response. In the *gsnor* mutant, an increased total SNO level was found and SA signalling was blunted; it was proposed that a high SNO environment would promote *S*-nitrosylation of NPR1 thus driving its oligomerization, resulting in compromised SA-dependent immunity (Feechan et al, 2005). GSNOR does not directly reduce *S*-nitrosylated proteins. Rather, recent data has suggested that Thioredoxin-h5 (TRX-h5) is involved in converting SNO in NPR1 into thiols, thus reversing the effect of *S*-nitrosylation (Kneeshaw et al, 2014). Conversely, it has been reported that exogenous 100 μM GSNO treatment can promote nuclear localization of NPR1 (Lindermayr et al, 2010). Further, NO has also been reported to induce defence gene expression (Durner et al, 1998). These contradictory findings may suggest the physiological deference between whole plant and protoplast studies. Also, the impact of exogenous NO addition has been scored at relatively late time points, thus the impact of NO in these cases might be indirect.

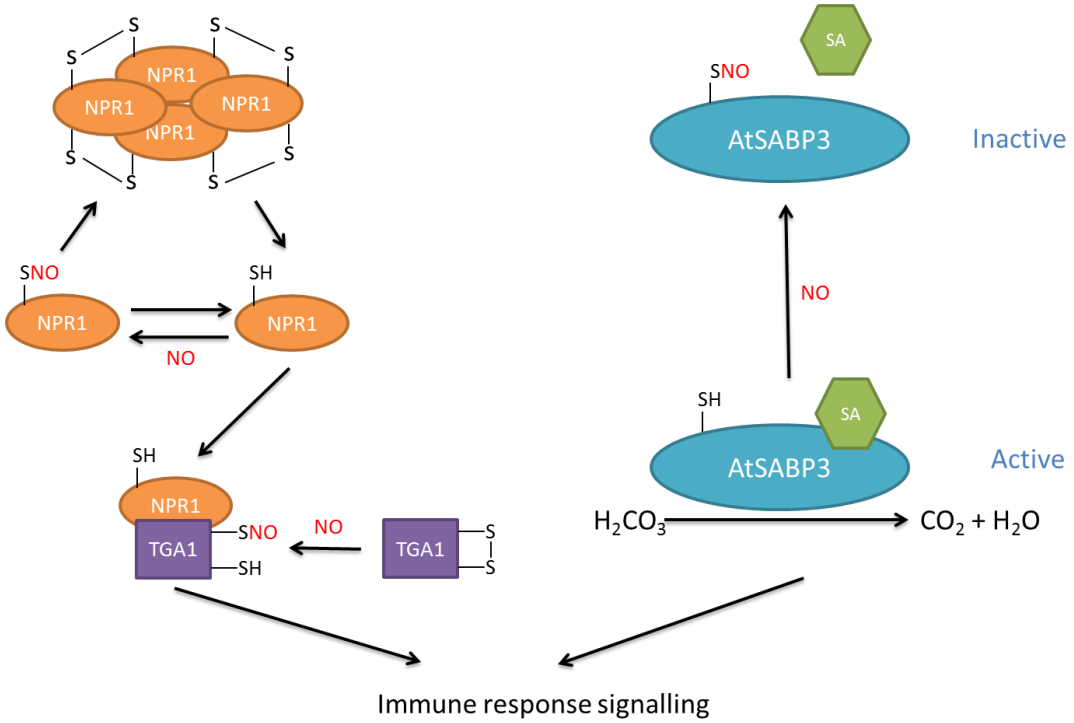

Figure 1.4. Role of NO and *S*-nitrosylation in plant immunity. Reduction of NPR1 oligomer to

monomer is important for NPR1 activity, and NPR1 oligomer-monomer homeostasis is important for plant immunity (Mou et al, 2003). In addition, NPR1 monomer is reported to bind TGA transcription factors to establish plant immunity in nucleus (Zhou et al, 2000). *S*-nitrosylation on NPR1 Cys156 has been reported to facilitate oligomerization of NPR1, which is vital to maintain NPR1 homeostasis and further establish proper NPR1 dependent plant defence (Tada et al, 2008). Adddtionally, *S*-nitrosylation of TGA1 has been reported to protect TGA1 from oxidative burst damage (Lindermayr et al, 2010). AtSABP3 is a positive regulator in plant immunity and is reported to have carbonic anhydrase activity and ability to bind SA. *S*-nitrosylation of *Arabidopsis* SABP3 abolishes its SA binding and the carbonic anhydrase activity which negatively regulate plant immunity (Wang et al, 2009b).

Nuclear localized NPR1 has been reported to interact with a subclass of basic leucine zipper transcription factors (TFs) / TGACG motif binding factors (TGAs), promoting them to bind the promoter region of *PR* genes (Zhang et al, 1999). *In vitro* assays have shown that TGA1 is S-nitrosylated and S-glutathionylated at Cys260 and Cys266 by GSNO respectively. It has been suggested these NO mediated modifications protect TGA1 from oxygen mediated modification, as well as enhancing DNA binding affinity to *as-1* elements (Lindermayr et al, 2010). Further, two other Cys residues, Cys172 and Cys287, have been suggested to be important in TGA1 activity. In non-reducing electrophoresis, a low mobility band has been observed in TGA1 protein with C260 and C266 mutations, suggesting intramolecular disulphide bond formation between C172 and C287. Interestingly, no disulphide bond formation was observed in the C172 and C287 double mutant. Further, *tga1 tga4* knock-out plants transformed with TGA-C172S/C287S mutants showed hyper-expression of the defence genes *PR-2* and *PR-5*, suggesting reduction of these Cys residues are important for TGA1 activity, as the mutants mimic their reduced states (Lindermayr et al, 2010). However, these findings are inconsistent with previous research that suggests TGA1 binding activity is not affected by redox regulation (Despres et al, 2003).

Salicylic acid binding protein 3 (SABP3), found in tobacco, has been reported to be a chloroplast localized carbonic anhydrase (CA), which exhibit both SA binding and CA activity (Slaymaker et al, 2002). In many plant species, CA activity is known to be required in lipid biosynthesis (Hoang

& Chapman, 2002). Additionally lipid-based molecules have been reported to be involved in NPR1 independent, jasmonic acid (JA) and SA related defence pathways (Kachroo et al, 2001). Recently, SABP3 in *Arabidopsis* has been shown can be S-nitrosylated both *in vitro* and *in vivo* at Cys280 (Wang et al, 2009b) (Fig 1.4). In *gsnor* plant, SABP3 is highly S-nitrosylated due to high SNO cellular environment. Further, both SA affinity and CA activity of SABP3 were blunted by *S*-nitrosylation. By investigating the pathogen resistance of *SABP3* knock-out plants, the growth of *Pst* DC3000 (*avrB*), which is known to trigger a strong SA response, was increased compare to wild type plants, suggesting a positive role of SABP3 in the SA dependent immune response (Wang et al, 2009b). Taken together, these data suggested *S*-nitrosylation of SABP3 would negatively regulate plant immunity.

1.5 NO function in the hypersensitive response (HR)

Upon detection of pathogen virulence factors, plants initiate programmed cell death called HR cell death to mount defence (Greenberg & Yao, 2004). It has been reported that during pathogen challenge, HR cell death is driven by reactive oxygen species (ROS) synthesized by NADPH oxidase and NO generated from nitrosative burst (Delledonne et al, 1998; Yun et al, 2011).

Analysis on the phenotypes of *Arabidopsis GSNOR* mutant during pathogen challenge suggested that GSNOR can govern the cellular SNO level and development of HR cell death (Yun et al, 2011). In *gsnor1-3,* where SNO concentration is elevated compared to wild type plants, although both total and free SA level are reduced, HR cell death is accelerated. Further, this phenotype is consistent in both *gsnor1-3* and *gsnor1-3 SA induction deficient 2 (sid2)* double mutant plants, where SA synthesis is compromised. In contrast, HR cell death is delayed and reduced in *gsnor1-1*, where SNO concentration is lower compared to wild type. Thus, increasing SNO levels promote cell death independent of SA (Yun et al, 2011).

SA has been shown to be involved in plant defence against biotrophic pathogens like *Erysiphe* and *Pseudomonas syringae* (Wildermuth et al, 2001). However, although the SA level is strikingly reduced in *gsnor1-3* and *gsnor1-3 sid2* double mutant plants, both plants showed increased resistance against an avirulent oomycete *Hyaloperonospora arabidopsidis* Emwa1 due to the

accelerated development of cell death (Yun et al, 2011). These results suggested high cellular SNO may drive biotrophic pathogen resistance even in the presence of low SA levels and a weak SA-dependent immunity environment.

Production of ROS in plants following pathogen recognition is catalysed by NADPH oxidases (AtRBOH), and a regulatory role of NO on these enzymes was investigated. Analysis has shown translation of RbohD is not affected by cellular SNO levels upon pathogen challenge, but *in vivo* and *in vitro* assays suggested enzyme activity is inhibited by NO modification. Further investigation suggested a conserved cysteine, Cys890, is S-nitrosylated. By computer modelling, C890 is believed to be important in binding a co-factor, Flavin adenine dinucleotide (FAD). *S*-nitrosylation of C890 results in disruption of FAD binding, reducing ROS synthesis (Yun et al, 2011). Thus, NO regulation on C890 has been suggested to function as a negative feed-back loop in the later stage of the HR (Fig 1.5).

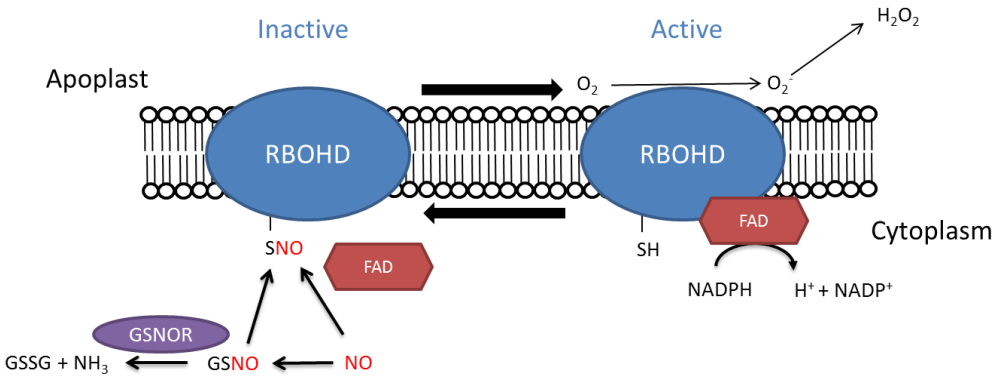

Figure 1.5. *S*-nitrosylation regulates activity of NADPH oxidase RBOHD that regulate oxidative burst during plant-pathogen interaction. *S*-nitrosylation on RBOHD C890 blocks its binding of the essential co-factor FAD, and blunt its activity in synthesizing reactive oxygen species (ROS)(Yun et al, 2011).

Peroxiredoxin II E (PrxII E) has been shown to be S-nitrosylated a few hours after pathogen infection (Romero-Puertas et al, 2007). PrxII E functions in detoxifying peroxynitrite, and *S*-nitrosylation of PrxII E abolishes its activity. Further, this event has been shown to synchronize

with accumulation of peroxynitrite in plants after avirulent pathogen challenge (Gaupels et al, 2011). Peroxynitrite has been suggested to be the substrate in tyrosine nitration (Vandelle & Delledonne, 2011) and nitrated proteins are known to be elevated in plant defence (Cecconi et al, 2009). Although the majority of the evidence is circumstantial NO may *S*-nitrosylate PrxII E to enhance the impact of its own derivative, peroxynitrite, during HR cell death development and further influence tyrosine signalling.

1.6 NO regulating transcription factors (TFs) activity

Apart from TGA1, NO has been reported to regulate activities of other TFs in plant (Serpa et al, 2007). AtMYB2, a typical R2R3 MYB transcription factor, has been reported to be S-nitrosylated at a conserved Cys53, resulting in blunted binding activity. Another R2R3 MYB, maize P1 protein, has an additional Cys49. It has been reported that an intramolecular disulphide bond formation between Cys49 and Cys53 under non-reducing condition, which inhibits P1 activity (Heine et al, 2004). Thus, *S*-nitrosylation on AtMYB2 Cys53 may mimic this inhibitory function in P1 protein.

2. Salicylic acid

2.1 Salicylic acid, a brief introduction

2.1.1 A historical view of SA

Salicylic acid (SA, 2-hydroxy benzoic acid) is one of a variety of phenolic compounds, consisting of an aromatic ring bearing a hydroxyl group or its functional derivative, produced in plants. Traditionally, plant phenolic acids were considered as non-essential or waste products. Until recently, SA was regarded as a secondary metabolite (Hadacek et al, 2011).

Before the physiological functions of SA have been recognized, the medical uses of SA have been studied for centuries. Since 5th century B.C., it has been known that chewing the salicylate-rich willow leaf and bark provides pain relief and Native Americans use compresses containing willow bark extract for the same purpose (Vlot et al, 2009). Later, the chemical essence of the folk remedy has been identified. A yellowish substrate salicin was isolated from willow bark and then

converted into a sugar and an acid named salicylic acid. Due to its pain relief effect, SA was in high demand. In the late 19th century, SA and its derivative acetyl salicylic acid (ASA) was successfully chemically synthesized and later brought to market with the trade name "Aspirin". To date, Aspirin is considered as one of the most successful drugs worldwide.

2.1.2 SA function in plants

Nowadays, SA has been recognized as an important signalling molecule in plant growth, development and immunity (Rivas-San Vicente & Plasencia, 2011; Vlot et al, 2009). In salicylic acid deficient plants, flowering time is delayed, and UV-C irradiation has been reported to induce *Arabidopsis* flowering in an SA dependent manner (Mart ńez et al, 2004). Additionally, study of a loss of function mutant, *siz1*, a SUMO E3 ligase, has revealed that *siz1* plants exhibit an early flowering phenotype due to elevated SA levels (Jin et al, 2008). This evidence has suggested SA may have function in the plant flowering process. SA also has been reported to regulate heat production in plants. SA was isolated from the male flower of *Sauromatum guttatum* Schott (Voodoo lily), which is a thermogenic plant. Exdogenously applying SA to a plant's appendix induced a rise in temperature (Raskin et al, 1987).

The major function of SA has been recognized as a key signalling molecule in establishment of disease resistance. First, studies on transgenic or mutant plants, which were transformed with a bacterial SA-degrading salicylate hydroxylase (*nahG*) gene (Delaney et al, 1994; Gaffney et al, 1993) or with mutations in SA synthesis genes (Nawrath & Metraux, 1999), have shown their enhanced susceptibility to both virulent and avirulent pathogens. Significantly, the resistance of these plants was restored by treatment of SA or its analogs. Second, SA treatment prior to pathogen inoculation has been proven to enhance plant resistance and further analysis revealed SA treatment can induce *PR* gene expression (Cao et al, 1994).

In addition to localized defence, SA has been known to function in SAR (Fu & Dong, 2013; Vlot et al, 2009). Studies on SA deficient mutants also showed they failed to establish SAR (Delaney et al, 1994; Gaffney et al, 1993; Nawrath & Metraux, 1999). Although SA itself is not be considered as a mobile signalling molecule for SAR, methyl salicylate (MeSA) has been put forward as a

possible signal (Park et al, 2007), although another reports have questioned this (Attaran et al, 2009).

2.2 SA receptors in plants

As mentioned above, SABP3 is a protein with high affinity for SA and CA activity. In addition, four SA receptors have been identified in tobacco (Vlot et al, 2009). SABP1 has been identified as a catalase, and its H_2O_2 degrading activity was inhibited by SA after binding. (Chen et al, 1993). Ascorbate peroxidase (APX), a key enzyme scavenging H_2O_2, activity has been shown to be inhibited by SA (Durner & Klessig, 1995). These data implies that SA may promote H_2O_2 accumulation by inhibiting multiple H_2O_2 degrading enzymes during oxidative burst. SABP2 is a methyl salicylate esterase with higher affinity to SA (Du & Klessig, 1997; Forouhar et al, 2005). Previous report has suggested SABP2 is responsible in converting MeSA to SA. Further, binding between SA and SABP2 inhibits SABP2 activity (Forouhar et al, 2005), and it has been suggested that SABP2 is required to establish SAR in tobacco (Park et al, 2007).

NPR1, a master gene in regulating plant defence, has been suggested to serve as a SA binding protein (Wu et al, 2012). Along with copper, Cys521 and Cys529 of NPR1 have been found to be required for the *in vitro* binding of SA. Additionally, mutation in Cys521 and Cys529 abolished its copper binding ability (Rochon et al, 2006). It has been suggested that SA binding of NPR1 is required for NPR1 oligomer dissociation (Wu et al, 2012). However, lack of crystal structure data makes this hypothesis debatable. Recently, NPR3 and NPR4 have been reported to be SA receptors in *Arabidopsis* (Fu et al, 2012). NPR3 and NPR4 were isolated as negative regulators in plant immunity (Zhang et al, 2006) and function in a NPR1 dependent manner. Both NPR3 and NPR4 interact with NPR1 and drive its degradation, a process mediated by SA. It has been reported that binding of SA to NPR3 facilitate its interaction with NPR1, in contrast, the constitutive interaction between NPR4 and NPR1 is disrupted by binding of SA to NPR4 (Fu et al, 2012).

2.3 SA synthesis in plants

Two distinct biosynthesis pathways have been uncovered for SA (An & Mou, 2011; Dempsey et

al, 2011)(Fig 1.6), one is the isochorismate synthase (ICS) mediated isochorismate pathway and the other is the phenylalanine ammonia-lyase (PAL) mediated phenylalanine pathway. Both pathways use chorismate as substrate. However, both pathways are not fully characterized.

Isotope feeding research in the 1960s has suggested two possible routes to synthesize SA from phenylalanine depending on the plant species. PAL is the first enzyme identified in this pathway. PAL is known to catalyse the reaction that converts phenylalanine (Phe) to trans-cinnamic acid (t-CA). Subsequently, t-CA is hydroxylated to form O-coumarate (Chadha & Brown, 1974; El-Basyouni et al, 1964) and its side chain is oxidized to form SA. Alternatively, the side chain of t-CA can be oxidized to form benzoic acid (Klämbt, 1962) and SA is yielded by following hydroxylation. The difference between the two pathways is the order of aromatic ring hydroxylation and side chain-shortening reactions.

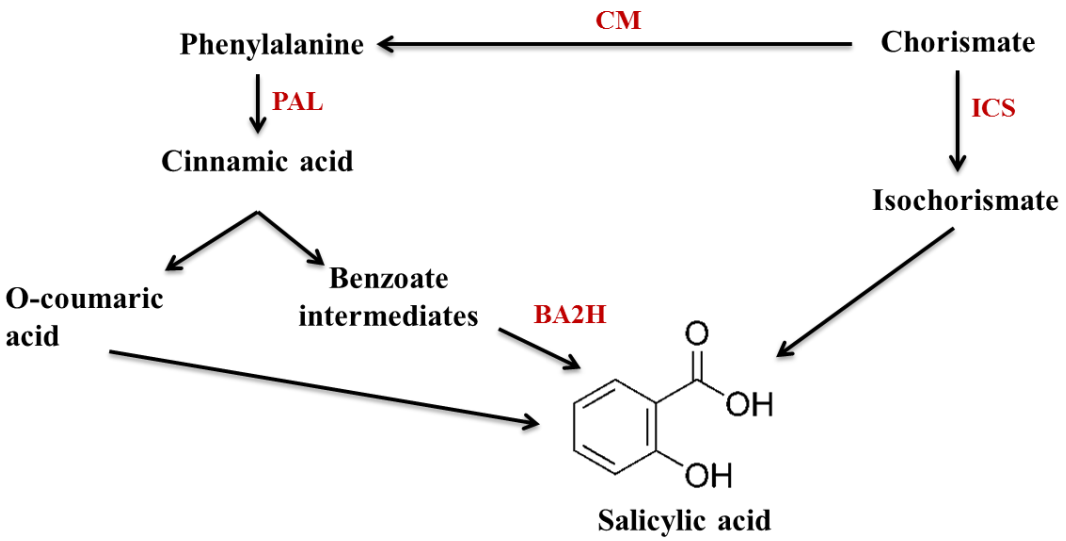

Figure 1.6. Current knowledge of SA synthesis pathways in *Arabidopsis*. Both chorismate and phenylalanine pathways are presented in Arabidopsis and use chorismate as initial substrate. The ICS mediated pathway plays a major role in *Arabidopsis* (Wildermuth et al, 2001), although the PAL pathway plays a minor role, its impact in *Arabidopsis* has been noticed (Huang et al, 2010). Unlike isochorismate pathway, several intermediates and synthesis routes have been found in PAL pathway. However, neither pathway has been fully resolved.

PAL is a key regulator of the phenylalanine pathway and also plays an important role in SA biosynthesis during the immune response. Four *PAL* genes are found in Arabidopsis, with different kinetic and functional properties (Cochrane et al, 2004). Mutations in all four *PAL* genes result in stunted and sterile plants and the quadruple mutants accumulate reduced levels of SA both at basal level and upon pathogen infection. Further, this line showed increased susceptibility to avirulent *Pseudomonas syringae* (Huang et al, 2010). However, the quadruple mutant still exhibited 10% of wild-type PAL activity, suggesting a leaky *pal* mutation or the presence of an unknown *PAL* gene. The importance of PAL in plant defence was also suggested in previous research, in the study of interaction of Arabidopsis and *Hyaloperonospora arabidopsidis*, when expression of *PAL* is reduced plants become vulnerable to oomycete infections. Also, exogenous application of PAL inhibitor results in increased susceptibility and reduced accumulation of SA. Further, treatment of SA can recover plant defence. These findings suggest the importance of *PAL* in localized defence against oomycete infection (Mauch-Mani & Slusarenko, 1996).

Some bacteria are known to synthesize SA from chorismate via a two-step enzymatic reaction. First, chorismate is isomerized to isochorismate (IC) by ICS, and IC is converted to SA and pyruvate by pyruvate lyase (IPL) (Mercado-Blanco et al, 2001; Serino et al, 1995). In bacteria like *Pseudomonas aeruginosa* and *Pseudomonas fluorescens*, this reaction is catalysed by two unifunctional enzymes, in contrast, a bifunctional enzyme that exhibit both ICS and IPL activity was found in *Yersinia enterocolitica* and *Mycobacterium tuberculosis*, this enzyme has been termed as SA synthase (SAS) (Harrison et al, 2006; Pelludat et al, 2003). In addition, transgenic plants that overexpress both bacterial *ICS* and *IPL* exhibit elevated levels of SA and increased pathogen resistance, indicating plants are capable to synthesize SA from chorismate by using these enzymes (Verberne et al, 2000).

A genetic study has confirmed the presence of a similar SA biosynthesis pathway in plants (Wildermuth et al, 2001). A mutant, *sid 2*, has been identified in *ICS1*. This mutant's phenotype includes accumulation of only 5-10% of SA compared to wild type. *sid2* plants are also susceptible to pathogen infection and are compromised in SAR. Further, exogenous SA treatment

may restore their resistance. Taken together, these findings suggested the ICS mediated pathway is the major pathway in pathogen induced SA synthesis (Wildermuth et al, 2001). Further, the importance of the ICS-mediated SA synthesis pathway has been highlighted in tobacco (Catinot et al, 2008) and tomato (Uppalapati et al, 2007).

Two isochorismate synthase genes, *ICS1* and *ICS2*, have been identified in *Arabidopsis*. Like *ICS1*, *ICS2* also encodes a functional isochorismate synthase. Mutant analysis on *ics1*, *ics2* and *ics1 ics2* revealed that *ICS2* also participates in Arabidopsis SA synthesis, but its contribution can only be detected in *ICS1* knock out. Upon UV irradiation, compared to wild type plants, the *ics1* mutant accumulated 10% of the expected SA level, and *ics1 ics2* double mutant accumulated about 4%. These findings not only indicate a minor role of ICS2 in ICS-mediated SA synthesis, but also the presence of a ICS independent SA synthesis pathway (Garcion et al, 2008). Further biochemical analysis has confirmed that ICS1 is a chloroplast localized enzyme; synchronized with the fact that the chloroplast is the major organelle of SA synthesis. Recombinant AtICS1 has been shown to convert chorismate into isochorismate *in vitro*, which suggested ICS1 is a unifunctional enzyme (Strawn et al, 2007). Although accumulated data suggested SA is synthesized in multiple plant species through the ICS-mediated pathway, the mechanism of converting IC into SA is still unclear. No IPL-like gene has been identified in *Arabidopsis*, thus half of the biochemical pathway is still unexplained.

2.4 Regulation of SA synthesis

Mutant screening has revealed many factors that regulate SA accumulation. Both positive and negative regulators have been identified that function in SA synthesis and those regulators include transcription factors, transporters and signalling modulators.

Enhanced Disease Susceptibility 1 (EDS1) and Nonspecific Disease Resistance 1 (NDR1) are proteins that required for induction of ETI. EDS1 has been shown to be required preferably by R proteins with a toll-interleukin-1 receptor (TIR) domain, and NDR1 is mainly required by R proteins with coiled-coil (CC) domain (Aarts et al, 1998). The putative lipase like protein, EDS1, has been reported to physically interact with its partners, Phytoalexin Deficient 4 (PAD4) and

Senescence Associated Gene 101 (SAG101) (Feys et al, 2001; Feys et al, 2005). A previous report placed EDS1 upstream of SA synthesis as *eds1* is not able to induce an SA dependent response upon pathogen infection (Falk et al, 1999). Further study on both *eds1*, *pad4* mutants plants showed there are unable to induce SA synthesis in both *P. syringae* pv. *tomato* DC3000 and DC3000/avrRps4 infection (Feys et al, 2001). In addition, SA treatment can induce defence gene expression in *eds1* and *pad4* mutants and enhance *EDS1/PAD4* expression in wild type, suggesting SA positively regulate EDS1 and PAD4 via a feedback loop (Feys et al, 2001; Zhou et al, 1998). NDR1 is another positive regulator which is independent from EDS1 mediated ETI. Previous research has shown the *ndr1* mutant has reduced SA accumulation in response to UV treatment and impaired *PR1* expression and SAR induction upon *P. syringae avrRpt2* infection (Shapiro & Zhang, 2001).

Transcription factors have been identified that regulate *ICS1* expression and thus impact on SA synthesis. Ethylene Insensitive 3 (EIN3) and EIN3-Like 1 (EIL1) are known as positive regulators of ethylene responses. A recent study suggested these transcription factors also function as negative regulators in SA synthesis (Chen et al, 2009a). The double mutant *ein3 eil1* shows elevated levels of SA without pathogen infection, enhanced pathogen resistance and constitutive expression of *PR1*, *PR2* and *ICS1*. In addition, a triple mutant *ein3 eil1 sid2* restored its susceptibility to pathogens. Further, EIN3 has been shown to specifically bind the P5 fragment of the *ICS1* promoter sequence *in vitro*. *In vivo*, removing this fragment from *ICS1* promoter resulted in increased *ICS1* promoter activity in wild type plants, but not in the *ein3 eil1* double mutant, suggesting EIN3 and EIL1 may play a role in cross-talk between ethylene and SA (Chen et al, 2009a).

NAC (petunia NAM and *Arabidopsis* ATAF1, ATAF2 and CUC2) transcription factors have been shown to be involved in negative regulation of *ICS1* expression during *P. syringae* infection (Zheng et al, 2012). During *P. syringae* infection, three NAC transcription factor genes, *ANAC019*, *ANAC055* and *ANAC072*, have been shown to be up-regulated. In the *nac* triple mutant, the basal expression of *ICS1* increased compared to wild type plants. Additionally, a ChIP assay has revealed that ANAC019 binds the ICS1 promoter directly *in vivo* (Zheng et al, 2012). It has been

reported that ANAC019, ANAC055 and ANAC072 share the same *cis*-element in a protoplast assay (Tran et al, 2004). Thus, it is reasonable to believe these three NAC transcription factors may all act as negative regulators in *ICS* expression.

Two positive regulators, Calmodulin-Binding Protein 60-like g (CBP60g) and SAR-Deficient 1 (SARD1), have been identified recently (Zhang et al, 2010). CBP60g and SARD1 appear to act redundantly as only the *sard1 cbp60g* double mutant, not the single mutants, exhibit a reduced SA level upon both virulent and avirulent pathogen infection. Further, the double mutant is also compromised in PTI, ETI and SAR (Wang et al, 2011; Zhang et al, 2010).

On the other hand, overexpression of *SARD1* results in elevated SA levels, SA-dependent gene expression and enhanced disease resistance (Zhang et al, 2010). Further analysis revealed SARD1 and CBP60g share the same binding motif on the *ICS1* promoter -1110 to -1290, with the highest binding affinity to the sequence GAAATTTTGG. A number of W-box motifs, which is the binding motif for WRKY transcription factors, are present on the *ICS1* promoter. Recently, in a protoplast assay, overexpression of *WRKY28* has been shown to enhance the expression of the *ICS::GUS* reporter (van Verk et al, 2011). A gel-shift assay indicated that WRKY28 binds the *ICS1* promoter at position -445 and -460. Additionally, mutations in these motifs result in reduced *ICS1* expression (van Verk et al, 2011).

The newest transcription factors identified to regulate *ICS1* are TCP8 and TCP9 (Wang et al, 2015b). It has been reported that expression of *ICS1* is significantly reduced in *tcp8 tcp9* double mutants during the immune response. The binding between TCP8 and *ICS1* promoter was confirmed both *in vitro* and *in vivo*. Interestingly, TCP8 was found to interact with the majority of the currently known transcription factors which regulate *ICS1* expression, suggesting a potential complex coordinated regulatory mechanism orchestrating *ICS1* expression (Wang et al, 2015b).

SA induction deficient 1 (*sid1*), also known as *Enhanced disease susceptibility 5* (*eds5*) has been shown to have reduced SA accumulation upon UV and pathogen induction, as well as increased susceptibility to pathogens (Nawrath et al, 2002). Studies revealed that EDS5 belongs to the

multidrug and toxin extrusion (MATE) transporter family which is presented in both prokaryotic and eukaryotic cells. A recent study has suggested that EDS5 is the transporter to export SA from chloroplasts into the cytosol, where SA functions to control immune responses. In the *eds5* mutant SA is thought to be trapped inside the chloroplast which inhibits its synthesis via a feedback loop and results in reduced SA levels in plants (Serrano et al, 2013).

3. Project aims

NO is known to regulate the plant immune response on multiple levels (Frederickson Matika & Loake, 2014; Skelly & Loake, 2013; Yu et al, 2014). Previous reports suggested in gsnor1-3 plants, elevated cellular SNO not only compromised SA signalling, but also impaired SA synthesis, resulting in a low SA level (Feechan et al, 2005). The ICS1 mediated pathway is responsible for pathogen induced SA synthesis (Dempsey et al, 2011; Vlot et al, 2009). Thus, it is reasonable to assume a high SNO content may influence either expression of the *ICS1* gene or activity of ICS1 protein. The aim of this project is to investigate the possible link between the high cellular SNO environment and SA synthesis and provide more depth of understanding of how NO regulates plant immunity.

Chapter 2 Material and Methods

1. Plant material and *E. coli* strains

Arabidopsis accession Col-0 and *gsnor1-3* were grown under 16 h of light at 22 ℃ and 8 h of darkness at 18 ℃. *E. coli* strain DH5α was used for normal plasmid propagation, *E. coli* strain Rosetta^{TM} 2 (DE3) was used for recombinant protein expression. Agrobacterium strain GV3101was used to transform *Arabidopsis*. Bacteria strains were normally cultivated in LB (10 g/L tryptone, 5 g/L yeast extract, 10 g/L NaCl) medium with antibiotics. For protein expression, terrific broth (TB) medium (12 g/L tryptone, 24g/L yeast extract, 4 mL/L glycerol, 10% potassium phosphate) with antibiotics (Rosetta^{TM} 2 (DE3), 25 ug/mL Chloramphenicol) was used.

2. Preparing pathogen and plant leaf samples

The bacterial strain *Pseudomonas syringae* ES4326 was used to induce plant immune response. Bacteria was grown at 30 ℃ overnight and diluted with $MgCl_2$ until OD at A_{600}=0.002. 1 mL of this bacteria preparation was used to inject into the whole mature leave of 4 week old *Arabidopsis* using a needless syringe. Infected leaves were collected 9 hour after infection, weighed, snap frozen in liquid nitrogen and stored at -80 ℃ for future use.

3. Plant RNA extraction and cDNA synthesis

Leave samples were ground to fine powder in liquid nitrogen, afterwards the powder was suspended in Trizol^{TM} (100 mg tissue/ mL Trizol^{TM}). The suspension was spun down at 12000 g for 5 min at 4 ℃, the supernatant was collected and transferred into new Eppendorf tube. Chloroform (200 μL/ mL Trizol) was added into supernatant, and the mixture was shaken and incubated at room temperature for 3 minutes. After incubation, the mixture was centrifuged at 12000 g for 15 minutes at 4 ℃. After centrifugation, the aqueous phase was transferred to a new Eppendorf tube. 0.5 mL of isopropyl alcohol was added into Eppendorf and was mixed, the mixture was then incubated at room temperature for 10 minutes. Then the mixture was centrifuged at 12000 g for 10 minutes at 4 ℃. After incubation, the supernatant was removed, 1 mL 75% ethanol was added to wash the pellet, followed by 5 min centrifuge at 12000 g. After

centrifugation, the supernatant was removed again and the pellet was left air dry. The dry pellet was dissolved in 20 µL of RNase-free water. The quantity of RNA was determined by NanoDrop. RNA preparation was stored at -20 ℃ until further use. Plant cDNA was synthesized using RevertAid First Strand cDNA synthesis Kit (Thermo Scientific) and 100 ng RNA sample as template via PCR.

4. Primer design

Sequence of primers used in this study

AtICS1 primer in pET28a

Forward: ATCGTCGACCCATATGAATGGTTGTGATGGA

Reverse: ATCGTCGACTCAATTAATCGCCTGTAGAGA

CBP60g Gateway cloning primers:

attB1:

GGGGACAAGTTTGTACAAAAAAGCAGGCTTCATGAAGATTCGGAACAGCCCTAGTTTT

attB2:

GGGGACCACTTTGTACAAGAAAGCTGGGTCCTATTACAAGCCTTCCCTCGGATTTCTG

SARD1 Gateway cloning primers:

attB1

GGGGACAAGTTTGTACAAAAAAGCAGGCTTCATGGCAGGGAAGAGGTTATTTCAAGA

attB2

GGGGACCACTTTGTACAAGAAAGCTGGGTCCTATTAGAAAGGGTTTATATGATTTTGAG

ACGAAGAT

ICS1 Gateway cloning primers:

attB1

GGGGACAAGTTTGTACAAAAAAGCAGGCTTCATGGCTTCACTTCAATTTTCTTCTCAG

attB2

GGGGACCACTTTGTACAAGAAAGCTGGGTCCTATTATTGTGAGAACCCCTTATCCCCCA

TACA

M13 sequence primer sets (for pDONR221)

Forward: GTAAAACGACGGCCAG

Reverse: CAGGAAACAGCTATGAC

ICS1 sequence primer sets:

Forward 1: ACAGGTTCCAATTGACCAGC

Forward 2: TGCATTTTACTTTTCAGTCCCTC

Forward 3: TGGCTAGCACAGTTACAGCG

Forward 4: CAGGGAGACTTACGAAGGAAGA

Sard1 sequence primer set:

Forward 1: ACAGGGAGTAAAATCAGTGACG

Forward 2: TTGTGGTTTGTGAAGCGATG

Forward 3: TGAAAGCACTTATCGATGGTCA

CBP60g sequence primer set:

Forward 1: CTTGTGATCGAGCTCGTGG

Forward 2: CCCAGTGATGAGGTTTGGAG

Forward 3: CAGCGGTTAACGATAGGACC

Forward 4: CTCAAGCTGGTCACCTGGTA

ICS1 promoter Gateway cloning primers:

AttB1:

GGGGACAAGTTTGTACAAAAAAGCAGGCTCTTGTTGAATTATGGTTTCATTCTATTGGA

TTATCT

AttB2:

GGGGACCACTTTGTACAAGAAAGCTGGGTTGCAGAAATTCGTAAAGTGTTTCTTGAAG

A

ICS1 EMSA fragment

Forward: TATGTACTTGGTGAGCCGTC
Reverse: AGGAATATTTGCTTTAATTTCATG

5. Quantitative RT-PCR analysis

Quantitative RT-PCR experiments were performed using Roche LightCycler® 480 system and LightCycler® 480 SYBR Green I Master, according to the protocols of the manufacturer (10 μL qRT-PCR reaction contains 5 μL of master, 1 μL forward primer, 1 μL reverse primer, 1 μL cDNA template and water). The thermal cycler program was 95 ℃ for 10 mins (denaturing), followed by 45 cycles of 95 ℃ for 10 sec, 58 ℃ for 15 sec and 72 ℃ for 15 sec, and the melting curve was set to be 95 ℃ for 5 sec and 65 ℃ for 1 min. *ACTIN2* was used as the internal reference.

6. Vector construction

Plant *ICS1*, *SARD1* and *CBP60g* were amplified from cDNA using designed primers via PCR using Pfu polymerase (Promega) (25 μL PCR reaction contains 1 μL DNA template, 4 μL 2.5 mM dNTP, 2.5 10X buffer, 1 μL polymerase, 1 μL forward primer, 1 μL reverse primer and water) at T_A=55 ℃ and elongation time for 4 mins, 40 cycles. The PCR products were examined using 1% agarose gel, the bands with right size were cut out under UV. And amplified PCR fragment was obtained using gel extraction method. To begin with, the cut-out gel was dissolved in approx. 500 μL of buffer QG (Qiagen) and was incubated at 65 °C until the gel was fully dissolved. The rest of purification steps were performed using PCR purification kit from Thermo Scientific. Briefly, the solution was passed through a spin column at maximum speed for 2 mins, the flow-through was

removed, the column was washed twice using wash buffer as the protocol suggested, and the purified PCR product was eluted with 30 µL of Milli-Q water. Purified PCR products were stored at -20 ℃.

For recombinant ICS1 construct, the purified PCR product and pET-28α were digested with *Nde*I and *Sal*I (Total amount of 40 µL of digesting reaction contains 10 µL of DNA, 1 µL of each digest enzyme, 4 µL of 10X buffer and water) at 37 °C for 1 hour. Digested products were examined on 1% agarose gel and fragments were cut out and purified. Purified products were ligated using T4 DNA ligase (Sigma) (A 15 µL ligation reaction contains of 7 µL insert, 3 µL digested vector, 1.5 µL ligation buffer, 1 µL of T4 ligase and water) at room temperature for a minimum of 1 hour. Ligation products were transformed to *E. coli* DH5α competent cells. For transforming DH5α, 10 µL of ligation product was added into 100 µL of thawed competent cells, after 10 minutes incubation on ice, the cells were heat shocked at 42 ℃ for 90 sec followed by incubating on ice for 5 mins, afterwards 1 mL LB medium was added into cell and incubate at 37 ℃ for 1 hour. After incubation, Transformed DH5α was selected by LB Agar plate containing 50 µg/ mL kanamycin. After overnight incubation, successful transformants were picked up and tested by colony PCR (Crimson taq polymerase, NEB) using gene specific primers. Transformed colonies confirmed via PCR were incubated in 5 mL LB medium with 50 µg/ mL kanamycin at 37 ℃ overnight. After incubation, the plasmid was extracted using Miniprep kit from ThermoScientific, the insert was confirmed by PCR. After PCR confirmation, the plasmid was sequenced to confirm its integrity. The sequenced plasmid was subsequently transformed into Rosetta^{TM} 2 (DE3) competent cells (GE Healthcare) for protein expression work.

For recombinant SARD1 and CBP60g, the purified PCR product was inserted into an entry vector (pDONR221 (Invitrogen)) via BP reaction (5 µL reaction contains 2 µL insert, 2 µL pDONR221, 1 µL BP clonase) and incubated at room temperature 2 hours. The reaction product was transformed into DH5α and selected on LB Agar plate with 50 µg/ mL kanamycin at 37 °C overnight. Colonies were evaluated using colony PCR with gene specific primers. Plasmids were obtained afterwards by miniprep and the sequence was confirmed by sequencing. After completing entry vector, the LR reaction was performed (5 µL reaction contains 2 µL entry clone,

2 μL destination vector, 1 μL LR clonase) to transfer insert into destination vector pDEST17 and pDEST-HisMBP (Addgene plasmid #11085)(Nallamsetty et al, 2005) vector and subsequently transformed into DH5α. Transformed cells were selected on LB agar plates with 100 μg/ mL ampicillin. And the complete plasmid was subsequently taken out from DH5α and transformed into Rosetta™ 2 (DE3) and BL21 pLysS cells for protein expression.

For overexpression ICS1, SARD1 and CBP60g in *Arabidopsis*, the similar Gataway cloning procedure was performed using pEarlyGate 202 (Earley et al, 2006) as destination vector. The completed plasmids in DH5α were selected on LB agar plates with 50 μg/ mL kanamycin. Afterwards plasmids were transformed into agrobacterium GV3101 and selected on LB agar plates with 100 μg/ mL rifampcin, 25 μg/ mL gentamycin, 50 μg/ mL kanamycin and 1 μg/ mL tetracycline. For transformation agrobacterium, the competent cells were thawed on ice for 30 minutes, 10 μL of plasmid was added into thawed cells, and the cells were snap-frozen in liquid nitrogen, and then put in 37 ℃ waterbath for 5 minutes, afterwards cells were incubated with 1 mL LB at 28 ℃ for 3 hours, and then selected on LB agar plates with antibiotics in 30 ℃ incubator.

7. Recombinant protein expression, extraction and purification

A single *E. coli* strain Rosetta™ 2 (DE3) colony with recombinant ICS1, SARD1 or CBP60g gene was picked up and grown in 5 mL LB with 25 μg/ mL chloramphenicol and 50 μg/ mL kanamycin or 100 μg/ mL ampicillin at 37 ℃ overnight. 1 mL overnight culture was then transferred into a 250 mL flask containing 50 mL TB media with the same antibiotic, the culture was then grown in a 37 ℃ shaker until its OD_{600} was at approx. 0.6. 1 mM IPTG was added into culture to induce protein expression. Then the induced culture was incubated at room temperature (approx. 20 ℃) for 16 hours. Afterwards, cells were harvested by centrifugation at 4000 rpm for 5 minutes, the supernatant was discarded and pellet was washed by PBS. After further centrifugation at 4000 rpm for 1 min, the washed pellet was resuspended in 1 mL lysis buffer (20 mM sodium phosphate, 500 mM sodium chloride, 1% Triton, 10 mM imidazole, pH 7.4) containing 1 mM DTT and protease inhibitor. Cells were subsequently lysed using sonication and the cell debris was spun down at 12000 g for 20 minutes at 4 ℃. The supernatant which is the total soluble protein expressed in *E.*

coli was transferred into a fresh Eppendorf tube. Protein samples were stored on ice for purification.

To purify recombinant proteins with His-tag, the HisPur™ Ni-NTA resin (Thermo Scientific) was used. 250 μL of resin was added into an Eppendorf tube and spun at 700 g for 2 minutes. The supernatant was removed and resin was equilibrated with 500 μL equilibrium buffer (20 mM sodium phosphate, 300 mM sodium chloride, 10 mM imidazole, pH 7.4), then the equilibrated resin was spun down at 700 g for 2 minutes and buffer was removed. The equilibration procedure may be repeated 2 or 3 times. Afterwards 500 μL cell lysate was added into pre-equilibrate resin and mixed properly. The mixture can be incubated at 4 ℃ for several hours to achieve better binding. After incubation the resin was spun down at 700 g for 2 minutes and the supernatant was collected as flow-through for analysis. The resin was washed using wash buffer (20 mM sodium phosphate, 300 mM sodium chloride, 25 mM imidazole, pH 7.4) for 5 times and the supernatant during washing steps can be collected for analysis. After washing, bound protein can be eluted using elution buffer (20 mM sodium phosphate, 300 mM sodium chloride, 250 mM imidazole, pH 7.4). Protein expression and purification can be evaluated using SDS-PAGE.

To purify MBP-SARD1 and MBP-CBP60g, Pierce™ 5 mL centrifuge column (Pierce #89897) and amylose resin (NEB E8021S) were used. 1 mL of amylose resin was added into 5 mL column, and resuspended by 3 volumes (3 mL) of column buffer (200 mM NaCl, 20 mM TrisHCl pH 7.4, 1 mM EDTA). After resuspension buffer has been removed, soluble fraction of cell lysate has been loaded onto resin bed, and the resin was washed by a total 6 volumes of column buffer. After washing, bounded protein was eluted by elution buffer (column buffer and 10 mM maltose). Eluted protein was collected, and its concentration was determined by Bradford assay (Bio-Rad #5000006).

8. *S*-nitrosylation **assays**

Biotin-switch was performed as a method to detect possible NO modification on protein *in vitro* (Forrester et al, 2009). First of all, Zeba™ Column was equilibrated with HEN buffer (250 mM Hepes-NaOH pH 7.7, 1 mM EDTA, 0.1 mM Neocuproine), and purified protein was desalted by

passing through the column. After desalting the protein, NO donor was added to the protein sample (0.1 mM CysNO) including a negative (No CysNO) and positive (CysNO + SDS) control. The reaction was incubated in the dark at room temperature for 20 minutes. After incubation, the NO donor was removed by passing the sample through new pre-equilibrated Zeba^{TM} column. And 3 volumes of blocking buffer (Mixture of HEN buffer and 25% SDS at 9:1 ratio, 20 mM MMTS) was added into protein sample which has passed through column to block the free thiols that were not linked to NO. The reaction was incubated in the dark at 50 ℃ with 5 minutes interval vortex for 20 minutes. After incubation, 1 total volume of pre-chilled acetone was added to each sample. The sample was then incubated in the dark at -20 ℃ for 20 minutes. Then the sample was centrifuged at 1000 g for 10 minutes at 4 ℃, the supernatant was removed and pellet was air dried in the dark. The pellet was resuspended with HENS (HEN buffer and 1%SDS) buffer and the sample was labeled by adding labeling solution (4 mM biotin-HPDP, 1 mM ascorbate), and subsequently incubated for 1 hour at room temperature. The biotinylated protein can be detected using SDS-PAGE and immunoblotting using anti-biotin antibody.

9. Western blot

Proteins separated by SDS-PAGE were transferred by electrophoresis to a nitrocellulose membrane (Whatman, UK) for further analysis. A sandwich structure was assembled in following manner: Scouring pad – 2× filter papers – gel – nitrocellulose membrane – 2× filter papers – Scouring pad. All components were equilibrated in transfer buffer before assembling. This sandwich was secured by a clasp and placed in a blotting tank; the nitrocellulose membrane was towards the anode side with gel behind it and the "sandwich" was immersed in transfer buffer. An box with ice was also put in the tank. The electrophoresis was run at constant 100V for 60 – 90 minutes or 10V overnight at 4 ℃.

After western blotting, the nitrocellulose membrane was blocked with 5% (w/v) skimmed milk (Marvel, UK) in PBST at room temperature for 30 mins. After blocking, solution was discarded and washed with PBST several times. The primary antibody was diluted in blocking reagent to an optimum dilution and the diluted primary antibody solution was incubated with the nitrocellulose membrane for 1 hour at room temperature or overnight at 4 ℃. After incubation, the diluted

primary antibody solution was removed and PBST was used to wash membrane for multiple times, each wash lasted about 5 minutes. After washing, a secondary antibody immunoglobulin G (IgG) – Horseradish Peroxidase) was diluted in blocking reagent at an optimum dilution and the diluted secondary antibody solution was incubated with the nitrocellulose membrane for 1 hour at room temperature. After incubation, the membrane was washed another 4 times in PBST.

Proteins were detected by the Pierce™ ECL Western Blotting Substrate (ThermoScientific), according to the manufacturer's guidelines, the result being darker bands on photographic film (ThermoScientific) when exposed in dark room. The exposure time was varied based on the initially observed result.

10. Plant transformation

Floral dipping is used as a method for inserting a foreign gene into *Arabidopsis* genome using agrobacterium (Clough & Bent, 1998). A single colony of agrobacterium that carries pEarlyGate 202 with the desired insert have been picked and grown in 5 mL LB medium with 100 μg/ mL rifampcin, 25 μg/ mL gentamycin, 50 μg/ mL kanamycin and 1 μg/ mL tetracycline overnight at 28 ℃. The next day 1 mL of overnight culture was added into 200 mL LB with same antibiotics and grown at 28 ℃ until its OD_{600} reached 0.8 to 1.5. The cell culture was centrifuged at 4000 rpm for 10 minutes the supernatant discarded and the pellet resuspended in 500 mL of 5% sucrose with 250 μL of Silwet L-77. Plants with clipped primary bolts and secondary bolts that were about 2-10 cm were ready to be transformed. Each *Arabidopsis* blot was dipped into *agrobacterium* resuspension for 30 sec, after dipping, plants were covered with bag for 1 day to maintain humidity. Seeds of transgenic plants were collected and grown up for selection.

Transgenic plants were confirmed to be transgenic by growing seeds on selection antibiotics. For pEarlyGate 202 with the insert, Murashige and Skoog (MS) plate with 50 μg/ mL kanamycin was used. Transgenic plants will maintain green on plate while non-transgenic plant will die. To determine the copy number of transgene in transgenic *Arabidopsis*, the segregation ratio of T1 transgenic plant was calculated. And a 3:1 ratio would suggest the single copy of transgene.

11. Electrophoretic mobility shift assay (EMSA)

To detect interactions between SARD1, CBP60g and *ICS1* promoter sequence, EMSA was used based on a previous method with slight modifications (Zhang et al, 2010). The 181-bp *ICS1* promoter fragment was amplified by PCR. First, the probe was end-labeled by incubating 10 pmol of double-stranded DNA in a 40 μL reaction with 100 units of T4 polynucleotide kinase (NEB M0201S) and 40 μCi of [γ-^{32}P]ATP (PerkinElmer) at 37 ℃ for at least 30 minutes. After incubation, 3 M sodium acetate was added to reach a final concentration of 0.3 M. After vortexing, 2 to 2.5 volumes of cold 100% ethanol were added to the sample. After mixing, DNA was precipitated at -20 ℃ overnight. Following precipitation, the reaction was centrifuged at maximum speed for 20 minutes, and the supernatant removed. The pellet was washed by 1 mL cold 70% ethanol, and spun at maximum speed for 2 minutes. After removing ethanol, the pellet was left to dry at 37 ℃. The dried pellet was resuspended with water to make the final concentration of labelled probe 0.1 pmol/μL. The labelled probe was kept at -20 ℃. Approximately 100 ng of purified MBP-SARD1 or MBP-CBP60g was mixed with 100 ng of poly[dI-dC] (Pierce) and 4 μL of 5X binding buffer (50 mM Hepes (pH 7.5), 375 mM KCl, 6.25 mM $MgCl_2$, 25% glycerol) in a 19 μL reaction. The reaction was incubated at 4 °C for 20 minutes. After incubation 1μL of labelled probe (0.1 pmol per reaction) was added, the mixture was further incubated at 4 ℃ for another 20 minutes and then run on 5% native polyacrylamide gel in 0.5X TGE buffer (12.5 mM Tris, 95 mM glycine, 0.5 mM EDTA). After electrophoresis, gel was dried and a piece of X-ray film was placed over the gel in a light-proof box. The X-ray film was developed afterwards.

12. GUS stain using X-Gluc

Plant tissue was immersed in staining solution (0.1 M $NaPO_4$ pH7.0, 10 mM EDTA, 0.1% Triton X-100, 1.0 mM $K_3Fe(CN)_6$, 2.0 mM X-Gluc) and vacuum infiltrated until the plant tissue was fully immersed in staining solution. The plant tissues were incubated at 37 ℃ overnight. Staining solution was removed after incubation and was washed subsequently with 50% ethanol and later with 70% ethanol until tissue become colorless.

Chapter 3 SA synthesis related gene expression

Introduction

Salicylic acid (SA) is a phytohormone that has a critical role in plant disease resistance. Plants with mutations that impact SA synthesis exhibited enhanced susceptibility to virulent and avirulent pathogens (Vlot et al, 2009). In *Arabiodopsis*, two genes were identified as essential for SA biosynthesis in response to pathogen challenge. *SID2* (*SA-induction-deficient 2*)/*ICS1* (*Isochorismate Synthase 1*) encodes an enzyme that convert chorismate to isochorismate, a precursor of SA (Wildermuth et al, 2001). Further, *EDS5* (*Enhanced-disease-susceptibility 5*) encodes a multi-drug and toxin extrusion (MATE) transporter (Nawrath et al, 2002). Recent results suggest the chloroplast membrane localized EDS5 functions as an SA transporter in *Arabidopsis* (Serrano et al, 2013). In addition, NPR1 is required downstream of SA to activate plant defence responses (Dong, 2004) and it is vital in establishing both local and systematic acquired resistance (SAR)(Fu & Dong, 2013).

Calmodulin (CaM) binding protein 60 G (CBP60g) was recognized to be involved in *Arabidopsis* disease resistance to *Pseudomonas syringe* (Wang et al, 2009a). *CBP60g* was reported to be induced between three and six hours after *Psm* ES4326 infection. *cbp60g* plants accumulated less SA and showed enhanced susceptibility compared to wild type. In addition, a CaM binding domain was identified at the N-terminus of CBP60g, which is essential for protein function in plant immunity (Wang et al, 2009a). A subsequent study identified CBP60g and its closely related protein SARD1 are transcription factors that directly bind to the *ICS1* promoter with high affinity to a GAAATTTGG motif (Zhang et al, 2010). SARD1 shares 39% similarity in amino acid sequence to CBP60g, both transcription factors have a DNA binding domain located in the centre of the protein. However, SARD1 does not contain a CaM binding domain (Zhang et al, 2010). Both *SARD1* and *CBP60g* were expressed in response to *Psm* ES4326 infection. In *sard1 cbp60g* plants, *ICS1* expression was significantly decreased, and the SA level was reduced compared to wild type plants (Zhang et al, 2010). Further, the expression of *SARD1* is later than *CBP60g*, with

Psm ES4326 infection, *SARD1* expression was not significantly induced until 24 hours (Wang et al, 2011).

S-nitrosoglutathione (GSNO), formed by *S*-nitroyslation of glutathione (GSH), functions as a stable reservoir for NO bioactivity. The importance of maintaining GSNO homeostasis was demonstrated via reverse genetic studies. *Arabidopsis* GSNO reductase (AtGSNOR1) is the enzyme that turnovers GSNO. Further, *atgsnor1-3* plants showed an elevated total cellular SNO concentration and resulted in compromised plant non-host, basal and *Resistance* (*R*) gene-mediated protection (Feechan et al, 2005; Kwon et al, 2012). Upon pathogen infection, *gsnor1-3* plants showed reduced SA accumulation, delayed and reduced *PR1* expression compared to wild-type *Arabidopsis* (Feechan et al, 2005).

We speculated that high cellular SNO levels may negatively regulate SARD1 and CBP60g activities and thus reduce *ICS1* expression, leading to a reduction in SA synthesis. However, increased cellular NO and SNO levels may not only regulate SARD1 and CBP60g activity, but also control their transcription. To evaluate this hypothesis, quantitative reverse transcription PCR (qRT-PCR) was used to monitor expression of these genes (Fig 3.1).

Results

Arabidopsis leaves were infiltrated with *Psm ES4326* (OD_{600}= 0.02), and samples were collected at different time points after inoculation. Expression of *ICS1*, *SARD1* and *CBP60g* were evaluated by qRT-PCR (Figure 3.1). Each bar represents normalized mean expression of *ICS1*, *SARD1* and *CBP60g* respectively after inoculation. Gene expression of *ICS1*, *SARD1* and *CBP60g* were normalized by *ACTIN2*, which has already been used as internal reference in previous research studying same genes using qRT-PCR (Truman & Glazebrook, 2012; Wang et al, 2009a).

Results are consistent with previous findings: *ICS1* (Fig 3.1C), *SARD1* (Fig 3.1A) and *CBP60g* (Fig 3.1C) transcripts accumulated after pathogen inoculation in *Arabidopsis* Col-0 and *gsnor1-3* plants. However, the expression levels of these genes in *gsnor1-3* plants were lower than their expression in Col-0 and their expression was also delayed. In Col-0 plants, expression of *CBP60g*

was increased 1 hour after inoculation (Fig 3.1B), and *SARD1* expression from 3 to 6 hours post inoculation (Fig 3.1A) (Wang et al, 2011). Increased expression of *SARD1* and *CBP60g* triggered the expression of *ICS1*, resulting in increased *ICS1* transcript levels at 6 hours after inoculation (Fig 3.1C). In *gsnor1-3* plants, *SARD1* expression was slightly increased 12 hours after inoculation (Fig 3.1A). Increased *CBP60g* and *ICS1* expression were detected at similar time points in both *gsnor1-3* and Col-0 plants, but the expression of these genes was significantly reduced in *atgsnor1-3* plants relative to Col-0.

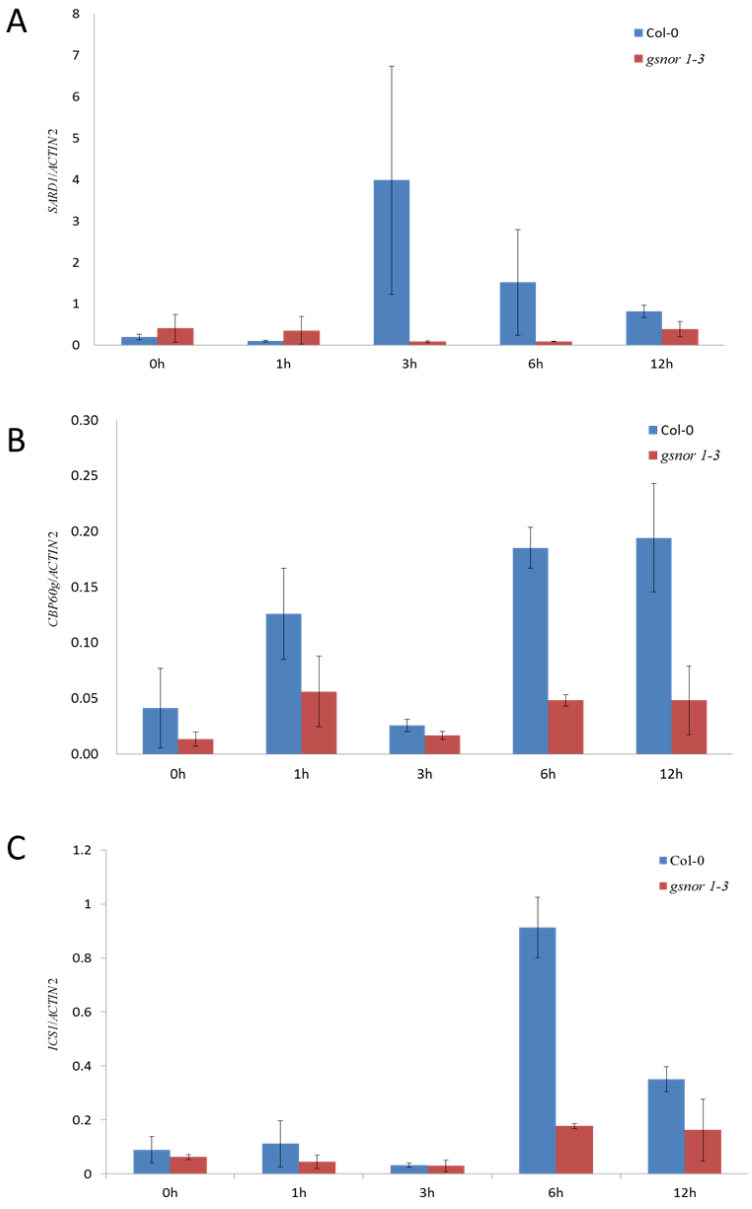

Figure 3.1. Induction of *ICS1*, *SARD1* and *CBP60g* in *Arabidopsis* Col-0 and *gsnor1-3* plants after pathogen challenge. Each bar represents the mean value of expression of *SARD1* (A), *CBP60g* (B)

and *ICS1* (C) in Col-0 (Blue) and *gsnor1-3* plants (Orange) at respective times after inoculation. Gene expression levels were normalized related to *ACTIN 2* level. Data was obtained from three biological replicates, error bar represent standard deviation.

Discussion

In *Arabidopsis sard1 cbp60g* double knockout plants, *ICS1* expression is significantly reduced (Zhang et al, 2010), which indicates the importance of the function of SARD1 and CBP60g in maintaining the integrity of the SA synthesis pathway. Our data shows that despite the presence of no mutations in *SARD1* and *CBP60g*, reduced *SARD1* and *CBP60g* transcript levels were observed in the presence of high cellular SNO levels. Thus, increased SNO content is a factor that contributes to reduced *ICS1* transcript accumulation in *gsnor1-3* plants during the immune response and consequently leads to reduction of SA levels in *gsnor1-3* plants. Currently, SA synthesis is thought to be triggered by two independent signalling cascades, PAD4/EDS1 and NDR1 (Dempsey et al, 2011). Previous research suggested that the SARD1/CBP60g node is located between the PAD4/EDS1 node and SA synthesis node (Wang et al, 2011). EDS1/PAD4 are key regulators of TIR-NBS-LRR triggered R-protein mediated resistance (Aarts et al, 1998), which is compromised in *gsnor1-3* plants (Feechan et al, 2005). Thus, low *SARD1* and *CBP60g* transcripts in *gsnor1-3* plant may be due to compromised R-protein mediated resistance including EDS1/PAD4 function.

Moreover, SARD1 or CBP60g may also be directly modified by NO via *S*-nitrosylation, which may control their activity. Recent researches have provided some evidences that plant transcription factor activity might be modulated by *S*-nitrosylation. *Arabidopsis* MYB transcription factors, MYB2 and MYB30, have been shown to be modified by NO result in inhibition of their DNA binding activities *in vitro* (Serpa et al, 2007; Tavares et al, 2014). *Arabidopsis gsnor1-3* plants show compromised SA synthesis due to high cellular GSNO content (Feechan et al, 2005). In addition to low *ICS1* transcript level we observed in qRT-PCR, we hypothesized that excessive NO level may inhibit transcription factors activities such as SARD1 and CBP60g via post-translational modification and result in suppression of *ICS1* expression.

Chapter 4 SARD1 and CBP60g protein expression

Introduction

Previous research demonstrated that SARD1 and CBP60g are transcription factors that bind to *ICS1* promoter region at -1110 and -1290 upstream of untranslated region. In *sard1 cbp60g* plants, *ICS1* expression and salicylic acid (SA) levels were significantly reduced upon pathogen infection compared to wild type plants (Zhang et al, 2010). Our previous results showed in *gsnor1-3* plants, *SARD1* and *CBP60g* expression was delayed and reduced after pathogen infection compared to *Arabidopsis* Col-0, which suggested reduced expression of these regulators in high SNO levels reduces *ICS1* expression and further leads to low SA levels. In addition, multiple proteins are found to be *S*-nitrosylated in *Arabidopsis*, many of these modifications are promoted in *gsnor1-3* plants (Wang et al, 2015a; Yun et al, 2011). Thus, we speculate that SARD1 and CBP60g are potential targets undergoing *S*-nitrosylation and this modification might impact their activity. To evaluate this hypothesis the production of recombinant SARD1 and CBP60g is required.

SARD1 and CBP60g were expressed previously (Truman et al, 2013; Wang et al, 2009a; Wang et al, 2011; Zhang et al, 2010). Full length and truncated CBP60g (1-76 aa) was expressed with a N-terminal glutathione S-transferase (GST) tag using a pET15 vector (Wang et al, 2009a). Full length and truncated (1-83 aa) SARD1 were expressed using the same vector (Zhang et al, 2010). The GST tag is a widely used affinity tag for its high expression efficiency and solubility (Harper & Speicher, 2011). In addition, the incorporation of a protease cleavage site within the GST-fusion protein for further tag cleavage after protein purification is a widely used strategy to support subsequent analysis by NMR and structural determinations by crystallography. However, GST was reported to be *S*-nitrosylated and thus may not be the optimal choice for our study (Ji et al, 2002).

Polyhistidine-tag (His-tag) is a string of nucleotides encoding at least six histidine residues fused at either end of the translated protein. The His-tag has high affinity to Cu^{2+}, Ni^{2+}, Co^{2+} or Zn^{2+},

that provides a purification strategy for its fusion proteins. Further, it has a small size which will minimize its impact on protein folding (Hengen, 1995). However, endogenous histidine-rich proteins from expression hosts like *E. coli* make purifying his-tagged proteins more difficult than GST-tagged proteins. In addition, the His-tag does not improve protein expression or solubility, thus lower protein yield is expected in expression and purification. Maltose-binding protein (MBP) is another affinity tag that is commonly used in fusion protein expression. Like GST tag, MBP tag is known for its high yields and solubility (Papaneophytou & Kontopidis, 2014). In addition, no cysteine residues are present in the tag, making it more attractive for assessing potential *S*-nitrosylation. However, MBP itself has a high molecular weight (40 kDa), thus further tag cleavage may be required after expression and purification.

In this chapter, recombinant HisMBP-SARD1 and HisMBP-CBP60g were successfully expressed and purified.

Results

SARD1 was initially fused with hexahistidine (His_6) for protein expression. *SARD1* cDNA was amplified from Col-0 cDNA library with the correct size of 1353 bp (Fig 4A) and cloned into pDEST^{TM}17 vector. After DNA sequencing validation, the finished construct was transferred into *E. coli* Rosetta^{TM} 2 (DE3). His-SARD1 was expressed and purified. Total soluble and purified protein were obtained and analyzed by SDS-PAGE. The resulting gel was subsequently analyzed using Coomassie staining (Fig 4.1A). However, no up-regulated band was visible in total soluble protein (Fig 4.1A, Lane 1 and 2) with/without addition of Isopropyl β-D-1-thiogalactopyranoside (IPTG). In addition, no protein was detected after purification, suggesting no SARD1 was expressed. Although several adjustments were made, the results were consistent. To circumvent this issue, another vector, pET28a, was used for SARD1 expression. His-SARD1 expressed from *E. coli* Rosetta^{TM} 2 (DE3) using pET28a was purified and analyzed by SDS-PAGE and western-blot (Fig 4.1B). After Coomassie staining, proteins were mainly detected in elution sample 3, 4 and 5, with a dominant band at 60 kDa size. The predicted molecular weight of SARD1 is 50 kDa and a 60 kDa band doesn't represent His-SARD1. In elution sample 4 and 5, coomassie stain also revealed non-dominant bands other than 50 kDa and 60 kDa, we suggest

those bands are non-specific *E. coli* proteins that co-purified during purification. In a western blot, a dominant band slightly below 50 kDa sign was detected by anti-His antibody (Fig 4.1B, lower half). This indicated the presence of His-SARD1, since this band was not visible in Coomassie staining, suggesting that His-SARD1 expression level was not optimal. Collectively, our data suggested that the His-tag may not be the best tag for SARD1 expression.

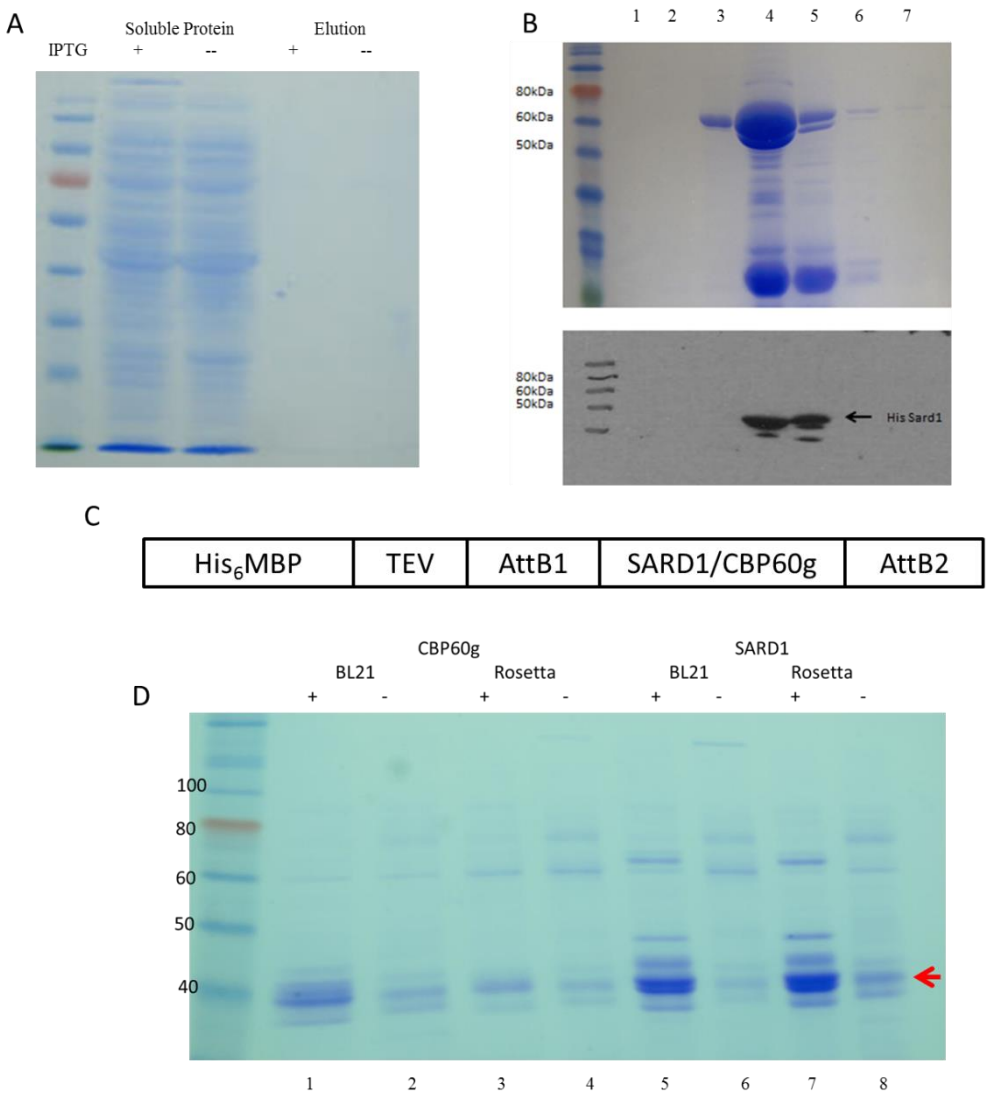

Figure 4.1. Expression and purification of SARD1 and CBP60g using different tags and expression hosts. (A) Coomassie stain of purified His-SARD1 protein from *E. coli* Rosetta™ 2 (DE3), + and – indicate presence/absence of IPTG during protein expression. Lane 1 and 2, total soluble protein. Lane 3 and 4, eluted protein. (B) Coomassie stain and western blot of purified His-SARD1 protein from *E. coli* BL21. Arrow indicates His-SARD1. 7 vials (500 µL each) of

eluted protein were collected during purification. Lanes 1-7 correspond to each vial of eluted protein. (C) Schematic drawing of fusion protein with pDEST-HisMBP construct including TEV protease cleavage site. (D) Coomassie stain of purified HisMBP-SARD1 protein from *E. coli*, + and – indicate presence/absence of IPTG during protein expression, red arrow indicates band correspond to MBP (40 kDa), molecular weight of protein markers indicated on the left (kDa). Lane 1 and 2 are purified CBP60g elution from *E. coli* BL21 cells. Lane 3 and 4 are purified CBP60g elution from *E. coli* Rosetta cells. Lane 5 and 6 are purified SARD1 elution from *E. coli* BL21 cells. Lane 7 and 8 are purified SARD1 elution from *E. coli* Rosetta cells.

To overcome the difficulties encountered during the expression of His-SARD1, a construct was designed to fuse a His_6MBP tag at the N-terminus of a TEV protease cleavage site followed by SARD1/CBP60g, based on the pDEST-HisMBP vector (Fig 4.1C). A TEV protease cleavage site was included for potential further tag cleavage (Sun et al, 2011). The completed construct was transferred into *E. coli*, recombinant SARD1 and CBP60g were expressed and purified using amylose resin as described in method section 7. Eluted proteins were analyzed via SDS-PAGE, the resulting gel was stained by Coomassie blue (Fig 4.1D). However, no HisMBP-SARD1 or HisMBP-CBP60g was detected after purification, only HisMBP tags were found at 40 kDa (Red arrow, Fig 4.1D). Both *E. coli* BL21 DE3 and *E.coli* Rosetta^{TM} 2 (DE3) were used for expression and the results were similar. This suggested recombinant SARD1/CBP60g may be degraded or insoluble thus only the tag remained in the soluble fraction and was purified, or the protein tag was cleaved from recombinant protein and no SARD1/CBP60g was purified. The different band intensity at 40 kDa with/without IPTG induction indicated a successful induction as it correspond to the size of the MBP protein (Fig 4.1D). The amount of MBP in the purified sample was significantly increased in both BL21 and Rosetta with IPTG induction, suggesting the MBP-tag is a better choice to the His-tag.

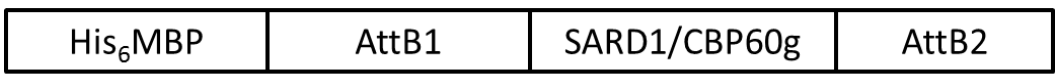

Figure 4.2. Schematic drawing of the pDEST-HisMBP fusion protein construct. 6X His

(Hexahistidine) tags are located at the N-terminus of MBP (Maltose binding protein) tag. The MBP tag is designed to improve the fusion protein's solubility and yield. AttB1/B2 sequences are used for cloning by recombination.

Based on previous results, the TEV protease cleavage site was removed from the previous construct (Fig 4.2). The resulting construct was transferred into *E. coli* Rosetta™ 2 (DE3), recombinant SARD1 and CBP60g were expressed and purified using amylose resin as per protocol. Purified proteins were analyzed by SDS-PAGE and western-blot. Following Coomassie staining, several up-regulated bands were observed in the SARD1 purified fraction with IPTG induction (Fig 4.3A). Among them, an up-regulated 90 kDa band indicated His-MBP SARD1 expression (Fig 4.3A, red arrow). However, there was no significant difference in CBP60g purified protein between presence/absence of IPTG induction. In the subsequent western-blot, both CBP60g and SARD1 were detected by anti-MBP antibody (Fig 4.3B, red arrow). In addition, free MBP-tag was also detected and there was a significant difference with addition of IPTG. However, the purity of the proteins was not optimal.

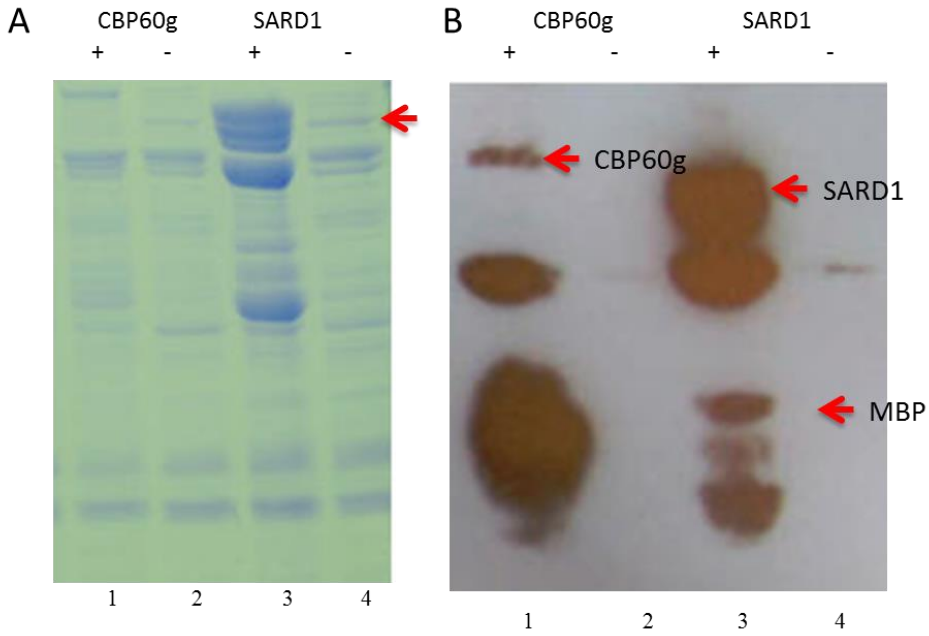

Figure 4.3. Purified HisMBP-SARD1 protein from *E. coli* Rosetta™ 2 (DE3). (A) Coomassie stain of purified recombinant CBP60g and SARD1 from *E. coli* Rosetta™ 2 (DE3) protein extract, + and – indicate presence/absence of IPTG during protein expression, red arrow indicates

predicted HisMBP-SARD1 size. (B) Western-blot of purified recombinant CBP60g and SARD1 from *E. coli* Rosetta^{TM} 2 (DE3) protein extract, + and – indicate presence/absence of IPTG during protein expression. Recombinant SARD1, CBP60g and the MBP-tag are indicated by red arrow with labels.

SARD1 and CBP60g cDNA was amplified from pathogen challenged Col-0 cDNA, with a size of 1353 bp and 1689 bp respectively (Fig 4.4A). SARD1 and CBP60g cDNA were cloned into pDEST-HisMBP destination vector. Constructs were subsequently transferred into *E. coli* BL21 pLysS cells for expression. Recombinant proteins were expressed as per protocol. Total soluble proteins from *E. coli* were obtained and analysed by SDS-PAGE. The resulting gels were stained by Coomassie blue (Fig 4.4B). For CBP60g, there was no significantly up-regulated expression found with the presence of the inducer IPTG (Fig 4.4B, lane 1). However, total protein expression in the SARD1 expression line was significantly up-regulated by adding IPTG (Fig 4.4B, lane 3), especially at 90 kDa (red arrow), 60 kDa and 40 kDa. The MBP-SARD1 protein has a predicted molecular weight of 90 kDa, the molecular weight of MBP-tag is 40 kDa and we suggest 60 kDa band may correspond to degraded MBP-SARD1 protein. Recombinant SARD1 and CBP60g was purified using an amylose resin (NEB E8021S) based purification technique. Purified protein was analysed using SDS-PAGE and Coomassie staining (Fig 4.4C and D), the concentration of purified protein was measured using the Bradford assay. Despite little up-regulation of expression (Fig 4.4B), CBP60g has been successfully purified (Fig 4.4C. Lane 1 and 2, red square). Further, SARD1 also has been purified using the same technique (Fig 4.4C. Lane 3 and 4, red square). By analysing the presence of recombinant proteins in different elution fractions (Fig 4.4D), elution fraction 2 for both recombinant proteins was chosen to be used in further experiments due to its greater purity, despite the fact it was less concentrated (Fig 4.4D).

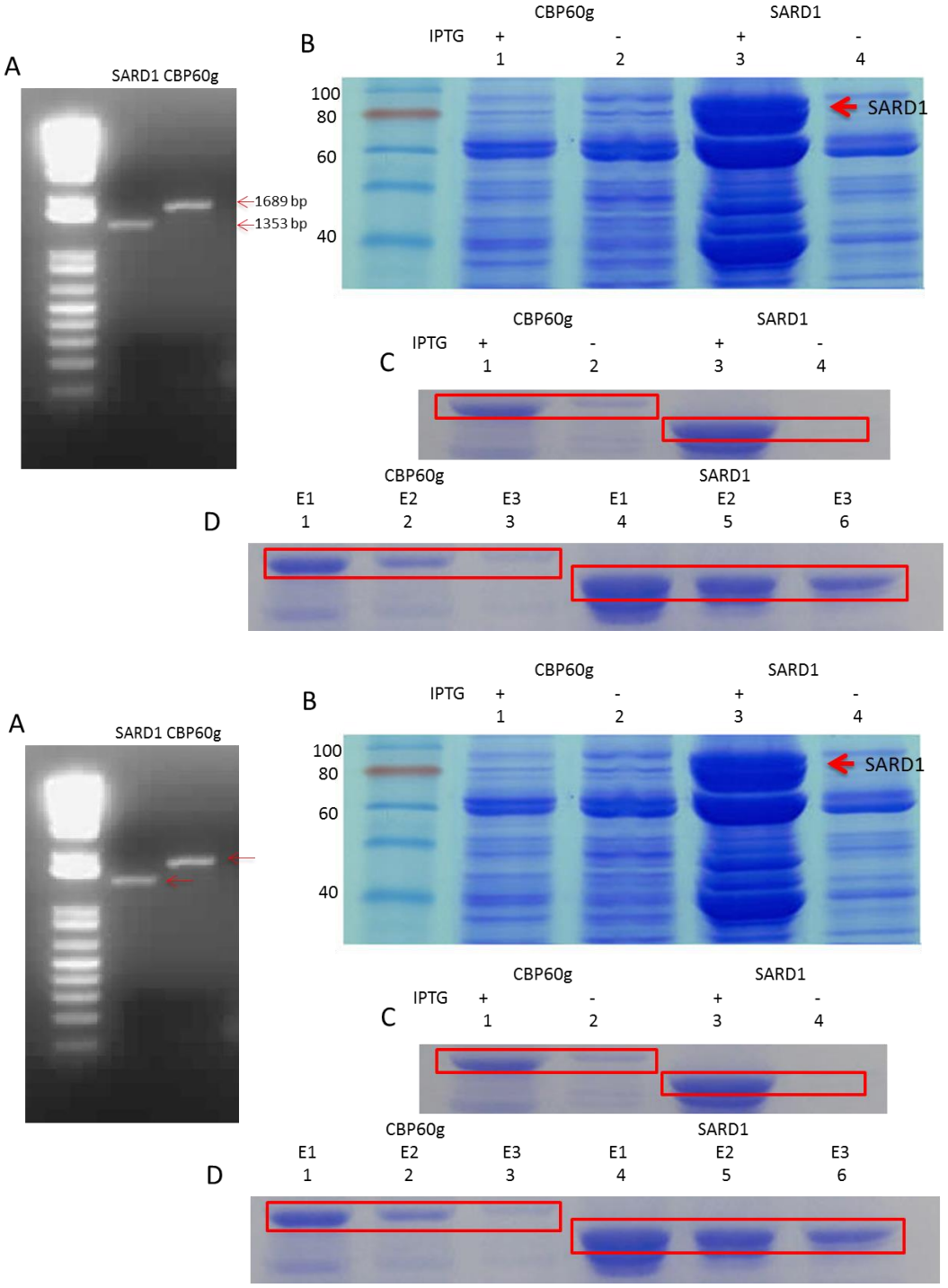

Figure 4.4. Expression and purification of recombinant SARD1 and CBP60g. (A) Amplification of *SARD1* and *CBP60g* from Col-0 cDNA, bands indicate successful amplification of target genes, as labelled. (B) Induction of recombinant CBP60g and SARD1 in *E. coli* BL21 pLysS (DE3), total soluble protein with (+) or without (-) IPTG, molecular weight of protein markers indicated on the left (kDa), land 1 and 2 are CBP60g total protein fractions, lane 3 and 4 are SARD1 total protein fractions, red arrow indicates up-regulated band corresponding to HisMBP-SARD1. (C)

Coomassie stain of purified recombinant CBP60g and SARD1 from *E. coli* BL21 pLysS (DE3) protein extract, + and – indicate presence/absence of IPTG during protein expression. Lane 1 and 2 are CBP60g, lane 3 and 4 are SARD1. (D) Coomassie stain of recombinant CBP60g and SARD1 in different elution fractions of purified protein. Lane 1-3 contain CBP60g, lane 4-6 contain SARD1.

Discussion

After several attempts, SARD1 and CBP60g were expressed and purified with HisMBP-tag in *E. coli* BL21 pLysS (DE3) (Fig 4.4D). Recombinant SARD1 and CBP60g were initially designed to tag with His_6. However, no protein was expressed when using Gateway® system pDEST17 (Fig 4.1A). A previous research indicated that expression vector pDEST17 containing the sequence AAA-AAA in its attB1 site which result in its susceptibility to -1 ribosomal frameshifting at the sequence C-AAA-AAA (Belfield et al, 2007). SARD1 was later expressed with His_6 tag using pET28a vector with low protein purity and concentration, which can only be detected using western-blot (Fig 4.1B). In fact, recombinant SARD1 was not the dominant band following Coomassie blue staining (Fig 4.1B). His-tag is one of smallest and most commonly used tags in protein expression and purification. SARD1 has a predicted molecular weight of 50 kDa, thus the dominant 60 kDa band is a contaminant during purification (Fig 4.1B, Lane 4 and 5). The *E .coli* chaperone GroEL, a 60 kDa heat shock protein, is a possible contaminant that co-eluted with His-SARD1. In addition, any endogenous histidine rich protein from *E. coli* may also interact with Ni-NTA resin and be purified later, which could explain the non-specific bands showed in Fig 4.1B. SARD1 was predicted to be insoluble when expressing in *E. coli*, such property may also contribute on SARD1 low expression level with His-tag. Taken together, the unsuccessful expression of His-SARD1 in *E. coli* suggested it was better to use protein tags which can improve protein solubility and expression level. GST-tag was used in previous research (Zhang et al, 2010) and was proven to be a suitable tag for SARD1 expression and subsequent experiments. However, GST contains multiple cysteines which were shown susceptible to *S*-nitrosylation (Ji et al, 2002). In addition, glutathione (GSH) is used in GST fusion protein purification, which can interfere in subsequent redox regulation study of SARD1. Thus, MBP-tag is chosen to fuse with SARD1 for recombinant protein expression.

SARD1 and CBP60g were expressed using an N-terminal His-MBP tag, which included a TEV protease site. However, this was not successful, as no protein was detected in SDS-PAGE (Fig 4.1D). The *E. coli* BL21 pLysS strain appears to be superior relative to the Rosetta^{TM} 2 strain in the expression of these recombinant proteins. More non-specific bands and stronger basal expression were observed in proteins expressed from Rosetta^{TM} 2 than *E. coli* BL21 pLysS (Fig 4.3). *E. coli* carrying the pLysS plasmid produce bacteriophage T7 lysozyme, which is a natural inhibitor of T7 RNA polymerase, this can reduce basal expression from the T7 promoter (Studier, 1991). In summary, after several attempts and adjustments, recombinant SARD1 and CBP60g were successfully expressed using an N-terminal HisMBP tag and *E. coli* BL21 pLysS as host with IPTG induction. Recombinant proteins were purified by a batch method using amylose resin and eluted with maltose for further study.

Chapter 5 SARD1 DNA binding assay

Introduction

Various transcription factors were found to bind on *ICS1* promoter to regulate its expression, including SARD1 and another closely related protein, CBP60g (Zhang et al, 2010). *SARD1* (*SAR deficient 1*) was named due to it is required for systemic acquired resistance (SAR). In previous research, *Arabidopsis sard1* plants showed reduced SAR to subsequent pathogen infection after pre-treatment with *Psm* ES4326 or *Psm* ES4326 *avrB* (Zhang et al, 2010). SARD1 and its closely related protein CBP60g were later identified as transcription factors which are required for *ICS1* induction and nuclear localization. Subsequent experiments showed SARD1 and CBP60g bind *ICS1* promoter at -1110 to -1290 bp upstream of the translational start site with high affinity to GAAATTTTGG motif (Zhang et al, 2010). A later study suggested that despite sharing the same binding motif, *SARD1* and *CBP60g* are expressed at different time point. CBP60g plays more important role in SA induction in calcium dependant manner at early stages of plant defence, while SARD1 has more important role later (Wang et al, 2011).

Developed in 1981 (Fried & Crothers, 1981), Electrophoretic mobility shift assay (EMSA) is used to detect interaction between protein and nucleic acid. This technique is based on the theory that electrophoretic mobility of free nucleic acids is faster than a protein-nucleic acid complex (Hellman & Fried, 2007; Lane et al, 1992). Nucleic acids are labelled by radioisotopes and ran through acrylamide or agarose gel. Signals from radioisotopes can be viewed using autoradiography. By adding specific proteins, e.g. respective transcription factors, resulting radiolabelled nucleic acid-protein complex will run slower than free nucleic acid, resulting position “shift” on photographic film (Fig 5.1A). EMSA using radioisotopes can achieve its maximum sensitivity. Even though, fluorescence, chemiluminesence and immunohistochemical approaches are used in detecting mobility shift with less sensitivity but better safety.

Nitric oxide (NO) is reported to inhibit or increase plant transcription factors activities via

S-nitrosylation (Lindermayr et al, 2010; Serpa et al, 2007). In *Arabidopsis*, *AtMYB2* is expressed in response to abiotic stresses including water stress, low oxygen and high salinity. AtMYB2 is reported to bind the *ALCOHOL DEHYDROGENASE 1* gene (*ADH1*) to the GT-motif (TGGTTT) (Hoeren et al, 1998). Recent results suggested that the minimal DNA binding domain of AtMYB2, M2D, is able to bind the TGGTTT motif in EMSA. The binding is inhibited after adding 5 mM sodium nitroprusside (SNP) or *S*-nitrosyglutathione (GSNO), suggesting an inhibitory role of NO donors. Furthermore, this inhibition was reversed by adding the reducing reagent, dithiothreitol (DTT) (Serpa et al, 2007). Another plant transcription factor, TGA1, was reported to bind activation sequence-1 (as-1) elements (TGACG(N7)TCACG) (Despres et al, 2003). In EMSA, the His-TGA1-as-1 complex migrates with different mobility under different redox states. A high mobility band indicates presence of reduced or modified cysteine, while a low mobility bands indicates presence of intramolecular disulphide bonds (Despres et al, 2003). In addition, reduction of disulphide bridge within TGA1 and GSNO dependent modification were shown to increase its DNA binding activity in EMSA (Lindermayr et al, 2010).

Truncated SARD1 has been demonstrated to bind the *ICS1* promoter (Zhang et al, 2010). In this chapter, full length recombinant SARD1 was used in EMSA to test its DNA binding activity, and NO donors were used to examine the impact of NO on its DNA binding ability.

Results

To evaluate the DNA binding ability of recombinant SARD1, HisMBP-SARD1 was assayed using EMSA. A 181 bp *ICS1* promoter fragment described previously (Zhang et al, 2010) was amplified from Col-0 genomic DNA and used as the binding target for recombinant protein. Utilising an agarose gel, an increased amount of SARD1 protein in the assay resulted in increased formation of a low mobility DNA-protein complex between SARD1 and the *ICS1* promoter fragment (Fig 1A, upper arrow, labelled as shift). While the intensity of the DNA probe, which moved much faster than the DNA-protein complex, decreased in intensity correspondent to an increasing amount of SARD1 (Fig 5.1A, lower arrow, labelled as free probe). This demonstrated that recombinant SARD1 has similar DNA binding ability as previously reported for its truncated form (Zhang et al. 2010).

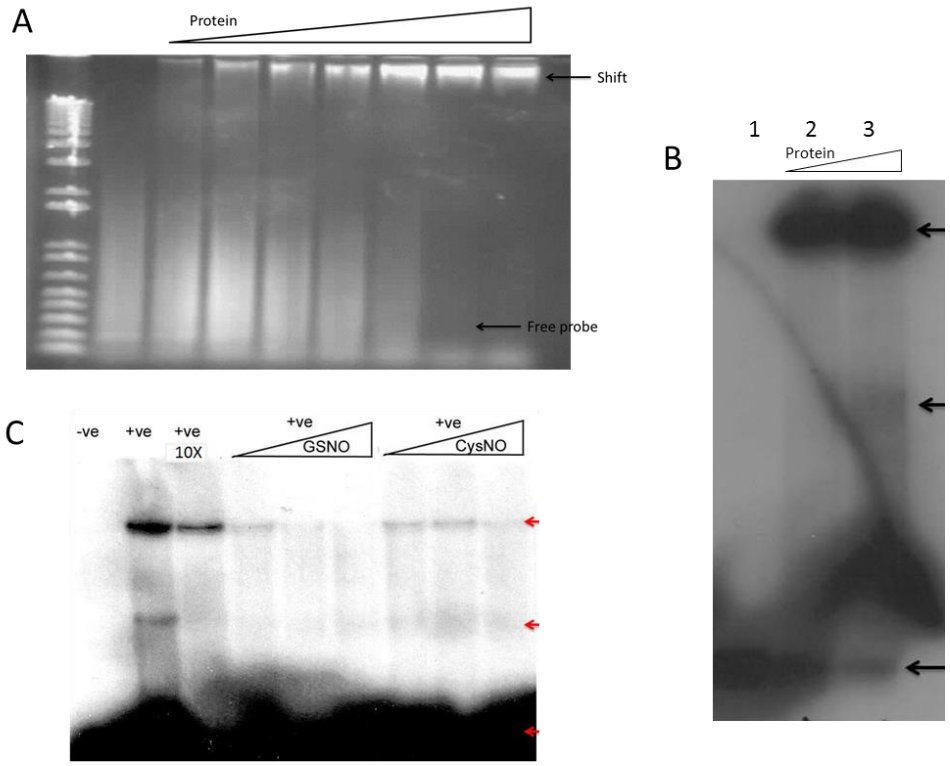

Figure 5.1. DNA binding assay of SARD1. (A) Binding between increasing amount of SARD1 and a constant amount of DNA probe subsequently fractionated on an agarose gel. Lane 1, no protein. Lane 2, 1 μg protein. Lane 3, 2 μg protein. Lane 4, 5 μg protein. Lane 5, 10 μg protein. Lane 6, 20 μg protein. Lane 7, 50 μg protein. Lane 8, 100 μg protein. (B) Binding between SARD1 and DNA probe subsequently analysed by native PAGE. Lane 1, 1 pmol labelled probe. Lane 2, 1 pmol labelled probe, 5 μg protein. Lane 3, 1 pmol labelled probe, 10 μg protein. (C) Binding of SARD1 with DNA probe in presence of NO donor. –ve: no protein; +ve: 10 μg protein loaded; 10X: 10X unlabelled DNA probe. Arrows indicate position of DNA probe signal. CysNO: nitrosocysteine. GSNO: S-nitroysoglutathione.

To increase the sensitivity of this assay, the same assay was performed on a native polyacrylamide gel (Fig 5.1B). In this assessment, consistent with our previous results, SARD1 exhibited DNA binding ability. However, two shifts were observed with an increasing amount of SARD1 (Fig 5.1B, lane 3). Initially, this observation was speculated to be due to protein aggregation, but after several adjustments (changing amount of protein, polyacrylamide gel concentration, addition of nonionic detergent), this phenomenon was not resolved. This protein-DNA complex (Fig 5.1B,

upper arrow) may be formed by binding between the DNA probe and a SARD1 polymer, which results in a large complex with low mobility. In addition, a SARD1 monomer may also bind with the DNA probe forming a complex with higher mobility (Fig 5.2B lane 3, middle arrow). Further, by adding 10X non-radiolabelled DNA probe, the intensity of the DNA-protein complex was reduced (Fig 5.1C, lane 3, upper and middle arrows) compared to reactions without non-labelled probe (Fig 5.1C, lane 2, upper and middle arrows).

To test if NO is capable of modifying SARD1 activity, different NO donors have been included in DNA binding assay. The assay has been performed using SARD1 which was pre-treated with different concentrations of GSNO or CysNO (0.1 mM, 0.5 mM and 5 mM, Fig 1C, lane 4-9). In both scenarios, the binding complex between SARD1 and DNA was reduced with the presence of NO. This finding suggests that SARD1 is a potential target for NO-based modifcation *in vitro* and the outcome of such modification may lead to inhibition of its DNA binding ability.

Discussion

Recombinant full length HisMBP-SARD1 was shown to bind the 181 bp *ICS1* promoter sequence which was previously described by Zhang et al (Zhang et al, 2010). The DNA binding activity of HisMBP-SARD1 was demonstrated by increased amount of SARD1-DNA complex observed in the presence of increased SARD1 input (Fig 1AB). It is noteworthy that in previous research (Zhang et al, 2010), only truncated SARD1 was tested for its binding ability. In addition, truncated SARD1 was tagged with GST-tag (26 kDa), which is smaller than MBP-tag (40 kDa). Above all, despite its large molecular weight, MBP-tag showed its ability on preserving protein activity upon expression of a eukaryotic less-soluble protein in prokaryotic system.

The binding between SARD1 and DNA probe was competed by presence of un-labelled probe (Fig 5.1C, lane 3), indicates the specificity of SARD1 binding. Moreover, the DNA binding ability of SARD1 was inhibited by adding GSNO or CysNO (Fig 5.1C). Unlike CysNO which directly transfer nitrosonium (NO^+) moiety from one thiol to another, GSNO was shown to produce disulphide bond with protein sulfhydryls (Giustarini et al, 2005). Nevertheless, the inhibitory role of CysNO on SARD1 DNA binding activity suggested that presence of *S*-nitrosylation on SARD1

cysteine residue. *S*-nitrosylation was reported to inhibit DNA binding activity of multiple transcription factors across kingdoms, like AtMYB2 (Serpa et al, 2007), AtMYB30 (Tavares et al, 2014), c-MYB (Brendeford et al, 1998) and myocyte enhancer factor 2 (MEF2) (Okamoto et al, 2014). As the first transcription factors showed to be *S*-nitrosylated in its protein family, there is little insight on how *S*-nitrosothiol (SNO) formation blocks its DNA binding ability. A well characterized plant R2R3 MYB transcription factor, AtMYB30, was shown to be S-nitrosylated at C49 and C53 *in vitro* and SNO formation on either site result in inhibition of its DNA binding ability (Tavares et al, 2014). Both cysteines were studied extensively on maize R2R3 MYB transcription factor P1 (Heine et al, 2004). C49 is the redox sensor in R2R3 MYB DNA binding domain and its reduction state is critical for DNA binding. On the secondary structure level, both cysteines are positioned in the hydrophobic core and are susceptible to *S*-nitrosylation. It was suggested *S*-nitrosylation on either cysteine is sufficient to inhibit DNA binding via induction of subtle structural modification (Tavares et al, 2014). As for SARD1, *S*-nitrosylation may introduce a similar structural change on its DNA binding domain that block DNA access. It is important to identify the modified cysteine residue in SARD1 and study the DNA activity of its cysteine mutant. SARD1 forms polymers without reducing reagents like DTT. In addition, DNA binding was observed in EMSA without reducing reagent, suggesting that reducing conditions may not be required for SARD1 DNA binding activity (Fig 5.1C, lane 2).

The inhibitory role of NO on SARD1 DNA binding also has biological significance. SARD1 is known to bind *ICS1* promoter region to activate *ICS1* expression and further promotes salicylic acid (SA) accumulation (Zhang et al, 2010). We previously reported in *gsnor1-3* plants, SA accumulation is reduced upon pathogen infection, suggesting that the SA synthesis pathway was compromised (Feechan et al, 2005). Previous result suggested in *gsnor1-3* plants, *SARD1* expression is reduced possibly due to compromised R-gene mediated resistance upstream of SA synthesis. Here, we demonstrated that possible *S*-nitrosylation of SARD1 inhibits its DNA binding activity, which provide a direct *in vitro* explanation of how a high SNO environment may supress *ICS1* expression and SA accumulation. On the other hand, the inhibitory role of NO on *ICS1* expression may provide a feed-back loop to control plant defence response once the pathogen is contained. Previously we have described the inhibitory role of NO on *Arabidopsis* NADPH

oxidase AtRBOHD (Yun et al, 2011), which itself is required for reactive oxygen species (ROS) synthesis during plant defence, but later its activity is inhibited by elevated NO concentration during pathogen-triggered nitrosative burst. In addition, higher SA level was observed in *Arabidopsis* enhanced GSNO reductase 1 (GSNOR1) activity mutant, *gsnor1-1* plants, after pathogen infection (Feechan et al, 2005). This phenomenon indicates that potential less inhibition of SARD1 activity in *gsnor1-1* plants due to lower cellular SNO level in compare to wild type plants may result in higher *ICS1* expression thus more SA synthesis.

Chapter 6 *S*-nitrosylation of SARD1

Introduction

S-nitrosylation is a post-translational modification that involves covalent attachment of a NO moiety to a cysteine thiol. It is suggested that *S*-nitrosylation plays an important role in plant defence and development (Feechan et al, 2005; Kwon et al, 2012; Yun et al, 2011). In animals, a number of transcription factors were shown to be *S*-nitrosylated, including NF-kB, HIF-1 and Activator protein-1 (AP-1), resulting in either inhibition or activation of their activity (Sha & Marshall, 2012). AP-1 is a bZIP transcription factor, which is a heterodimer formed by a Fos and Jun subunit (Shaulian & Karin, 2002). AP-1 is important in controlling gene expression during cell proliferation, transformation and apoptosis. AP-1 is shown to be regulated by *S*-nitrosylation for decades (Abate et al, 1990). C154 and C272 in c-Fos and c-Jun subunits respectively are *S*-nitrosylated resulting in inhibition of their DNA binding ability. Recently, another transcription factor, myocyte enhancer factor 2C (MEF2C), was also found to be *S*-nitrosylated resulting in inhibition of its transcriptional activity (Okamoto et al, 2014). MEF2 isoforms were shown to regulate neurogenesis and neuronal survival in the brain (Dietrich, 2013). *S*-nitrosylation of MEF2 C39 results in inhibition of its binding to the Bcl-xL promoter and thereby decreases Bcl-xL promoter activity *in vivo* (Okamoto et al, 2014). In plants, a MYB transcription factor, AtMYB2, was shown to be *S*-nitrosylated at C53 (Serpa et al, 2007), which reduces its DNA binding activity after *S*-nitrosylation. Another bZIP transcription factor in plants, TGA1, is also S-nitrosylated *in vitro* (Lindermayr et al, 2010). Unlike AtMYB2, *S*-nitrosylation of TGA1 C260 and C266 was reported to enhance its DNA binding activity and protect it from oxidative modification (Lindermayr et al, 2010).

To detect *S*-nitrosylation *in vitro*, a technique called biotin-switch was used (Forrester et al, 2009; Jaffrey & Snyder, 2001) (Fig 6.1A). The flow-chart in Fig 6.1A shows the process of biotin-switch. Protein with reactive cysteines serves as a potential *S*-nitrosylating target to NO donors, like GSNO and CysNO. First, the target protein is incubated with NO donor to allow *S*-nitrosylation to

occur, other unoccupied thiols are then blocked by the blocking reagents MMTS (*methyl methanethiosulfonate)* or NEM (N-Ethylmaleimide). After blocking, the *S*-nitrosylated thiol is reduced by ascorbate, which can subsequently react with biotin HPDP (N-[6-(Biotinamido)hexyl]-3 ´-(2 ´-pyridyldithio)propionamide). The biotinylated protein is then detected by western blot using anti-biotin antibody.

In EMSA, the DNA binding activity of SARD1 was inhibited by addition of NO donors, which may be due to potential *S*-nitrosylation. Here, recombinant SARD1 was shown to be *S*-nitrosylated *in vitro*. Further, subsequent site-direct mutagenesis revealed that SARD1 C438 was the site of *S*-nitrosylation.

Results

To detect if SARD1 is *S*-nitrosylated, the biotin-switch assay was performed using recombinant HisMBP-SARD1 as substrate. It is noteworthy that the MBP tag and His tag do not contain any cysteine residues, thus any signal detected upon biotin-switch would indicate the presence of S-nitrosylated SARD1. Fig 6.1B suggests that SARD1 is *S*-nitrosylated in the biotin-switch assay. Ponceau S is a dye that reversibly stains protein on nitrocellulose or PVDF membranes, which indicates the amount of protein in the assay. Bands appeared in western blot indicating SARD1 was labelled by biotin-HPDP, which is due to *S*-nitrosylation of SARD1. The sample in Lane 1 serves as negative control, as no CysNO was added, thus all free thiols were blocked and cannot be linked with biotin-HPDP later. The sample in Lane 4 is positive control, as SARD1 was treated by SDS prior NO treatment. Addition of SDS linearized the protein and exposed all free thiols to NO donor regardless of structure. In lane 5, ascorbate is not added during the process, without its reduction, the S-nitrosylated cysteine cannot react with biotin, resulting in no signal in the western blot. An increased amount of CysNO was added into samples in lane 2 and 3, which resulted in increased signal in the western blot corresponding to CysNO input. In sum,, the biotin-switch experiment demonstrated recombinant SARD1 is S-nitrosylated *in vitro*.

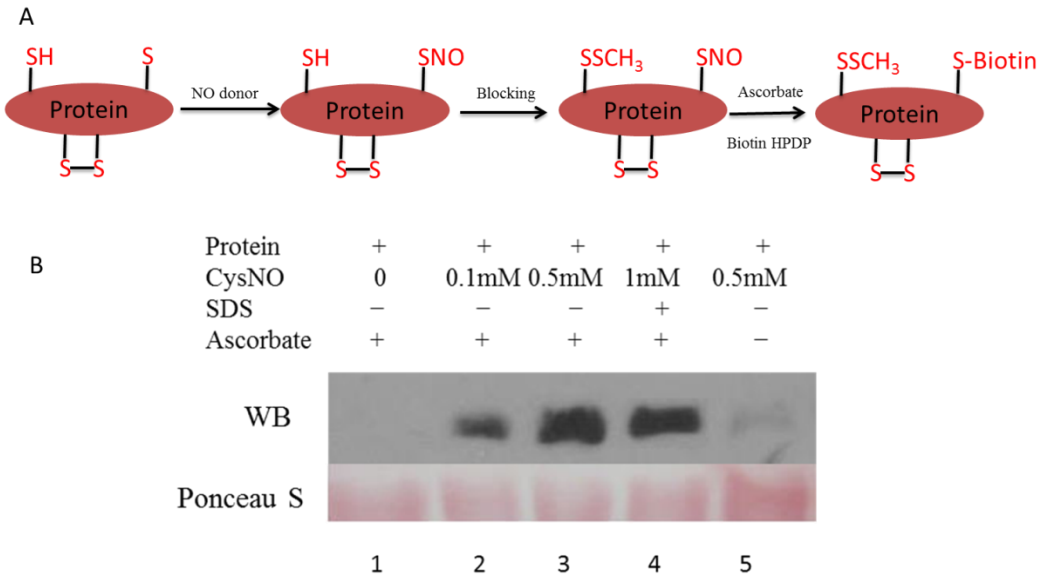

Figure 6.1. Biotin-switch of recombinant SARD1. (A) Schematic drawing of biotin-switch process. As the flow-chart shows, biotin-switch involves three steps: 1. *S*-nitrosylation of reactive cysteiene (indicate by red S) with NO donor. 2. blocking other non-occupied cysteine using blocking reagents. 3. Reduction of S-nitrosylated cysteine with ascorbate and labelling newly generated cysteine with biotin-HPDP, labelled protein can be detected using western-blot. (B) Detection of *S*-nitrosylated protein SARD1 using different concentrations of CysNO. WB: western blot. SDS: sodium dodecyl sulphate. Lane 1: negative control with no CysNO added. Lane 2 and 3, *S*-nitrosylation of SARD1 with 0.1 mM and 0.5 mM CysNO, respectively. Lane 4, positive control, SARD1 was linearized prior to biotin-switch by SDS to expose all free cysteines. Lane 5, negative control, no ascorbate was added during biotin-switch assay.

After confirming SARD1 is *S*-nitrosylated *in vitro*, it is important to determine which cysteine in SARD1 is the site of this modification (Fig 6.2). From studying DNA binding activity of truncated SARD1, Zhang and his colleagues have identified that the amino acid sequence in the middle of SARD1 corresponds to its DNA binding domain (Fig 6.2A, highlighted in orange) (Zhang et al, 2010). SARD1 contains four cysteines (Fig 6.2A, highlighted in red) and none of these residues were located within the DNA binding domain. A software, GPS-SNO 1.0, was used to predict the potential SARD1 *S*-nitrosylation site (Xue et al, 2010)(Table 1). Four cysteines were scored by the software based on their position, a higher score suggests a higher chance to be S-nitrosylated.

According to GPS-SNO, C311 and C333 have a higher score than other cysteines.

Position	Peptide	Score
221	SGQGVVVCEAMTEAI	0.393
311	TLKHARECILGNKLY	20.577
333	FMILNPICEVMKALI	15.139
438	TPAEFNICFTGSSSQ	1.158

Table 6.1. Identifying possible S-nitrosylated cysteine using GPS-SNO. SARD1 *S*-nitrosylation site was predicted using GPS-SNO 1.0 (Xue et al, 2010) without any threshold. Cysteines were labelled with red with corresponding to their position in SARD1. Scores indicate the likelihood of *S*-nitrosylation site based on known database and calculation.

To identify which cysteine is *S*-nitrosylated *in vitro*, four individual SARD1 mutants were made, each containing a single cysteine to serine mutation (C221S, C311S, C333S, C438S). Four HisMBP-SARD1 proteins were successfully expressed and purified with the same conditions as HisMBP-SARD1 (Fig 6.2B). Subsequently, the biotin-switch was performed to determine which cysteine(s) might be *S*-nitrosylated *in vitro*.

A

MAGKRLFQDLDSDQENKSEKRIKSVLPSLASPISSVFGALISENTLRSVLEPVIRKVVRQEVEYGIS
KRFRLSRSSSFRIEAPEATTPTLKLIFRKNLMTPIFTGSKISDVDNNPLEIILVDDSNKPVNLNRPIKL
DIVALHGDFPSGDKWTSDEFESNIIKERDGKRPLLAGEVSVTVRNGVATIGEIVFTDNSSWIRSRK
FRIGAKVAKGSSGQGVVVCEAMTEAIVVRDHRGELYKKHHPPMLEDEVWRLEKIGKDGAFHKK
LSSRHINTVQDFLKLSVVDVDELRQILGPGMSDRKWEVTLKHARECILGNKLYISRGPNFFMILN
PICEVMKALIDGHVLSSQESLNQPYVKNLVRDAYSKGNFLEVGERTANEAALLTQGDDLDQQYA
ASHYQNIEIDKSYQQNGYVQERSTNNLEIVNEGYITTPAEFNICFTGSSSQNHINPF_

B

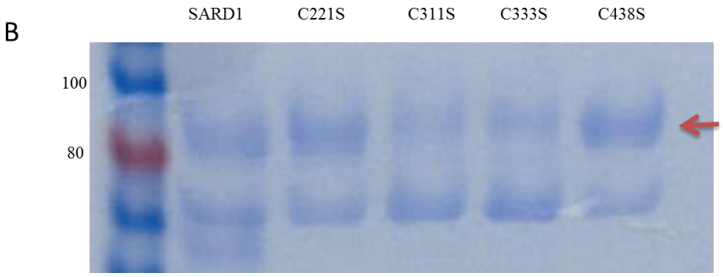

Figure 6.2. (A) SARD1 amino acid sequence. Amino acids highlighted in orange indicate the SARD1 DNA binding region. Amino acids in red indicate cysteine residues in SARD1. (B) Protein expression of SARD1 and its cysteine mutants. Purified SARD1 and its mutants were stained by Coomassie blue. Red arrow indicates SARD1 and its mutants. Molecular weight (kDa) of corresponding band was labelled at left.

Biotin-switch experiments with SARD1 and its cysteine mutants suggested that C438, is *S*-nitrosylated (Fig 6.3). In the biotin-switch assay, with 1 mM CysNO, a signal from the anti-biotin antibody was observed from SARD1 and its mutants C221S, C311S and C333S.No signal was also observed in mutant C438S (Fig 6.3A, upper half), which suggested that cysteine 438 of SARD1 is the target site for *S*-nitrosylation. To confirm this observation, the experiment was repeated with a focus on the SARD1 C438S mutant (Fig 6.3B, upper half). In a biotin-switch assay, after electrophoresis, purified recombinant SARD1 and its mutants on nitrocellulose membrane were detected by anti-MBP antibody (Fig 6.3, lower half), indicating the presence of HisMBP-SARD1 in all samples. In the western blot using anti-MBP antibody, several bands were observed on the film, the dominant bands with molecular weight of 90 kDa indicate presence of MBP-SARD1. Bands with lower molecular weight suggest existence of degraded MBP-SARD1 proteins present in the sample. Bands with higher molecular weight suggest presence of dimerized or oligomerized MBP-SARD1 protein.

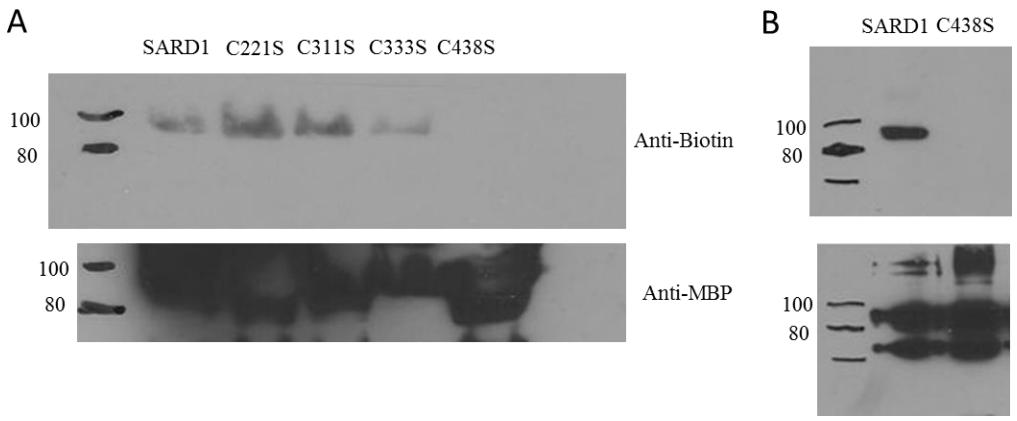

Figure 6.3. Determination of the *S*-nitrosylated cysteine in SARD1. (A) Biotin-switch assay results of SARD1 and its associated cysteine mutants. Upper half: western blot using anti-biotin antibody. Lower half: western blot using anti-MBP antibody. (B) Biotin-switch results of SARD1 and its C438S mutant. Upper half: western blot using anti-biotin antibody. Lower half: western blot using anti-MBP antibody.

Discussion

The results from EMSA analysis suggested that SARD1 is *S*-nitrosylated *in vitro*, which may result in inhibition of its DNA binding activity. Subsequent biotin-switch assays showed SARD1 is indeed *S*-nitrosylated *in vitro*. Examination of the SARD1 amino acid sequence suggested none of its cysteines were located within the DNA binding domain (Fig 6.2A). GPS-SNO 1.0 was used to predict the *S*-nitrosylation site in SARD1. However, even using the default setting, no threshold for prediction, the software was not able to identify a cysteine target with high probability. This may be due to the fact that the algorithm of GPS-SNO is based on identified *S*-nitrosylated proteins from both animals and plants. However, SARD1 belongs to a plant specific calmodulin binding protein family which is newly identified as a transcription factors, perhaps making it difficult for GPS-SNO to predict an *S*-nitrosylation site with high accuracy. Nevertheless, GPS-SNO predicted C311 and C333 have a higher chance to be *S*-nitrosylated than other cysteines.

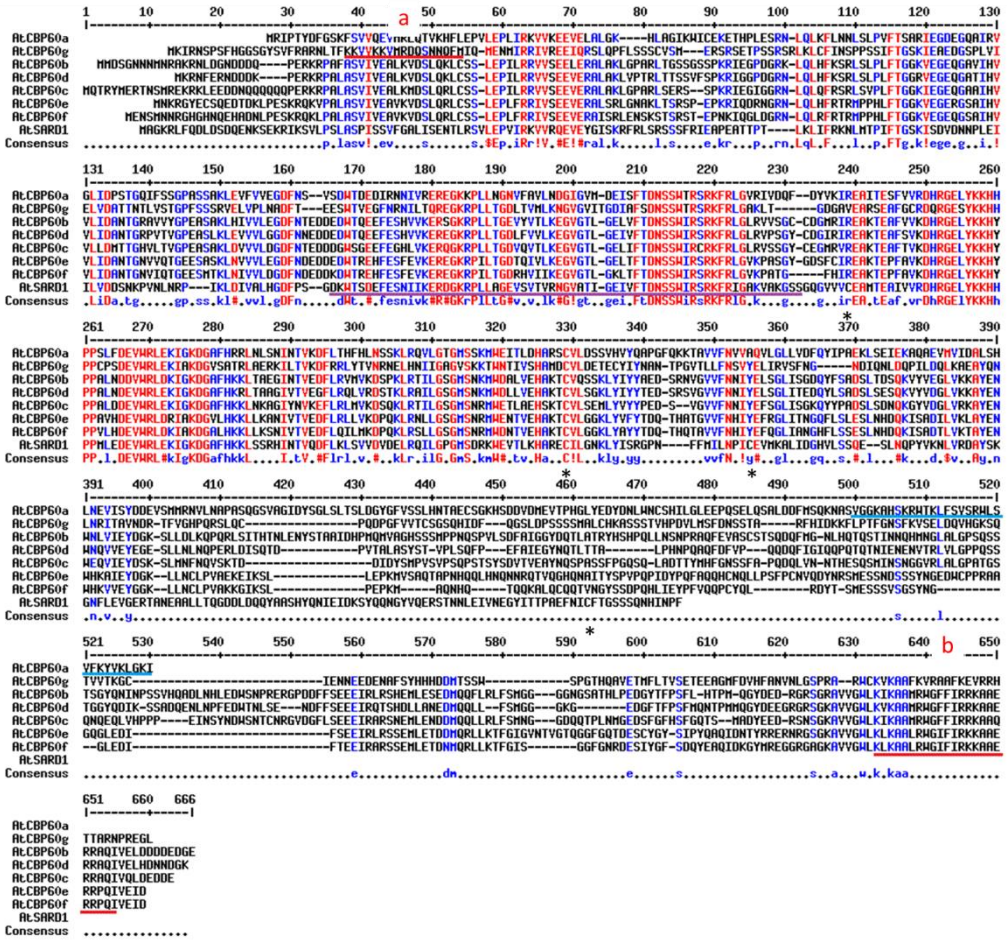

Figure 6.4. Sequence alignment of *Arabidopsis* CBP60 family proteins and SARD1. *Arabidospsis* CBP60 family proteins and SARD1 were aligned using MultAlin (Corpet, 1988) with default settings (http://bioinfo.genopole-toulouse.prd.fr/multalin/multalin.html). Amino acids with high consensus value (>90%) were coloured in red, amino acids with low consensus value (>50%) were coloured in blue. Red underline marked "a" indicates calmodulin-binding domain in CBP60g. Red underline marked "b" indicates calmodulin-binding domain in other CBP60 proteins. Blue underline indicates calmodulin-binding domain in CBP60a. Purple underline indicates SARD1 DNA binding domain. Stars indicate cysteine residues in SARD1.

In subsequent site-directed mutagenesis, followed by the biotin-switch assay, we found C438, was the site of *S*-nitrosylation, as opposed to the prediction. There is currently little known about SARD1, besides the position of its DNA binding domain. Apart from acting as potential switches

for redox regulation, cysteine residues are able to covalently interact with other cysteine thiols to create inter- and intramolecular bonds. This process is important in maintaining protein folding and structure. In addition, cysteine residues can coordinate a variety of metals and metalloids. Thus, cysteine residues are commonly incorporated into metal binding sites (Marino & Gladyshev, 2012). A well-studied example is zinc-finger proteins. A classic "zinc-finger" domain comprises of two cysteines and two histidines forming a tetrahedral coordination motif with Zn^{2+} in the centre (Kroncke & Klotz, 2009).

In general, there is no preference for substitution with any other amino acids (Betts & Russell, 2003). It is common to mutate cysteine into serine or alanine or histidine if there is a "zinc finger" domain involved. Alanine is non-bulky, chemically inert amino acid. However, alanine substitution was shown before to change transcription factor binding activity (Heine et al, 2004). In some cases, valine can also be used since it is as bulky as cysteine. Here, cysteine residues in SARD1 were mutated into serine residues as it is the closest amino acid to cysteine in terms of structure, also it is cannot be *S*-nitrosylated.

Interestingly, in the biotin-switch assay, SARD1 C221S and C311S showed increased signal compared to wild-type SARD1. This may indicate the presence of a disulphide bond within SARD1. Thus, mutation of cysteines involved in disulphide bond formation may have resulted in one or more cysteine residues becoming more solvent exposed and therefore exhibiting increased susceptibilty to *S*-nitrosylation.

SARD1 is a plant specific transcription factor that shares the same DNA binding site with CBP60g (Zhang et al, 2010). Both transcription factors play a partially redundant role in plant defence (Wang et al, 2011). The amino acid sequence alignment revealed SARD1 and CBP60g share 39% similarity and alignment of the CBP60 family proteins and SARD1 indicate that SARD1 and CBP60 family proteins have high similarity in their DNA binding domain (Fig 6.4). The C-terminal domain of SARD1 does not contain either a predictive CBP60 calmodulin binding site (Fig 6.4, region b) or an actual calmodulin binding site, as present in CBP60a (Fig 6.4) (Truman et al, 2013). Previous results also suggested that unlike CBP60g, the N-terminal domain of SARD1

was not capable of calcium binding (Zhang et al, 2010). Cysteine 438 of SARD1, the site of *S*-nitrosylation, is surprisingly not conserved between SARD1 and CBP60 proteins. This may suggest that this redox-based post-translational modification might be unique to SARD1. Although C438 is distant from the DNA binding domain, based on the primary sequence, this cysteine may be located close to DNA binding region based on secondary structure. However, the structure of SARD1 and CBP60G proteins remains to be determined. *S*-nitrosylation of SARD1 at C438 may change the secondary structure of this protein, for instance within the DNA binding motif which may block DNA binding domain, consistent with an inhibitory role for *S*-nitrosylation in this case.

Chapter 7 SARD1 C438S analysis

Introduction

Previous results have shown that *S*-nitrosylation of SARD1 results in inhibition of its DNA binding ability *in vitro*. To identify the S-nitrosylated residue, four single mutants were made. Amino acid mutation is a common strategy used in studying amino acid function. Cysteine plays an important and flexible role in protein function despite it being one of least abundant residues among the 20 common amino acids (Marino & Gladyshev, 2011).

Cysteine mutation was used in studying plant R2R3 MYB transcription factor activities under redox regulation (Heine et al, 2004; Serpa et al, 2007; Tavares et al, 2014). Two conserved cysteines, C49 and C53, are positioned within the DNA binding domain of *Arabidopsis* R2R3 MYB transcription factor AtMYB30. The minimum DNA binding domain (DBD) of AtMYB30 is sufficient for binding a 48-nucleotide MYB binding motif *in vitro*. Both cysteine residues were found to be *S*-nitrosylated *in vitro* and *S*-nitrosylation of either cysteine was shown to inhibit the DNA binding acivity of AtMYB30 DBD (Tavares et al, 2014). Cysteine residues were substituted by alanine residues during subsequent mutagenesis. The single mutants, AtMYB30 C49A and C53A, showed the same DNA binding activity compared to wild-type. The double mutant, however, lost its DNA binding ability despite the absence of *S*-nitrosylation (Tavares et al, 2014). This result is contradictory to a previous study in the maize transcription factor P1 (Heine et al, 2004), which is another R2R3 MYB transcription factor sharing high similarity to AtMYB30 within the DBD. The P1 C49A/C53A double mutant showed the same binding affinity to its target DNA as wild type protein. However, another P1 double mutant, C49I/C53S, which was believed to mimic the DNA binding domain mutation c-MYB C130S, showed the same compromised DNA binding activity (Myrset et al, 1993). Interestingly, substituting cysteine with alanine seemed to enhance P1 DNA binding activity and resulting in this protein becoming resistant to redox regulation (Heine et al, 2004). However, serine substitution at C53 was shown to preserve P1 activity to a large extent. The P1 C49S mutant showed similar DNA binding activity to the wild type protein and resistance to oxidation (Heine et al, 2004).

Four single cysteine mutants were made to identify the *S*-nitrosylated cysteine of SARD1. Serine residues were used to substitute for cysteine, due to this residue being isosteric to cysteine. In a subsequent biotin-switch assay, C438 was found to be susceptible to *S*-nitrosylation. The amino acid sequence of SARD1 showed no cysteine is located within its DNA binding domain. In fact, C438 is likely to be the cysteine most distant from the SARD1 DNA binding domain. Amino acid sequence alignment showed C438 is not conserved among the SARD1 and CBP60 protein family, therefore this regulatory mechanism may be exclusive to SARD1. We show that SARD1 C438S is not *S*-nitrosylated *in vitro* since the cysteine susceptible to NO modification was mutated to serine residue. To further investigate the function of this cysteine, we tested the SARD1 DNA binding activity in an electrophoresis mobility shift assay (EMSA) described earlier. In addition, we show that SARD1 has an ability to form oligomers in non-reducing conditions.

Results

To test the DNA binding activity of SARD1 mutants, purified recombinant protein was used in EMSA compared to wild-type SARD1 protein (Fig 7.1A). No shift was observed in the negative control. Protein-DNA complexes were observed in reactions with SARD1 and sard1 protein, indicating C438S has DNA binding activity. Increasing the amount of unlabelled probe (5X-20X) was used as competitor to determine if this binding is specific. With increased competitor, the shift decreased, as expected (Fig 7.1A). In addition, an increased amount of SARD1 and C438S were used in EMSA (Fig 7.1B), with 2 μg of protein and 0.1 pmol radio-labelled probe. DNA binding was observed at top of the gel. By increasing the amount of protein to 4 μg, the observed shift was seen in the middle of the gel (Fig 7.1B, upper arrow) and a stronger signal was detected at the top of the gel. In addition, the signal from the free-probe (Fig 7.1B, lower arrow) was significantly reduced in proportion to an increased protein level. These EMSAs suggested that SARD1 C438S is capable of binding the *ICS1* promoter sequence described previously (Zhang et al, 2010) with similar activity to wild-type SARD1.

To investigate if C438S is resistant to NO regulation, C438S was used in EMSA with an NO donor, CysNO (Fig 7.2). In EMSA, a C438S-DNA complex was observed as showed in our

previous experiment. The signal from this protein-DNA complex was reduced by addition of 10X unlabelled probe. With 1 mM CysNO, there was no reduction of the observed DNA-protein complex, suggesting the DNA binding activity of C438S was not influenced by NO.

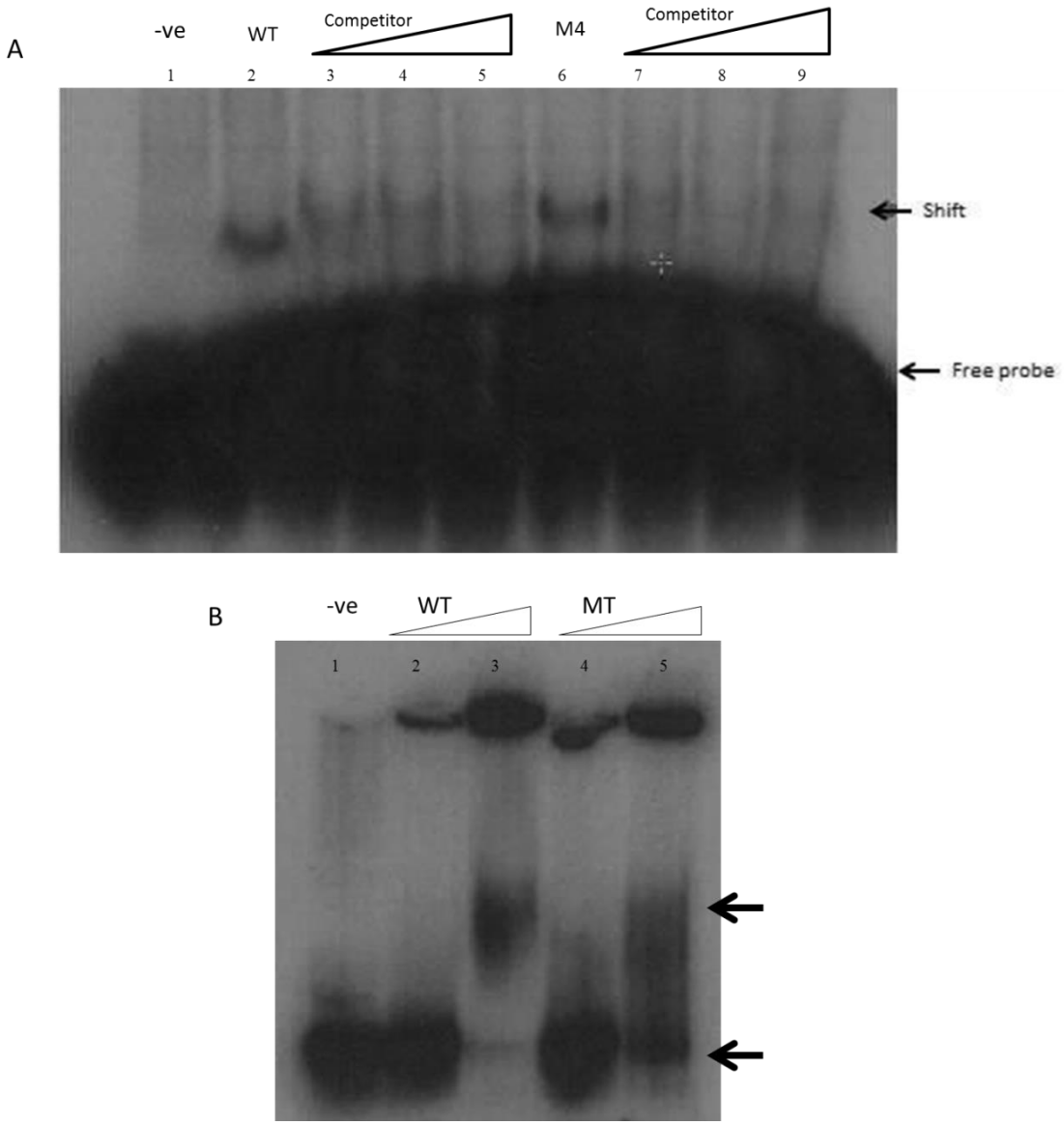

Figure 7.1. DNA binding assay of wild-type SARD1 and SARD1 C438S. (A) Binding between constant amount (10 μg) of SARD1/SARD1 C438S and an increasing amount of unlabelled probe subsequently analysed by native PAGE. Lane 1, labelled DNA probe. Lane 2, 10 μg wild type SARD1 recombinant protein without competitor. Lane 3, 10 μg wild type SARD1 recombinant protein with 1X competitor. Lane 4, 10 μg wild type SARD1 recombinant protein with 5X competitor. Lane 5, 10 μg wild type SARD1 recombinant protein with 10X competitor. Lane 6, 10

μg sard1 C438S recombinant protein without competitor. Lane 7, 10 μg sard1 C438S recombinant protein with 1X competitor. Lane 8, 10 μg sard1 C438S recombinant protein with 5X competitor. Lane 9, 10 μg sard1 C438S recombinant protein with 10X competitor. Competitor: unlabelled probe. (B) Binding between an increasing amount of SARD1/SARD1 C438S and a constant amount of DNA probe subsequently analysed by native PAGE. Upper arrow: SARD1-DNA complex. Lower arrow: labelled DNA that not bound to protein. Lane 1, labelled DNA probe. Lane 2, 5 μg wild type SARD1 recombinant protein. Lane 3, 10 μg wild type SARD1 recombinant protein. Lane 4, 5 μg sard1 C438S recombinant protein. Lane 5, 10 μg sard1 C438S recombinant protein. Competitor: 10X unlabelled probe.

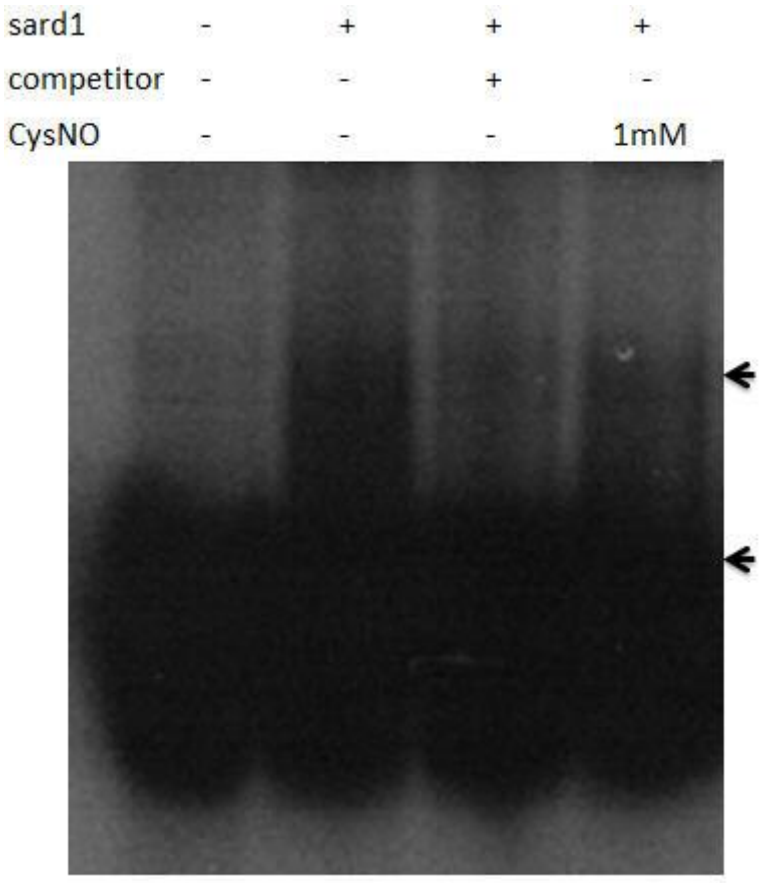

Figure 7.2. Binding of SARD1 C438S with DNA probe in presence of NO donor. +/-: presence/absence of indicated reagents within reaction. Reagents are labelled as left panel. Upper arrow: sard1-DNA complex. Lower arrow: free probe. CysNO: nitrosocysteine. Competitor: 10X unlabelled probe.

Cysteine is not only functional as a redox-switch in proteins. Another critical function is forming intra/inter-molecular disulphide bonds to maintain protein folding and conformation. We therefore tested the oligomerization of SARD1 (Fig 7.3). Purified SARD1 and its cysteine mutants were analysed by SDS-PAGE with/without reducing reagent DTT. In the presence of DTT, proteins were observed with molecular weight of 90 kDa (Fig 7.3, lower arrow), corresponding to recombinant HisMBP-SARD1 molecular weight. In non-reducing condition, two protein bands with higher molecular weight were observed in a Coomassie stain, which are below 230 kDa and above 230 kDa. SARD1 oligomers were observed in all samples. However, SARD1 C438S seemed to form less oligomers compare to SARD1 and its other mutants. An addition 55 kDa band was observed in wild-type SARD1 but not in mutant sard1 proteins, which may correspond to degradation of purified protein as its molecular weight is lower than the molecular weight MBP-SARD1 monomer.

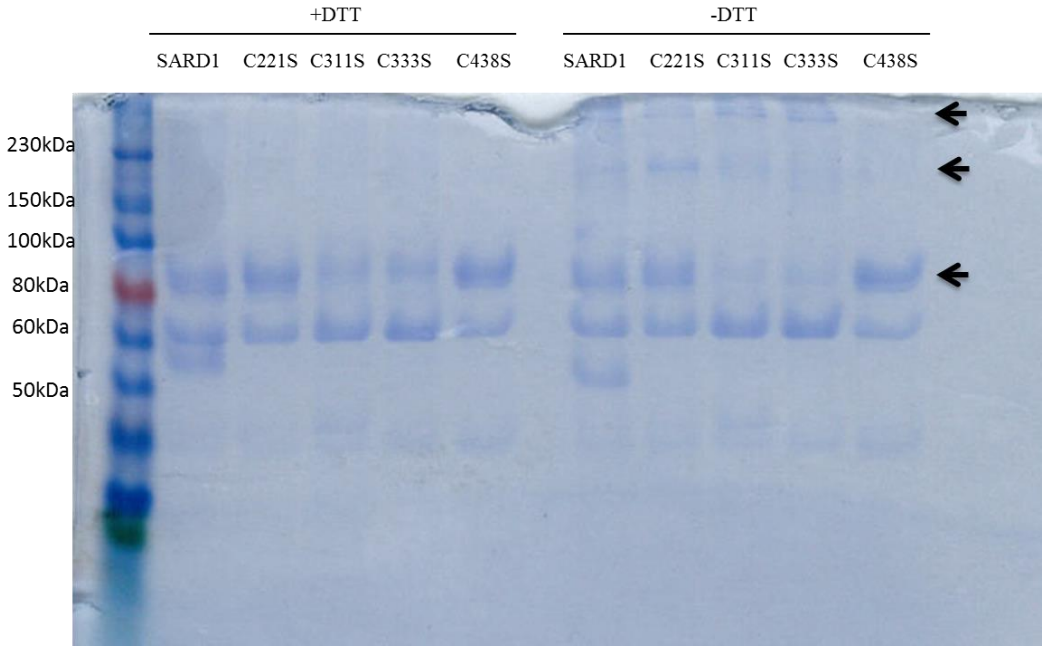

Figure 7.3. Oligomerization of SARD1 proteins. SARD1 and its mutants were analysed using SDS-PAGE, presence/absence of dithiothritol were labelled as above. Molecular weight of protein markers were indicated on the left (kDa). Upper arrow: oligomers with molecular weight more than 230 kDa. Middle arrow: oligomers with molecular weight about 230 kDa. Lower arrow:

HisMBP-SARD1 monomer with molecular weight of 90 kDa.

Discussion

Here, we showed HisSARD1 and the corresponding C438S mutant has the same DNA binding activity as wild type SARD1 protein. C438 was shown to be *S*-nitrosylated in the previous biotin-switch assay. Additionally, *S*-nitrosylated SARD1 lost its DNA binding ability *in vitro*. Unlike some transcription factors which were shown to be redox regulated, C438 is most distant from the SARD1 DNA binding domain among four cysteine residues found in SARD1. Thus, we speculated that C438S will maintain its DNA binding ability. Indeed, in EMSA, we demonstrated that SARD1 C438S is capable of binding the 181 bp probe isolated from the *ICS1* promoter region (Fig 7.1). The DNA binding ability of SARD1 C438S was not impaired by an NO donor, as the mutant is resistant to NO regulation. Our results also show that SARD1 forms a dimer and oligomers in the absence of the reducing reagent, DTT. Therefore, suggesting that SARD1 may exist as oligomer in an oxidized environment and require reducing conditions to function. Interestingly, fewer oligomers were observed in the SARD1 C438S mutant (Fig 7.3), suggesting C438 may not only be regulated via *S*-nitrosylation, but may also be susceptible to intermolecular disulphide bond formation. Based on SDS-PAGE, it is pre-mature to be certain about polymerization of SARD1 under non-reducing condition. To evaluate this observation further, it is possible to mutate other cysteines in SARD1 to identify the cysteines responsible to disulphide bond formation.

Previously, SARD1 was reported to bind the *ICS1* promoter region and induce *ICS1* expression (Zhang et al, 2010). In addition, the Arabidopsis GSNO reductase knock-out mutant, *atgsnor1-3*, was shown to have a reduced salicylic level and *Pathogenesis Related* (*PR*) gene expression upon pathogen infection (Feechan et al, 2005). Currently, there is few understanding about how high cellular SNO levels directly supress SA accumulation. The inhibitory role of NO on SARD1 DNA binding activity provides a significant insight into this issue. Although SARD1 and CBP60g were shown to bind the *ICS1* promoter at the same binding motif, expression of CBP60g was observed after pathogen infection with a peak expression level 9 hours post-infection (Wang et al, 2009a). A subsequent report suggested that *SARD1* is expressed at 24 hours after pathogen infection to

provide prolonged *ICS1* expression and SA synthesis (Wang et al, 2011). Previously we have reported that cellular SNO content increased after *Pseudomanas syringae* DC3000 avrB (*Pst* DC3000 *avrB*) and Pst DC3000 *avrRrps4* challenge while NADPH oxidase activity in *Arabidopsis* was increased and later reduced as plant resistance is developed. In addition, the NADPH oxidase, AtRBOHD, is *S*-nitrosylated both *in vivo* and *in vitro* resulting in supressed activity (Yun et al, 2011). In this case, SARD1 binding activity may be supressed by increasing cellular SNO levels, resulting in decreased *ICS1* expression and a reduced SA level after pathogen challenge. Oligomerization of SARD1 in non-reducing conditions suggests SARD1 monomerization may require a reducing cellular environment, which may be synchronized with decreased reactive oxygen species (ROS) levels after the initial ROS burst (Yun et al, 2011). Further, monomerization of SARD1 may facilitate its nuclear localization, as found in Arabidopsis (Zhang et al, 2010).

Chapter 8 Constructing *ICS1 promoter::GUS* reporter *Arabidopsis* plants

Introduction

Currently, it is suggested that the majority of salicylic acid (SA) synthesis in *Arabidopsis* induced by pathogen infection is mediated by Isochorismate Synthase (ICS) activity (Vlot et al, 2009). The ICS activity in *Arabidopsis* is largely due to expression of one gene, *AtICS1* (Wildermuth et al, 2001). Thus, numerous studies have focused on regulatory factors that influence SA accumulation (Dempsey et al, 2011). Among them, several transcription factors were identified that directly regulate *ICS1* expression (Chen et al, 2009a; van Verk et al, 2011; Wang et al, 2015b; Zhang et al, 2010; Zheng et al, 2012).

Ethylene Insensitive 3 (EIN3) and EIN3-like 1 (EIL1) are transcription factors that are known to positively regulate ethylene-dependant gene expression (Solano et al, 1998). A recent report also suggested that EIN3 and EIL1 are negative regulators of *ICS1* expression (Chen et al, 2009a). Accumulation of SA and constant expression of *Pathogenesis-Related* (*PR*) genes were found in *ein3 eil1* double mutant plants without pathogen infection. Further, EIN3 and EIL1 were found to bind the P5 fragment of the *ICS1* promoter, which is -117 to -324 bp upstream of the translational start site, both *in vitro* and *in vivo* (Chen et al, 2009a). WRKY28, a gene induced by avirulent *Pseudomonas syringae* pv *tomato* (*Pst*) infection (Navarro et al, 2004), was found to actively regulate *ICS1* expression in *Arabidopsis* protoplasts (van Verk et al, 2011). Enhanced *ICS1* promoter activity was detected in *Arabidopsis* protoplasts that overexpress *WRKY28*. *In vitro*, WRKY28 was shown to bind two W-box motifs on the *ICS1* promoter at position -445 and -460 (van Verk et al, 2011). In a recent study, a member of the Teosinte Branched 1/Cycloidea/PCF (TCP) family, TCP8, was identified to positively regulate *ICS1* expression (Wang et al, 2015b). TCP8 was shown to bind a GGGCCCAC motif on the *ICS1* promoter at approximately -150 bp upstream of the translational start site. The double knockout plants, *tcp8 tcp9*, were shown to have reduced *ICS1* expression (Wang et al, 2015b). Interestingly, this TCP binding site overlaps the

previously reported EIN3 and EIL1 binding site, suggesting a potential antagonistic interaction between these transcription factors. As mentioned in previous chapters, SARD1 and CBP60g were found to positively regulate *ICS1* expression (Zhang et al, 2010). SARD1 and CBP60g were reported to bind on a previously unidentified motif -1110 to -1280 upstream of the translational start site with high affinity to a GAAATTTTGG motif. A later study suggested that although SARD1 and CBP60g share the same binding motif, they act addictively and are partially redundant in *Arabidopsis* (Wang et al, 2011).

Fusing a promoter with *β-glucuronidase* (*GUS)* is a widely used strategy to study promoter activity (Hull & Devic, 1995). β-glucuronidase catalyses the hydrolysis of a variety of β-glucuronides which are commercially available. Further, the absence of endogenous GUS activity in higher plants allows detection of GUS activity even at low levels in transformed tissue. In addition, tissue specific GUS activity can be visualized using the substrate X-Gluc (Jefferson, 1989). The production and analysis of an *IS1::GUS* fusion would allow discrimination between either the transcriptional or post-transcriptional regulation of *ICS* expression by increased SNO levels.

Here, the *ICS1 promoter* fragment was fused with *GUS* and transferred into the pGWB3 vector (Nakagawa et al, 2007). Subsequently, the construct was transformed into *Arabidopsis* Col-0. GUS activity in successful transformants was then assessed.

Results

A 1500 bp *ICS1* promoter fragment including the 5' untranslated region was amplified from *Arabidopsis* Col-0 gDNA and analysed using an agarose gel (Fig 8.1A, arrow). The fragment was excised from the gel and purified as per protocol. The resulting DNA fragment was transferred into pGWB3 vector (Nakagawa et al, 2007) to fuse with *GUS*. The construct was transferred into *Agrobacterium tumefaciens* GV3101 and subsequently transformed into *Arabidopsis* Col-0 using floral dipping (Clough & Bent, 1998). Successful transgenic plants with kanamycin resistance were selected and later infiltrated by *Psm* ES4326 (OD_{600} = 0.02, Fig 8.1B, "+") or mock treated (10 mM $MgCl_2$, Fig 8.1B, "-") along with a negative control of Col-0 plants. Infected leaves were

collected 24 hours after inoculation and stained using X-Gluc. The GUS activity was visualized after destaining (Fig 8.1B, blue stain). Among 22 individual T1 transgenic plants, GUS activity was detected in 13 plants (Fig 8.1B, plant lines 1, 2, 7, 10, 11, 12, 13, 16, 17, 18, 19, 20 and 21). However, GUS activity was detected in plant lines 7, 10, 11 and 17 with mock treatment. Relatively weak GUS activity was observed in plant lines 1, 12, 13, 16 and 19. Induction of *GUS* expression was observed in plant lines 2, 18, 20 and 21. In Col-0, no GUS activity was observed after pathogen challenge or mock treatment. The copy number of transgene was not determined in the transgenic plants, as it will be determined in T1 generation by calculating Mendelian ratio.

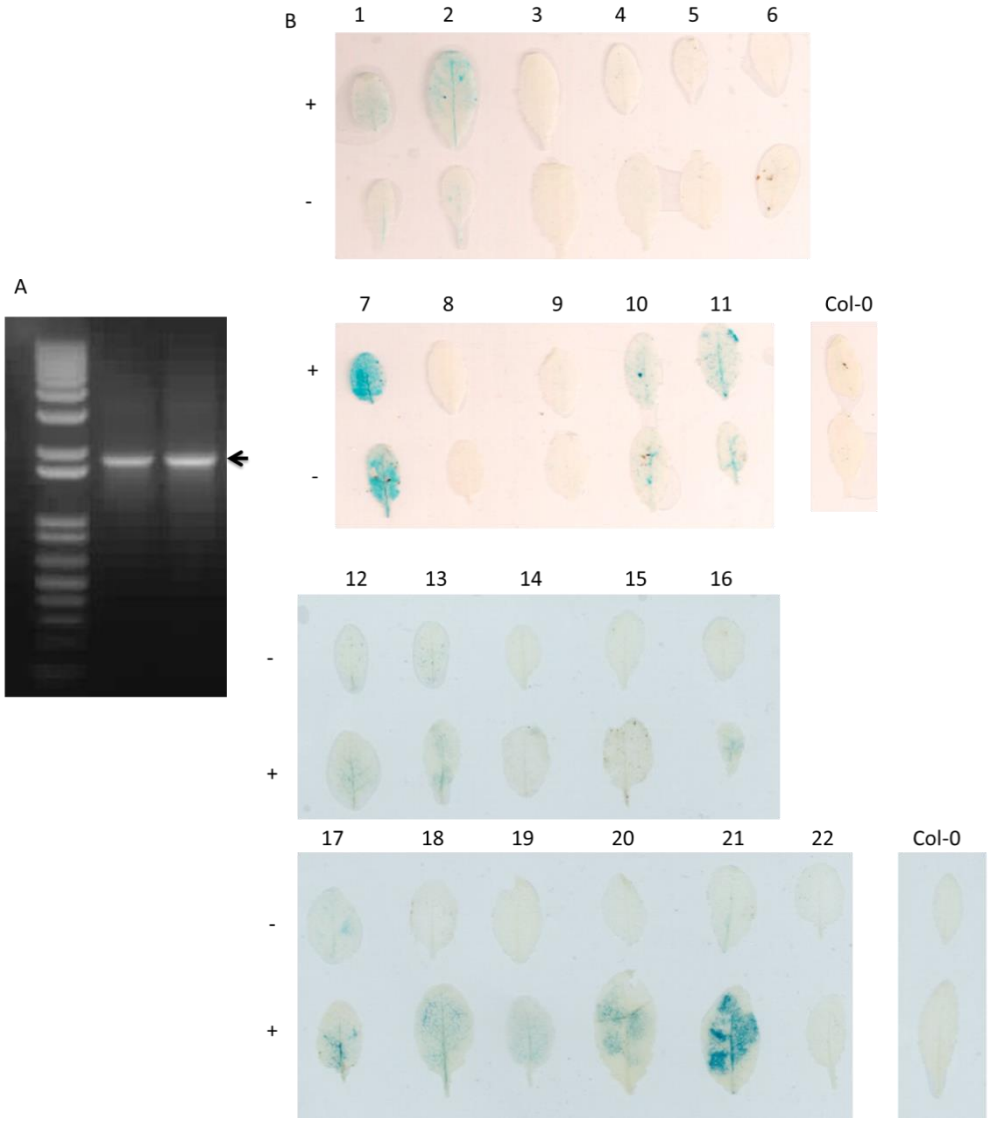

Figure 8.1. Construction of *AtICS1::GUS* Arabidopsis plants. (A) Amplification of *ICS1* promoter

sequence from *Arabidopsis* genomic DNA (gDNA). A 1500 bp *ICS1* promoter fragment was amplified from *Arabidopsis* Col-0 gDNA and analysed using agarose gel. Arrow indicates the DNA band corresponding to 1500 bp. (B) *GUS* expression in T1 transgenic plants 24 hours after pathogen infection. Plant leaves were collected from transgenic *Arabidopsis* Col-0 T1 plants 24 hours after *Pseudomonas syringae* (*Pst*) ES4326 and subsequently stained with X-Gluc (5-bromo-4-chlro-3-inolyl glucuronide). Each transformant is labelled with numbers above. Col-0 plants were used as a negative control. +: Pathogen infected. -: mock treatment. Blue staining indicates GUS activity.

Discussion

The full length *ICS1* promoter region is 3173 bp. We amplified a 1500 bp fragment since it contains all currently confirmed transcription binding site including SARD1/CBP60g (-1110 to -1280). Over 20 successful transformants were isolated following selection on Murashige & Skoog (MS) medium kanamycin plates and subsequently grown on soil. *Psm* ES4326 was used to inoculate transformed *Arabidopsis* leaves along with Col-0. In our hypothesis, the *ICS1* promoter will be triggered due to pathogen infection to induce *GUS* expression and the GUS activity could then be observed using its substrate, X-Gluc. GUS activity should not be detected in Col-0 or transgenic plants infiltrated by $MgCl_2$. 4 out of 22 transgenic plants fit our hypothesis (Fig 8.1B). It is expected that no GUS activity was detected in Arabidopsis Col-0 due to the absence of *GUS* in its genome. Integrating *ICS1 promoter::GUS* into the *Arabidopsis* genome mediated by *A. tumefaciens* is completely random, thus, the GUS activity in transgenic plants is largely dependent on the genomic location of the transgene insert (Gelvin, 2003). Several transgenic plants showed no or low *GUS* expression after pathogen infection, indicating that the T-DNA may be inserted into a low expression region on the genome. Also, 4 transgenic plants showed GUS activity without pathogen induction suggested the transgene was inserted into a genome region where there is a high level of transcription.

Arabidopsis ICS1 promoter::GUS plants will be useful tools to study *ICS1* promoter activity. To directly assess *ICS1* expression under high cellular SNO conditions, the *ICS1 promoter::GUS* transgene needs to be crossed into a *gsnor1-3* genetic background and GUS activity to compare to

that produced from the same transgene in a wild-type background. Since SA accumulation in *gsnor1-3* plants was reduced (Feechan et al, 2005), it is anticipated that *ICS1* transcription might be reduced in these plants. In addition, *ICS1 promoter::GUS* plants can be used to test *ICS1* promoter activity and SA biosynthesis with variables, for example pathogens and temperatures.

Chapter 9 Discussion and conclusion

Salicylic acid (SA) plays a critical role in inducing both local and systemic disease resistance against pathogen infection in Arabidopsis (Vlot et al, 2009). Numerous efforts were made to study SA biosynthesis and metabolism (Dempsey et al, 2011). Isochorismate synthase 1 (ICS1) was identified previously that is a key enzyme in SA synthesis in response to pathogen infection (Wildermuth et al, 2001). Recently, several transcription factors were identified to control *ICS1* expression including CBP60g, SARD1, WRKY28, TCP8 and NAC019 (Chen et al, 2009a; Wang et al, 2011; Wang et al, 2015b; Zhang et al, 2010; Zheng et al, 2012). Nitric oxide (NO) has been recognized as a signal molecule that contributes to plant immunity for decades (Delledonne et al, 1998; Durner et al, 1998). However, *S*-nitrosoglutathione (SNO) is believed to be a more stable carrier for NO bioactivity (Malik et al, 2011). Previously we identified that GSNO reductase (GSNOR) is critical in maintaining cellular SNO homeostasis. Loss of GSNOR function in *Arabidopsis* results in reduced SA accumulation and compromised plant disease resistance on multiple levels (Feechan et al, 2005). To identify the link between cellular SNO levels and SA biosynthesis, we investigated a potential regulatory role of NO on SARD1, a transcriptional activator of *ICS1*.

It has been suggested previously that SARD1/CBP60g node is located between EDS1/PAD4 and *ICS1* (Wang et al, 2011). In addition, we have reported that R-gene mediated defence response was compromised in *atgsnor1-3* plants (Feechan et al, 2005). It is reasonable to assume that in *atgsnor1-3* plants, *SARD1*, *CBP60g* and *ICS1* expression were delayed and reduced after pathogen infection, which may be due to compromised *R*-gene mediated response in high cellular SNO levels. Recombinant SARD1 was expressed and purified from *E. coli*. In subsequent experiments, NO was shown to regulate SARD1 DNA binding activity through *S*-nitrosylation on C438 *in vitro*. To determine if SNO levels modulate ICS transcription, the *ICS1 promoter* was fused to a *GUS* reporter gene and transferred into *Arabidopsis*. Successful transgenic plants were obtained and GUS activity was confirmed, providing a future tool to address this fundamental question. *ICS1::GUS* plants can be crossed with *gsnor1-3 plants*, and test the *ICS1* promoter activity using

GUS stain after pathogen challenging in high cellular SNO level. Based on our *in vitro* result, we hypothesize the *ICS1* promoter activity will be reduced in *gsnor1-3* plants.

NO was demonstrated to modulate plant disease resistance via *S*-nitrosylation of proteins involved in plant immune signalling. *S*-nitrosylation of SA-binding protein 3 (SABP3) at Cys280 resulted in inhibition of its SA binding and carbonic anhydrase (CA) activity and negatively regulated plant immunity, suggesting a potential feed-back loop modulated by NO (Wang et al, 2009b). SNO also has been shown to promote pathogen induced hypersensitive cell death in plants including those with reduced SA accumulation (Yun et al, 2011). Furthermore, *S*-nitrosylation of NADPH oxidase AtRBOHD at Cys890 inhibits its activity resulting in decreased reactive oxygen intermediate (ROI) accumulation (Yun et al, 2011). Taken together, these findings suggest a vital role of NO governing plant cell death both positively and negatively. NO has also been shown to facilitate oligomerization of non-expresser of pathogenesis-related genes 1 (NPR1) and contribute to the maintenance of NPR1 oligomer-monomer homeostasis, which is key in NPR1-dependent immunity (Feechan et al, 2005; Tada et al, 2008). In addition, *S*-nitrosylation and S-glutathionylation of TGA1 was demonstrated to increase its DNA binding activity *in vitro* (Lindermayr et al, 2010).

Thus, despite significant progress in understanding how NO modulates plant SA signaling, there is little knowledge on how NO regulates SA accumulation. Our results provide the first demonstration that *S*-nitrosylation of a known transcription activator, SARD1, resulting in inhibition of its DNA binding activity, may supress *ICS1* expression and thereby reduce SA biosynthesis during plant immune function. This finding in part might explain the reduction in SA accumulation found in plants with high SNO content (Feechan et al, 2005). In addition, SA was reported to trigger NO synthesis (Zottini et al, 2007), and constant SNO accumulation was observed in plants infected by pathogens along with accumulation of SA (Yun et al, 2011). However, over-accumulation of SA results gratuitous cell death and inhibition of plant growth (Rivas-San Vicente & Plasencia, 2011). In this context, *S*-nitrosylation of SARD1 may provide a feed-back loop to precisely control the magnitude of SA accumulation. It is noteworthy that as a transcription factor, SARD1 may not only regulate expression of *ICS1*. A bioinformatics study

suggested that clusters of genes enriched with a GAAATT motif within their promoter sequence were down-regulated in *sard1 cbp60g* double mutant plants (Truman & Glazebrook, 2012), suggesting additional genes that may be regulated by SARD1. A recent ChIP-seq revealed that SARD1 not only binds to *ICS1* promoter during plant defense response, but also bind to a number of genes involve in SAR, PTI and ETI (Sun et al, 2015), including positive and negative regulators. Thus, *S*-nitrosylation of SARD1 might regulate the expression of numerous other genes in addition to *ICS1*. With information of known targets for SARD1, ChIP-seq can be used to evaluate SARD1 binding activity to its targets under high SNO environment.

Redox regulation has been shown to regulate transcription in both plants and animals (Brigelius-Flohe & Flohe, 2011; Dietz, 2014). However, *S*-nitrosylation has only been suggested to regulate the activity of R2R3 MYB transcription factors, as these proteins have been shown to undergo this modification *in vitro* (Serpa et al, 2007; Tavares et al, 2014). Our results suggest an additional class of transcription factors is also regulated by NO. SARD1 belongs to a plant specific calmodulin-binding protein family CBP60 (Zhang et al, 2010), which have only recently been identified as transcription factors. These features may suggest a novel structure of this class of transcription factors, and possibly a novel regulatory mechanism mediated by NO.

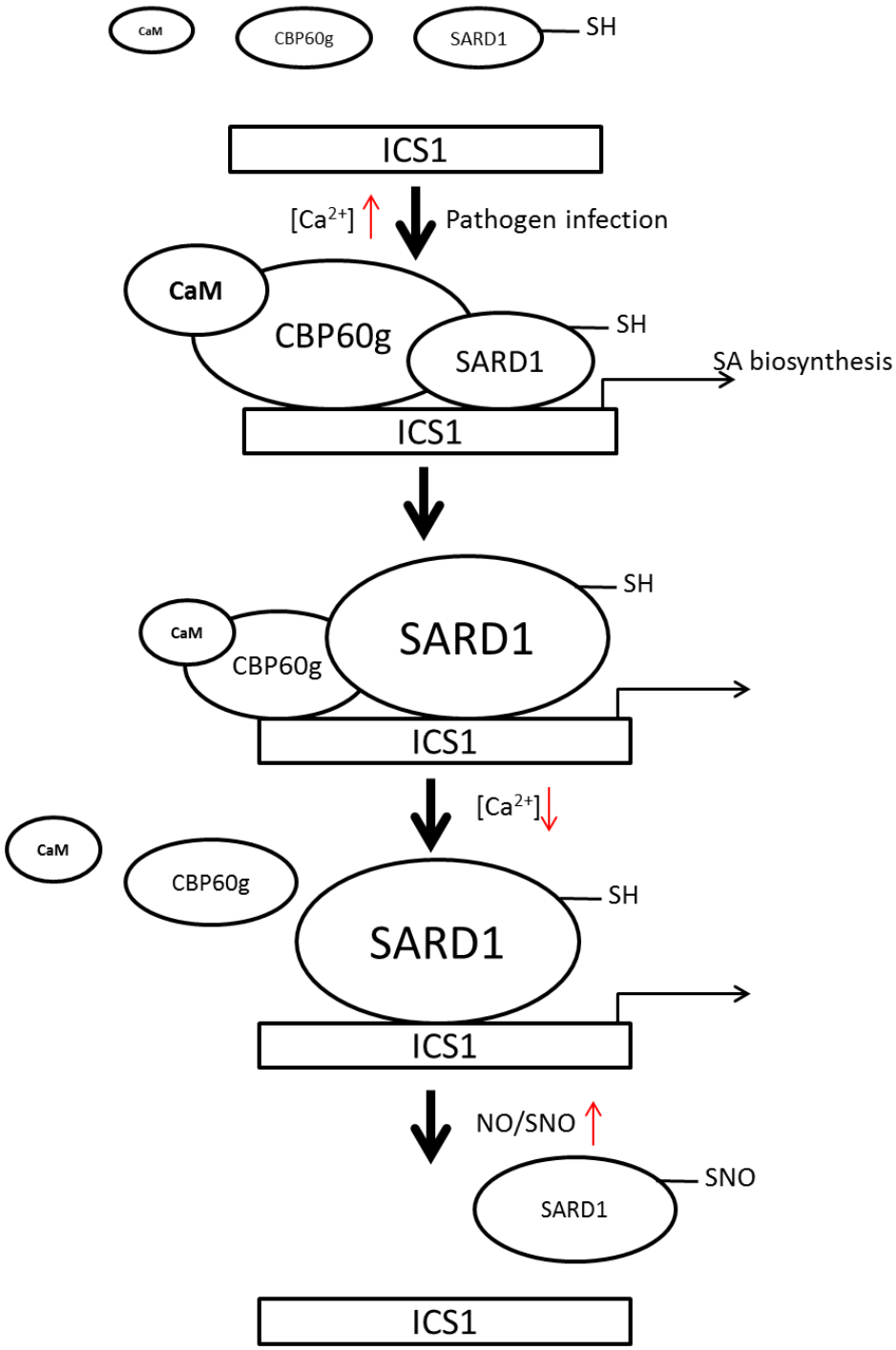

Figure 9.1 Model for control of *ICS1* expression by CBP60g, SARD1 and NO during plant defence response. SARD1 and CBP60g act largely redundantly to active ICS1 expression during plant defence response. At early stage, CBP60g is activated by calmodulin (CaM) binding and bind to *ICS1* promoter and induce SA synthesis, while SARD1 has less effect due to its low expression. At later stage, CBP60g and SARD1 bind to ICS promoter but SARD1 has greater

effect. As cellular calcium level decreased, CBP60g activity may be supressed while SARD1 bind to *ICS1* promoter to prolong SA synthesis. Binding between SARD1 and *ICS1* promoter may be inhibited by *S*-nitrosylation of SARD1 result in suppression of SA synthesis and fading of plant defence response once pathogen infection is contained. Circles indicate gene expression level of *SARD1* and *CBP60g*.

Here, we propose a model (Fig 9.1) the how NO may modulate SARD1 activity during plant immune response. It is showed previously that Ca^{2+} flux after PAMP recognition facilitates binding between CaM and CBP60g result in SA synthesis, while *SARD1* expression is low (Wang et al, 2009a). As plant immune response progress, CBP60g activity is supressed due to decreased Ca^{2+} level and expression of SARD1 is increased (Wang et al, 2011). Previously we have reported that cellular NO level is increased during plant immune response (Yun et al, 2011). It is possible the increased cellular NO level may *S*-nitrosylate SARD1 to inhibit its DNA binding activity result in turning off plant defence response. In this occasion, NO may act as a negative control preventing uncontrolled immune response in plant.

To further investigate this area, *Arabidopsis* plants expressing tagged-SARD1 in both wild-type and *gsnor1-3* plants first need to be obtained. Subsequently, the *in vivo* biotin-switch assay needs to be performed to demonstrate SARD1 is *S*-nitrosylated in *vivo*. Transgenic plants expressing SARD1 C438S also need to be included in the *S*-nitrosylation assay, to establish if C438 is the site of *S*-nitrosylation *in vivo*. Furthermore, to investigate if SARD1 DNA binding activity is impaired by *S*-nitrosylation *in vivo*, chromatin immunoprecipitation (ChIP) assays need to be performed to determine a possible difference in SARD1 DNA binding ability between wild-type and *gsnor1-3* plants. In addition, since we speculate that SARD1 C438S is insensitive to NO regulation, overexpression of SARD1 C438S may result in improved pathogen resistance than overexpression of wild-type SARD1. To test this, pathogen assays will need to be performed in *Arabidopsis* plants overexpressing the different SARD1 proteins.

Taken together, our results might partly explain the observation that reduced SA levels are found in *gsnor1-3* plants. Further, they reveal a new redox-switch target that is regulated by NO. In

addition, we suggested a potential feed-back mechanism for the regulation of SA synthesis which may also contribute to maintaining the delicate balance between plant immunity and cell death/growth/development.

References

Aarts N, Metz M, Holub E, Staskawicz BJ, Daniels MJ, Parker JE (1998) Different requirements for EDS1 and NDR1 by disease resistance genes define at least two R gene-mediated signaling pathways in Arabidopsis. *Proceedings of the National Academy of Sciences of the United States of America* **95:** 10306-10311

Abate C, Patel L, Rauscher F, Curran T (1990) Redox regulation of fos and jun DNA-binding activity in vitro. *Science* **249:** 1157-1161

Alderton WK, Cooper CE, Knowles RG (2001) Nitric oxide synthases: structure, function and inhibition. *Biochemal Journal* **357:** 593-615

An C, Mou Z (2011) Salicylic acid and its function in plant immunity. *Journal of Integrative Plant Biology* **53:** 412-428

Astier J, Lindermayr C (2012) Nitric oxide-dependent posttranslational modification in plants: an update. *International Journal of Molecular Sciences* **13:** 15193-15208

Attaran E, Zeier TE, Griebel T, Zeier J (2009) Methyl salicylate production and jasmonate signaling are not essential for systemic acquired resistance in Arabidopsis. *The Plant cell* **21:** 954-971

Babbs CF, Pham JA, Coolbaugh RC (1989) Lethal Hydroxyl Radical Production in Paraquat-Treated Plants. *Plant Physiology* **90:** 1267-1270

Basu S, Keszler A, Azarova NA, Nwanze N, Perlegas A, Shiva S, Broniowska KA, Hogg N, Kim-Shapiro DB (2010) A novel role for cytochrome c: Efficient catalysis of S-nitrosothiol formation. *Free Radical Biology & Medicine* **48:** 255-263

Belfield EJ, Hughes RK, Tsesmetzis N, Naldrett MJ, Casey R (2007) The gateway pDEST17 expression vector encodes a -1 ribosomal frameshifting sequence. *Nucleic Acids Research* **35:** 1322-1332

Benamar A, Rolletschek H, Borisjuk L, Avelange-Macherel MH, Curien G, Mostefai HA, Andriantsitohaina R, Macherel D (2008) Nitrite-nitric oxide control of mitochondrial respiration at the frontier of anoxia. *Biochimica et Biophysica Acta* **1777:** 1268-1275

Benhar M, Forrester MT, Stamler JS (2009) Protein denitrosylation: enzymatic mechanisms and cellular functions. *Nature Reviews Molecular Cell biology* **10:** 721-732

Betts MJ, Russell RB (2003) Amino Acid Properties and Consequences of Substitutions. 289-316

Blokhina O, Fagerstedt KV (2010) Oxidative metabolism, ROS and NO under oxygen deprivation. *Plant Physiology and Biochemistry : PPB / Societe francaise de physiologie vegetale* **48:** 359-373

Brendeford EM, Andersson KB, Gabrielsen OS (1998) Nitric oxide (NO) disrupts specific DNA binding of the transcription factor c-Myb in vitro. *FEBS Letters* **425:** 52-56

Brigelius-Flohe R, Flohe L (2011) Basic principles and emerging concepts in the redox control of transcription factors. *Antioxidants & Redox Signaling* **15:** 2335-2381

Cao H, Bowling SA, Gordon AS, Dong X (1994) Characterization of an Arabidopsis Mutant That Is Nonresponsive to Inducers of Systemic Acquired Resistance. *The Plant Cell* **6:** 1583-1592

Catinot J, Buchala A, Abou-Mansour E, Metraux JP (2008) Salicylic acid production in response to biotic and abiotic stress depends on isochorismate in Nicotiana benthamiana. *FEBS Letters* **582:** 473-478

Cecconi D, Orzetti S, Vandelle E, Rinalducci S, Zolla L, Delledonne M (2009) Protein nitration during defense response in Arabidopsis thaliana. *Electrophoresis* **30:** 2460-2468

Chadha KC, Brown SA (1974) Biosynthesis of phenolic acids in tomato plants infected withAgrobacterium tumefaciens. *Canadian Journal of Botany* **52:** 2041-2047

Chen H, Xue L, Chintamanani S, Germain H, Lin H, Cui H, Cai R, Zuo J, Tang X, Li X, Guo H, Zhou JM (2009a) ETHYLENE INSENSITIVE3 and ETHYLENE INSENSITIVE3-LIKE1 repress SALICYLIC ACID INDUCTION DEFICIENT2 expression to negatively regulate plant innate immunity in Arabidopsis. *The Plant Cell* **21:** 2527-2540

Chen R, Sun S, Wang C, Li Y, Liang Y, An F, Li C, Dong H, Yang X, Zhang J, Zuo J (2009b) The Arabidopsis PARAQUAT RESISTANT2 gene encodes an S-nitrosoglutathione reductase that is a key regulator of cell death. *Cell Research* **19:** 1377-1387

Chen Z, Silva H, Klessig DF (1993) Active oxygen species in the induction of plant systemic acquired resistance by salicylic acid. *Science* **262:** 1883-1886

Clough SJ, Bent AF (1998) Floral dip: a simplified method for Agrobacterium-mediated transformation of Arabidopsis thaliana. *The Plant Journal : for cell and molecular biology* **16:** 735-743

Cochrane FC, Davin LB, Lewis NG (2004) The Arabidopsis phenylalanine ammonia lyase gene family: kinetic characterization of the four PAL isoforms. *Phytochemistry* **65:** 1557-1564

Corpas FJ, Barroso JB, Carreras A, Valderrama R, Palma JM, Leon AM, Sandalio LM, del Rio LA (2006) Constitutive arginine-dependent nitric oxide synthase activity in different organs of pea seedlings during plant development. *Planta* **224:** 246-254

Corpas FJ, Palma JM, del Rio LA, Barroso JB (2009) Evidence supporting the existence of L-arginine-dependent nitric oxide synthase activity in plants. *The New Phytologist* **184:** 9-14

Corpet F (1988) Multiple sequence alignment with hierarchical clustering. *Nucleic Acids Research* **16:** 10881-10890

Cristovao AC, Choi DH, Baltazar G, Beal MF, Kim YS (2009) The role of NADPH oxidase 1-derived reactive oxygen species in paraquat-mediated dopaminergic cell death. *Antioxidants & Redox Signaling* **11:** 2105-2118

D'Autreaux B, Toledano MB (2007) ROS as signalling molecules: mechanisms that generate specificity in ROS homeostasis. *Nature Reviews Molecular Cell Biology* **8:** 813-824

del Rio LA, Corpas FJ, Barroso JB (2004) Nitric oxide and nitric oxide synthase activity in plants. *Phytochemistry* **65:** 783-792

Delaney TP, Uknes S, Vernooij B, Friedrich L, Weymann K, Negrotto D, Gaffney T, Gut-Rella M, Kessmann H, Ward E, Ryals J (1994) A central role of salicylic Acid in plant disease resistance. *Science* **266:** 1247-1250

Delledonne M, Xia Y, Dixon RA, Lamb C (1998) Nitric oxide functions as a signal in plant disease resistance. *Nature* **394:** 585-588

Dempsey DA, Vlot AC, Wildermuth MC, Klessig DF (2011) Salicylic Acid biosynthesis and metabolism. *The Arabidopsis book / American Society of Plant Biologists* **9:** e0156

Despres C, Chubak C, Rochon A, Clark R, Bethune T, Desveaux D, Fobert PR (2003) The Arabidopsis NPR1 Disease Resistance Protein Is a Novel Cofactor That Confers Redox Regulation of DNA Binding Activity to the Basic Domain/Leucine Zipper Transcription Factor TGA1. *The Plant Cell* **15:** 2181-2191

Dietrich JB (2013) The MEF2 family and the brain: from molecules to memory. *Cell and Tissue Research* **352:** 179-190

Dietz KJ (2014) Redox regulation of transcription factors in plant stress acclimation and development. *Antioxidants & Redox Signaling* **21:** 1356-1372

Dong X (2004) NPR1, all things considered. *Current Opinion in Plant Biology* **7:** 547-552

Du H, Klessig DF (1997) Identification of a Soluble, High-Affinity Salicylic Acid-Binding Protein in Tobacco. *Plant Physiology* **113:** 1319-1327

Durner J, Klessig DF (1995) Inhibition of ascorbate peroxidase by salicylic acid and 2,6-dichloroisonicotinic acid, two inducers of plant defense responses. *Proceedings of the National Academy of Sciences of the United States of America* **92:** 11312-11316

Durner J, Shah J, Klessig DF (1997) Salicylic acid and disease resistance in plants. *Trends in Plant Science* **2:** 266-274

Durner J, Wendehenne D, Klessig DF (1998) Defense gene induction in tobacco by nitric oxide, cyclic GMP, and cyclic ADP-ribose. *Proceedings of the National Academy of Sciences of the United States of America* **95:** 10328-10333

Durrant WE, Dong X (2004) Systemic acquired resistance. *Annual Review of Phytopathology* **42:** 185-209

Earley KW, Haag JR, Pontes O, Opper K, Juehne T, Song K, Pikaard CS (2006) Gateway-compatible vectors for plant functional genomics and proteomics. *The Plant Journal* **45:** 616-629

El-Basyouni SZ, Chen D, Ibrahim R, Neish A, Towers G (1964) The biosynthesis of hydroxybenzoic acids in higher plants. *Phytochemistry* **3:** 485-492

Falk A, Feys BJ, Frost LN, Jones JDG, Daniels MJ, Parker JE (1999) EDS1, an essential component of R gene-mediated disease resistance in Arabidopsis has homology to eukaryotic lipases. *Proceedings of the National Academy of Sciences* **96:** 3292-3297

Feechan A, Kwon E, Yun BW, Wang Y, Pallas JA, Loake GJ (2005) A central role for S-nitrosothiols in plant disease resistance. *Proceedings of the National Academy of Sciences of the United States of America* **102:** 8054-8059

Feys BJ, Moisan LJ, Newman MA, Parker JE (2001) Direct interaction between the Arabidopsis disease resistance signaling proteins, EDS1 and PAD4. *The EMBO Journal* **20:** 5400-5411

Feys BJ, Wiermer M, Bhat RA, Moisan LJ, Medina-Escobar N, Neu C, Cabral A, Parker JE (2005) Arabidopsis SENESCENCE-ASSOCIATED GENE101 stabilizes and signals within an ENHANCED DISEASE SUSCEPTIBILITY1 complex in plant innate immunity. *The Plant Cell* **17:** 2601-2613

Foresi N, Correa-Aragunde N, Parisi G, Calo G, Salerno G, Lamattina L (2010) Characterization of a Nitric Oxide Synthase from the Plant Kingdom: NO Generation from the Green Alga Ostreococcus tauri Is Light Irradiance and Growth Phase Dependent. *The Plant Cell* **22:** 3816-3830

Forouhar F, Yang Y, Kumar D, Chen Y, Fridman E, Park SW, Chiang Y, Acton TB, Montelione GT, Pichersky E, Klessig DF, Tong L (2005) Structural and biochemical studies identify tobacco SABP2 as a methyl salicylate esterase and implicate it in plant innate immunity. *Proceedings of the National Academy of Sciences of the United States of America* **102:** 1773-1778

Forrester MT, Foster MW, Benhar M, Stamler JS (2009) Detection of protein S-nitrosylation with the biotin-switch technique. *Free Radical Biology & Medicine* **46:** 119-126

Foster MW, Liu L, Zeng M, Hess DT, Stamler JS (2009) A genetic analysis of nitrosative stress. *Biochemistry* **48:** 792-799

Frederickson Matika DE, Loake GJ (2014) Redox regulation in plant immune function. *Antioxidants & Redox Signaling* **21:** 1373-1388

Fried M, Crothers DM (1981) Equilibria and kinetics of lac repressor-operator interactions by polyacrylamide gel electrophoresis. *Nucleic Acids Research* **9:** 6505-6525

Fu ZQ, Dong X (2013) Systemic acquired resistance: turning local infection into global defense. *Annual Review of Plant Biology* **64:** 839-863

Fu ZQ, Yan S, Saleh A, Wang W, Ruble J, Oka N, Mohan R, Spoel SH, Tada Y, Zheng N, Dong X (2012) NPR3 and NPR4 are receptors for the immune signal salicylic acid in plants. *Nature* **486:** 228-232

Gaffney T, Friedrich L, Vernooij B, Negrotto D, Nye G, Uknes S, Ward E, Kessmann H, Ryals J (1993) Requirement of salicylic Acid for the induction of systemic acquired resistance. *Science* **261:** 754-756

Garcion C, Lohmann A, Lamodiere E, Catinot J, Buchala A, Doermann P, Metraux JP (2008) Characterization and biological function of the ISOCHORISMATE SYNTHASE2 gene of Arabidopsis. *Plant Physiology* **147:** 1279-1287

Gaupels F, Spiazzi-Vandelle E, Yang D, Delledonne M (2011) Detection of peroxynitrite accumulation in Arabidopsis thaliana during the hypersensitive defense response. *Nitric oxide* **25:** 222-228

Gelvin SB (2003) Agrobacterium-Mediated Plant Transformation: the Biology behind the "Gene-Jockeying" Tool. *Microbiology and Molecular Biology Reviews* **67:** 16-37

Giustarini D, Milzani A, Aldini G, Carini M, Rossi R, Dalle-Donne I (2005) S-nitrosation versus S-glutathionylation of protein sulfhydryl groups by S-nitrosoglutathione. *Antioxidants & Redox Signaling* **7:** 930-939

Godber BL, Doel JJ, Sapkota GP, Blake DR, Stevens CR, Eisenthal R, Harrison R (2000) Reduction of nitrite to nitric oxide catalyzed by xanthine oxidoreductase. *The Journal of Biological Chemistry* **275:** 7757-7763

Greenberg JT, Yao N (2004) The role and regulation of programmed cell death in plant-pathogen interactions. *Cellular Microbiology* **6:** 201-211

Gupta KJ, Fernie AR, Kaiser WM, van Dongen JT (2011) On the origins of nitric oxide. *Trends in Plant Science* **16:** 160-168

Gupta KJ, Stoimenova M, Kaiser WM (2005) In higher plants, only root mitochondria, but not leaf mitochondria reduce nitrite to NO, in vitro and in situ. *Journal of Experimental Botany* **56:** 2601-2609

Hadacek F, Bachmann G, Engelmeier D, Chobot V (2011) Hormesis and a Chemical Raison D'etre for Secondary Plant Metabolites. *Dose Response : a publication of International Hormesis Society* **9:** 79-116

Hara MR, Thomas B, Cascio MB, Bae BI, Hester LD, Dawson VL, Dawson TM, Sawa A, Snyder SH (2006) Neuroprotection by pharmacologic blockade of the GAPDH death cascade. *Proceedings of the National Academy of Sciences of the United States of America* **103:** 3887-3889

Harper S, Speicher DW (2011) Purification of proteins fused to glutathione S-transferase. *Methods in Molecular Biology* **681:** 259-280

Harrison AJ, Yu M, Gardenborg T, Middleditch M, Ramsay RJ, Baker EN, Lott JS (2006) The structure of MbtI from Mycobacterium tuberculosis, the first enzyme in the biosynthesis of the siderophore mycobactin, reveals it to be a salicylate synthase. *Journal of Bacteriology* **188:** 6081-6091

Harrison R (2002) Structure and function of xanthine oxidoreductase: where are we now? *Free Radical Biology and Medicine* **33:** 774-797

He Y, Tang RH, Hao Y, Stevens RD, Cook CW, Ahn SM, Jing L, Yang Z, Chen L, Guo F, Fiorani F, Jackson RB, Crawford NM, Pei ZM (2004) Nitric oxide represses the Arabidopsis floral transition. *Science* **305:** 1968-1971

Hedberg JJ, Griffiths WJ, Nilsson SJF, Hoog J-O (2003) Reduction of S-nitrosoglutathione by human alcohol dehydrogenase 3 is an irreversible reaction as analysed by electrospray mass spectrometry. *European Journal of Biochemistry* **270:** 1249-1256

Heine GF, Hernandez JM, Grotewold E (2004) Two cysteines in plant R2R3 MYB domains participate in REDOX-dependent DNA binding. *The Journal of Biological Chemistry* **279:** 37878-37885

Hellman LM, Fried MG (2007) Electrophoretic mobility shift assay (EMSA) for detecting protein-nucleic acid interactions. *Nature Protocols* **2:** 1849-1861

Hengen PN (1995) Purification of His-Tag fusion proteins from Escherichia coli. *Trends in Biochemical Sciences* **20:** 285-286

Hess DT, Matsumoto A, Kim SO, Marshall HE, Stamler JS (2005) Protein S-nitrosylation: purview and parameters. *Nature Reviews Molecular Cell Biology* **6:** 150-166

Hoang CV, Chapman KD (2002) Biochemical and molecular inhibition of plastidial carbonic anhydrase reduces the incorporation of acetate into lipids in cotton embryos and tobacco cell suspensions and leaves. *Plant Physiology* **128:** 1417-1427

Hoeren FU, Dolferus R, Wu Y, Peacock WJ, Dennis ES (1998) Evidence for a role for AtMYB2 in the

induction of the Arabidopsis alcohol dehydrogenase gene (ADH1) by low oxygen. *Genetics* **149:** 479-490

Huang J, Gu M, Lai Z, Fan B, Shi K, Zhou YH, Yu JQ, Chen Z (2010) Functional analysis of the Arabidopsis PAL gene family in plant growth, development, and response to environmental stress. *Plant Physiology* **153:** 1526-1538

Hull GA, Devic M (1995) The beta-glucuronidase (gus) reporter gene system. Gene fusions; spectrophotometric, fluorometric, and histochemical detection. *Methods in Molecular Biology* **49:** 125-141

Jaffrey SR, Snyder SH (2001) The biotin switch method for the detection of S-nitrosylated proteins. *Science's STKE : Signal Transduction Knowledge Environment* **2001:** pl1

Jansson EA, Huang L, Malkey R, Govoni M, Nihlen C, Olsson A, Stensdotter M, Petersson J, Holm L, Weitzberg E, Lundberg JO (2008) A mammalian functional nitrate reductase that regulates nitrite and nitric oxide homeostasis. *Nature Chemical Biology* **4:** 411-417

Jefferson RA (1989) The GUS reporter gene system. *Nature* **342:** 837-838

Jensen DE, Belka GK, Bois GCD (1998) S-Nitrosoglutathione is a substrate for rat alcohol dehydrogenase class III isoenzyme. *Biochemical Journal* **331:** 659-668

Ji Y, Toader V, Bennett BM (2002) Regulation of microsomal and cytosolic glutathione S-transferase activities by S-nitrosylation. *Biochemical Pharmacology* **63:** 1397-1404

Jin JB, Jin YH, Lee J, Miura K, Yoo CY, Kim WY, Van Oosten M, Hyun Y, Somers DE, Lee I, Yun DJ, Bressan RA, Hasegawa PM (2008) The SUMO E3 ligase, AtSIZ1, regulates flowering by controlling a salicylic acid-mediated floral promotion pathway and through affects on FLC chromatin structure. *The Plant Journal* **53:** 530-540

Jones JD, Dangl JL (2006) The plant immune system. *Nature* **444:** 323-329

Kachroo P, Shanklin J, Shah J, Whittle EJ, Klessig DF (2001) A fatty acid desaturase modulates the activation of defense signaling pathways in plants. *Proceedings of the National Academy of Sciences of the United States of America* **98:** 9448-9453

Kaiser W, Brendle-Behnisch E (1995) Acid-base-modulation of nitrate reductase in leaf tissues. *Planta* **196**

Klämbt HD (1962) Conversion in Plants of Benzoic Acid to Salicylic Acid and its βd-Glucoside. *Nature* **196:** 491-491

Kneeshaw S, Gelineau S, Tada Y, Loake GJ, Spoel SH (2014) Selective protein denitrosylation activity of

Thioredoxin-h5 modulates plant Immunity. *Molecular Cell* **56:** 153-162

Kolbert Z, Bartha B, Erdei L (2008) Exogenous auxin-induced NO synthesis is nitrate reductase-associated in Arabidopsis thaliana root primordia. *Journal of Plant Physiology* **165:** 967-975

Kolbert Z, Ortega L, Erdei L (2010) Involvement of nitrate reductase (NR) in osmotic stress-induced NO generation of Arabidopsis thaliana L. roots. *Journal of Plant Physiology* **167:** 77-80

Kroncke KD, Klotz LO (2009) Zinc fingers as biologic redox switches? *Antioxidants & Redox Signaling* **11:** 1015-1027

Kubienova L, Kopecny D, Tylichova M, Briozzo P, Skopalova J, Sebela M, Navratil M, Tache R, Luhova L, Barroso JB, Petrivalsky M (2013) Structural and functional characterization of a plant S-nitrosoglutathione reductase from Solanum lycopersicum. *Biochimie* **95:** 889-902

Kwon E, Feechan A, Yun BW, Hwang BH, Pallas JA, Kang JG, Loake GJ (2012) AtGSNOR1 function is required for multiple developmental programs in Arabidopsis. *Planta* **236:** 887-900

Lane D, Prentki P, Chandler M (1992) Use of gel retardation to analyze protein-nucleic acid interactions. *Microbiological Reviews* **56:** 509-528

Lee U, Wie C, Fernandez BO, Feelisch M, Vierling E (2008) Modulation of nitrosative stress by S-nitrosoglutathione reductase is critical for thermotolerance and plant growth in Arabidopsis. *The Plant Cell* **20:** 786-802

Lindermayr C, Saalbach G, Durner J (2005) Proteomic identification of S-nitrosylated proteins in Arabidopsis. *Plant Physiology* **137:** 921-930

Lindermayr C, Sell S, Muller B, Leister D, Durner J (2010) Redox regulation of the NPR1-TGA1 system of Arabidopsis thaliana by nitric oxide. *The Plant Cell* **22:** 2894-2907

Liu L, Hausladen A, Zeng M, Que L, Heitman J, Stamler JS (2001) A metabolic enzyme for S-nitrosothiol conserved from bacteria to humans. *Nature* **410:** 490-494

Loake G, Grant M (2007) Salicylic acid in plant defence--the players and protagonists. *Current Opinion in Plant Biology* **10:** 466-472

Malik SI, Hussain A, Yun BW, Spoel SH, Loake GJ (2011) GSNOR-mediated de-nitrosylation in the plant defence response. *Plant Science* **181:** 540-544

Marino SM, Gladyshev VN (2011) Redox biology: computational approaches to the investigation of functional cysteine residues. *Antioxidants & Redox Signaling* **15:** 135-146

Marino SM, Gladyshev VN (2012) Analysis and functional prediction of reactive cysteine residues. *The*

Journal of Biological Chemistry **287:** 4419-4425

Martínez C, Pons E, Prats G, León J (2004) Salicylic acid regulates flowering time and links defence responses and reproductive development. *The Plant Journal* **37:** 209-217

Mauch-Mani B, Slusarenko AJ (1996) Production of Salicylic Acid Precursors Is a Major Function of Phenylalanine Ammonia-Lyase in the Resistance of Arabidopsis to Peronospora parasitica. *The Plant Cell* **8:** 203-212

May MJ, Vernoux T, Leaver C, Montagu MV, Inze D (1998) Glutathione homeostasis in plants: implications for environmental sensing and plant development. *Journal of Experimental Botany* **49:** 649-667

Mercado-Blanco J, van der Drift KM, Olsson PE, Thomas-Oates JE, van Loon LC, Bakker PA (2001) Analysis of the pmsCEAB gene cluster involved in biosynthesis of salicylic acid and the siderophore pseudomonine in the biocontrol strain Pseudomonas fluorescens WCS374. *Journal of Bacteriology* **183:** 1909-1920

Meyer C, Stöhr C (2004) Soluble and Plasma Membrane-bound Enzymes Involved in Nitrate and Nitrite Metabolism. *Photosynthetic Nitrogen Assimilation and Associated Carbon and Respiratory Metabolism***:** 49-62

Moche M, Stremlau S, Hecht L, Gobel C, Feussner I, Stohr C (2010) Effect of nitrate supply and mycorrhizal inoculation on characteristics of tobacco root plasma membrane vesicles. *Planta* **231:** 425-436

Mou Z, Fan W, Dong X (2003) Inducers of Plant Systemic Acquired Resistance Regulate NPR1 Function through Redox Changes. *Cell* **113:** 935-944

Mur LA, Mandon J, Persijn S, Cristescu SM, Moshkov IE, Novikova GV, Hall MA, Harren FJ, Hebelstrup KH, Gupta KJ (2013) Nitric oxide in plants: an assessment of the current state of knowledge. *AoB plants* **5:** pls052

Myrset AH, Bostad A, Jamin N, Lirsac PN, Toma F, Gabrielsen OS (1993) DNA and redox state induced conformational changes in the DNA-binding domain of the Myb oncoprotein. *The EMBO Journal* **12:** 4625-4633

Nakagawa T, Kurose T, Hino T, Tanaka K, Kawamukai M, Niwa Y, Toyooka K, Matsuoka K, Jinbo T, Kimura T (2007) Development of series of gateway binary vectors, pGWBs, for realizing efficient construction of fusion genes for plant transformation. *Journal of Bioscience and Bioengineering* **104:** 34-41

Nallamsetty S, Austin BP, Penrose KJ, Waugh DS (2005) Gateway vectors for the production of combinatorially-tagged His6-MBP fusion proteins in the cytoplasm and periplasm of Escherichia coli. *Protein Science : a Publication of the Protein Society* **14:** 2964-2971

Nathan C (2003) Specificity of a third kind: reactive oxygen and nitrogen intermediates in cell signaling. *Journal of Clinical Investigation* **111:** 769-778

Navarro L, Zipfel C, Rowland O, Keller I, Robatzek S, Boller T, Jones JD (2004) The transcriptional innate immune response to flg22. Interplay and overlap with Avr gene-dependent defense responses and bacterial pathogenesis. *Plant Physiology* **135:** 1113-1128

Nawrath C, Heck S, Parinthawong N, Métraux J-P (2002) EDS5, an Essential Component of Salicylic Acid-Dependent Signaling for Disease Resistance in Arabidopsis, Is a Member of the MATE Transporter Family. *The Plant Cell* **14:** 275-286

Nawrath C, Metraux JP (1999) Salicylic acid induction-deficient mutants of Arabidopsis express PR-2 and PR-5 and accumulate high levels of camalexin after pathogen inoculation. *The Plant Cell* **11:** 1393-1404

Nicaise V, Roux M, Zipfel C (2009) Recent advances in PAMP-triggered immunity against bacteria: pattern recognition receptors watch over and raise the alarm. *Plant Physiology* **150:** 1638-1647

Noctor G, Mhamdi A, Chaouch S, Han Y, Neukermans J, Marquez-Garcia B, Queval G, Foyer CH (2012) Glutathione in plants: an integrated overview. *Plant, Cell & Environment* **35:** 454-484

Okamoto S, Nakamura T, Cieplak P, Chan SF, Kalashnikova E, Liao L, Saleem S, Han X, Clemente A, Nutter A, Sances S, Brechtel C, Haus D, Haun F, Sanz-Blasco S, Huang X, Li H, Zaremba JD, Cui J, Gu Z, Nikzad R, Harrop A, McKercher SR, Godzik A, Yates JR, 3rd, Lipton SA (2014) S-nitrosylation-mediated redox transcriptional switch modulates neurogenesis and neuronal cell death. *Cell Reports* **8:** 217-228

Okmen B, Doehlemann G (2014) Inside plant: biotrophic strategies to modulate host immunity and metabolism. *Current Opinion in Plant Biology* **20:** 19-25

Papaneophytou CP, Kontopidis G (2014) Statistical approaches to maximize recombinant protein expression in Escherichia coli: a general review. *Protein Expression and Purification* **94:** 22-32

Park SW, Kaimoyo E, Kumar D, Mosher S, Klessig DF (2007) Methyl salicylate is a critical mobile signal for plant systemic acquired resistance. *Science* **318:** 113-116

Pawloski JR, Hess DT, Stamler JS (2001) Export by red blood cells of nitric oxide bioactivity. *Nature* **409:** 622-626

Pelludat C, Brem D, Heesemann J (2003) Irp9, Encoded by the High-Pathogenicity Island of Yersinia enterocolitica, Is Able To Convert Chorismate into Salicylate, the Precursor of the Siderophore Yersiniabactin. *Journal of Bacteriology* **185:** 5648-5653

Planchet E, Jagadis Gupta K, Sonoda M, Kaiser WM (2005) Nitric oxide emission from tobacco leaves

and cell suspensions: rate limiting factors and evidence for the involvement of mitochondrial electron transport. *The Plant Journal* **41:** 732-743

Raskin I, Ehmann A, Melander WR, Meeuse BJ (1987) Salicylic Acid: a natural inducer of heat production in arum lilies. *Science* **237:** 1601-1602

Rivas-San Vicente M, Plasencia J (2011) Salicylic acid beyond defence: its role in plant growth and development. *Journal of Experimental Botany* **62:** 3321-3338

Rochon A, Boyle P, Wignes T, Fobert PR, Despres C (2006) The coactivator function of Arabidopsis NPR1 requires the core of its BTB/POZ domain and the oxidation of C-terminal cysteines. *The Plant Cell* **18:** 3670-3685

Rockel P, Strube F, Rockel A, Wildt J, Kaiser WM (2002) Regulation of nitric oxide (NO) production by plant nitrate reductase in vivo and in vitro. *Journal of Experimental Botany* **53:** 103-110

Romero-Puertas MC, Laxa M, Matte A, Zaninotto F, Finkemeier I, Jones AM, Perazzolli M, Vandelle E, Dietz KJ, Delledonne M (2007) S-nitrosylation of peroxiredoxin II E promotes peroxynitrite-mediated tyrosine nitration. *The Plant Cell* **19:** 4120-4130

Rumer S, Gupta KJ, Kaiser WM (2009) Plant cells oxidize hydroxylamines to NO. *Journal of Experimental Botany* **60:** 2065-2072

Russwurm M, Koesling D (2004) NO activation of guanylyl cyclase. *The EMBO Journal* **23:** 4443-4450

Sakamoto A, Ueda M, Morikawa H (2002) Arabidopsis glutathione-dependent formaldehyde dehydrogenase is an S-nitrosoglutathione reductase. *FEBS Letters* **515:** 20-24

Sang J, Jiang M, Lin F, Xu S, Zhang A, Tan M (2008) Nitric oxide reduces hydrogen peroxide accumulation involved in water stress-induced subcellular anti-oxidant defense in maize plants. *Journal of Integrative Plant Biology* **50:** 231-243

Sanghani PC, Robinson H, Bosron WF, Hurley TD (2002) Human glutathione-dependent formaldehyde dehydrogenase. Structures of apo, binary, and inhibitory ternary complexes. *Biochemistry* **41:** 10778-10786

Seligman K, Saviani EE, Oliveira HC, Pinto-Maglio CA, Salgado I (2008) Floral transition and nitric oxide emission during flower development in Arabidopsis thaliana is affected in nitrate reductase-deficient plants. *Plant & Cell Physiology* **49:** 1112-1121

Serino L, Reimmann C, Baur H, Beyeler M, Visca P, Haas D (1995) Structural genes for salicylate biosynthesis from chorismate in Pseudomonas aeruginosa. *Molecular and General Genetics MGG* **249:** 217-228

Serpa V, Vernal J, Lamattina L, Grotewold E, Cassia R, Terenzi H (2007) Inhibition of AtMYB2 DNA-binding by nitric oxide involves cysteine S-nitrosylation. *Biochemical and Biophysical Research Communications* **361:** 1048-1053

Serrano M, Wang B, Aryal B, Garcion C, Abou-Mansour E, Heck S, Geisler M, Mauch F, Nawrath C, Metraux JP (2013) Export of salicylic acid from the chloroplast requires the multidrug and toxin extrusion-like transporter EDS5. *Plant Physiology* **162:** 1815-1821

Sha Y, Marshall HE (2012) S-nitrosylation in the regulation of gene transcription. *Biochimica et Biophysica Acta* **1820:** 701-711

Shapiro AD, Zhang C (2001) The Role of NDR1 in Avirulence Gene-Directed Signaling and Control of Programmed Cell Death in Arabidopsis. *Plant Physiology* **127:** 1089-1101

Shaulian E, Karin M (2002) AP-1 as a regulator of cell life and death. *Nature Cell Biology* **4:** E131-136

Shiva S (2010) Mitochondria as metabolizers and targets of nitrite. *Nitric Oxide : biology and chemistry / official journal of the Nitric Oxide Society* **22:** 64-74

Singh SP, Wishnok JS, Keshive M, Deen WM, Tannenbaum SR (1996) The chemistry of the S-nitrosoglutathione/glutathione system. *Proceedings of the National Academy of Sciences of the United States of America* **93:** 14428-14433

Skelly MJ, Loake GJ (2013) Synthesis of redox-active molecules and their signaling functions during the expression of plant disease resistance. *Antioxidants & Redox Signaling* **19:** 990-997

Slaymaker DH, Navarre DA, Clark D, del Pozo O, Martin GB, Klessig DF (2002) The tobacco salicylic acid-binding protein 3 (SABP3) is the chloroplast carbonic anhydrase, which exhibits antioxidant activity and plays a role in the hypersensitive defense response. *Proceedings of the National Academy of Sciences of the United States of America* **99:** 11640-11645

Solano R, Stepanova A, Chao Q, Ecker JR (1998) Nuclear events in ethylene signaling: a transcriptional cascade mediated by ETHYLENE-INSENSITIVE3 and ETHYLENE-RESPONSE-FACTOR1. *Genes & Development* **12:** 3703-3714

Spadaro D, Yun BW, Spoel SH, Chu C, Wang YQ, Loake GJ (2010) The redox switch: dynamic regulation of protein function by cysteine modifications. *Physiologia Plantarum* **138:** 360-371

Srivastava N, Gonugunta VK, Puli MR, Raghavendra AS (2009) Nitric oxide production occurs downstream of reactive oxygen species in guard cells during stomatal closure induced by chitosan in abaxial epidermis of Pisum sativum. *Planta* **229:** 757-765

Stamler JS, Simon DI, Osborne JA, Mullins ME, Jaraki O, Michel T, Singel DJ, Loscalzo J (1992) S-nitrosylation of proteins with nitric oxide: synthesis and characterization of biologically active

compounds. *Proceedings of the National Academy of Sciences of the United States of America* **89:** 444-448

Stohr C, Strube F, Marx G, Ullrich WR, Rockel P (2001) A plasma membrane-bound enzyme of tobacco roots catalyses the formation of nitric oxide from nitrite. *Planta* **212:** 835-841

Stoimenova M, Igamberdiev AU, Gupta KJ, Hill RD (2007) Nitrite-driven anaerobic ATP synthesis in barley and rice root mitochondria. *Planta* **226:** 465-474

Straus MR, Rietz S, Ver Loren van Themaat E, Bartsch M, Parker JE (2010) Salicylic acid antagonism of EDS1-driven cell death is important for immune and oxidative stress responses in Arabidopsis. *The Plant Journal* **62:** 628-640

Strawn MA, Marr SK, Inoue K, Inada N, Zubieta C, Wildermuth MC (2007) Arabidopsis isochorismate synthase functional in pathogen-induced salicylate biosynthesis exhibits properties consistent with a role in diverse stress responses. *The Journal of Biological Chemistry* **282:** 5919-5933

Studier FW (1991) Use of bacteriophage T7 lysozyme to improve an inducible T7 expression system. *Journal of Molecular Biology* **219:** 37-44

Sun P, Tropea JE, Waugh DS (2011) Enhancing the solubility of recombinant proteins in Escherichia coli by using hexahistidine-tagged maltose-binding protein as a fusion partner. *Methods in Molecular biology* **705:** 259-274

Sun T, Zhang Y, Li Y, Zhang Q, Ding Y, Zhang Y (2015) ChIP-seq reveals broad roles of SARD1 and CBP60g in regulating plant immunity. *Nature Communications* **6:** 10159

Tada Y, Spoel SH, Pajerowska-Mukhtar K, Mou Z, Song J, Wang C, Zuo J, Dong X (2008) Plant immunity requires conformational changes of NPR1 via S-nitrosylation and thioredoxins. *Science* **321:** 952-956

Tavares CP, Vernal J, Delena RA, Lamattina L, Cassia R, Terenzi H (2014) S-nitrosylation influences the structure and DNA binding activity of AtMYB30 transcription factor from Arabidopsis thaliana. *Biochimica et Biophysica Acta* **1844:** 810-817

Tran LS, Nakashima K, Sakuma Y, Simpson SD, Fujita Y, Maruyama K, Fujita M, Seki M, Shinozaki K, Yamaguchi-Shinozaki K (2004) Isolation and functional analysis of Arabidopsis stress-inducible NAC transcription factors that bind to a drought-responsive cis-element in the early responsive to dehydration stress 1 promoter. *The Plant Cell* **16:** 2481-2498

Truman W, Glazebrook J (2012) Co-expression analysis identifies putative targets for CBP60g and SARD1 regulation. *BMC Plant Biol* **12:** 216

Truman W, Sreekanta S, Lu Y, Bethke G, Tsuda K, Katagiri F, Glazebrook J (2013) The CALMODULIN-BINDING PROTEIN60 family includes both negative and positive regulators of plant

immunity. *Plant Physiology* **163:** 1741-1751

Tun NN, Santa-Catarina C, Begum T, Silveira V, Handro W, Floh EI, Scherer GF (2006) Polyamines induce rapid biosynthesis of nitric oxide (NO) in Arabidopsis thaliana seedlings. *Plant & Cell Physiology* **47:** 346-354

Uppalapati SR, Ishiga Y, Wangdi T, Kunkel BN, Anand A, Mysore KS, Bender CL (2007) The phytotoxin coronatine contributes to pathogen fitness and is required for suppression of salicylic acid accumulation in tomato inoculated with Pseudomonas syringae pv. tomato DC3000. *Molecular Plant-Microbe Interactions : MPMI* **20:** 955-965

van Verk MC, Bol JF, Linthorst HJ (2011) WRKY transcription factors involved in activation of SA biosynthesis genes. *BMC Plant Biology* **11:** 89

Vandelle E, Delledonne M (2011) Peroxynitrite formation and function in plants. *Plant Science* **181:** 534-539

Verberne MC, Verpoorte R, Bol JF, Mercado-Blanco J, Linthorst HJ (2000) Overproduction of salicylic acid in plants by bacterial transgenes enhances pathogen resistance. *Nature Biotechnology* **18:** 779-783

Vlot AC, Dempsey DA, Klessig DF (2009) Salicylic Acid, a multifaceted hormone to combat disease. *Annual review of phytopathology* **47:** 177-206

Wang BL, Tang XY, Cheng LY, Zhang AZ, Zhang WH, Zhang FS, Liu JQ, Cao Y, Allan DL, Vance CP, Shen JB (2010) Nitric oxide is involved in phosphorus deficiency-induced cluster-root development and citrate exudation in white lupin. *The New Phytologist* **187:** 1112-1123

Wang L, Tsuda K, Sato M, Cohen JD, Katagiri F, Glazebrook J (2009a) Arabidopsis CaM binding protein CBP60g contributes to MAMP-induced SA accumulation and is involved in disease resistance against Pseudomonas syringae. *PLoS Pathogens* **5:** e1000301

Wang L, Tsuda K, Truman W, Sato M, Nguyen le V, Katagiri F, Glazebrook J (2011) CBP60g and SARD1 play partially redundant critical roles in salicylic acid signaling. *The Plant Journal* **67:** 1029-1041

Wang P, Du Y, Hou YJ, Zhao Y, Hsu CC, Yuan F, Zhu X, Tao WA, Song CP, Zhu JK (2015a) Nitric oxide negatively regulates abscisic acid signaling in guard cells by S-nitrosylation of OST1. *Proceedings of the National Academy of Sciences of the United States of America* **112:** 613-618

Wang X, Gao J, Zhu Z, Dong X, Wang X, Ren G, Zhou X, Kuai B (2015b) TCP transcription factors are critical for the coordinated regulation of isochorismate synthase 1 expression in Arabidopsis thaliana. *The Plant Journal* **82:** 151-162

Wang YQ, Feechan A, Yun BW, Shafiei R, Hofmann A, Taylor P, Xue P, Yang FQ, Xie ZS, Pallas JA, Chu CC,

Loake GJ (2009b) S-nitrosylation of AtSABP3 antagonizes the expression of plant immunity. *The Journal of Biological Chemistry* **284:** 2131-2137

Wildermuth MC, Dewdney J, Wu G, Ausubel FM (2001) Isochorismate synthase is required to synthesize salicylic acid for plant defence. *Nature* **414:** 562-565

Wilkinson JQ, Crawford NM (1993) Identification and characterization of a chlorate-resistant mutant of Arabidopsis thaliana with mutations in both nitrate reductase structural genes NIA1 and NIA2. *Molecular and General Genetics MGG* **239:** 289-297

Wu Y, Zhang D, Chu JY, Boyle P, Wang Y, Brindle ID, De Luca V, Despres C (2012) The Arabidopsis NPR1 protein is a receptor for the plant defense hormone salicylic acid. *Cell Reports* **1:** 639-647

Xue Y, Liu Z, Gao X, Jin C, Wen L, Yao X, Ren J (2010) GPS-SNO: computational prediction of protein S-nitrosylation sites with a modified GPS algorithm. *PloS One* **5:** e11290

Yamamoto-Katou A, Katou S, Yoshioka H, Doke N, Kawakita K (2006) Nitrate reductase is responsible for elicitin-induced nitric oxide production in Nicotiana benthamiana. *Plant & Cell Physiology* **47:** 726-735

Yamasaki H, Sakihama Y (2000) Simultaneous production of nitric oxide and peroxynitrite by plant nitrate reductase: in vitro evidence for the NR-dependent formation of active nitrogen species. *FEBS Letters* **468:** 89-92

Yan S, Dong X (2014) Perception of the plant immune signal salicylic acid. *Current Opinion in Plant Biology* **20:** 64-68

Yu M, Lamattina L, Spoel SH, Loake GJ (2014) Nitric oxide function in plant biology: a redox cue in deconvolution. *The New Phytologist* **202:** 1142-1156

Yu M, Yun BW, Spoel SH, Loake GJ (2012) A sleigh ride through the SNO: regulation of plant immune function by protein S-nitrosylation. *Current Opinion in Plant Biology* **15:** 424-430

Yun BW, Feechan A, Yin M, Saidi NB, Le Bihan T, Yu M, Moore JW, Kang JG, Kwon E, Spoel SH, Pallas JA, Loake GJ (2011) S-nitrosylation of NADPH oxidase regulates cell death in plant immunity. *Nature* **478:** 264-268

Zhang Y, Cheng YT, Qu N, Zhao Q, Bi D, Li X (2006) Negative regulation of defense responses in Arabidopsis by two NPR1 paralogs. *The Plant Journal* **48:** 647-656

Zhang Y, Fan W, Kinkema M, Li X, Dong X (1999) Interaction of NPR1 with basic leucine zipper protein transcription factors that bind sequences required for salicylic acid induction of the PR-1 gene. *Proceedings of the National Academy of Sciences of the United States of America* **96:** 6523-6528

Zhang Y, Xu S, Ding P, Wang D, Cheng YT, He J, Gao M, Xu F, Li Y, Zhu Z, Li X, Zhang Y (2010) Control of salicylic acid synthesis and systemic acquired resistance by two members of a plant-specific family of transcription factors. *Proceedings of the National Academy of Sciences of the United States of America* **107:** 18220-18225

Zheng XY, Spivey NW, Zeng W, Liu PP, Fu ZQ, Klessig DF, He SY, Dong X (2012) Coronatine promotes Pseudomonas syringae virulence in plants by activating a signaling cascade that inhibits salicylic acid accumulation. *Cell Host & Microbe* **11:** 587-596

Zhou JM, Trifa Y, Silva H, Pontier D, Lam E, Shah J, Klessig DF (2000) NPR1 differentially interacts with members of the TGA/OBF family of transcription factors that bind an element of the PR-1 gene required for induction by salicylic acid. *Molecular Plant-Microbe Interactions : MPMI* **13:** 191-202

Zhou N, Tootle TL, Tsui F, Klessig DF, Glazebrook J (1998) PAD4 functions upstream from salicylic acid to control defense responses in Arabidopsis. *The Plant Cell* **10:** 1021-1030

Zipfel C (2014) Plant pattern-recognition receptors. *Trends in Immunology* **35:** 345-351

Zottini M, Costa A, De Michele R, Ruzzene M, Carimi F, Lo Schiavo F (2007) Salicylic acid activates nitric oxide synthesis in Arabidopsis. *Journal of Experimental Botany* **58:** 1397-1405